Interactions between Soil Organic Matter and Water with special respect to the Glass Transition Behavior

vorgelegt von

Dipl.-Ing.

Julia Hurraß

von der Fakultät III – Prozesswissenschaften –

der Technischen Universität Berlin

zur Erlangung des akademischen Grades

Doktorin der Naturwissenschaften

- Dr. rer.nat. -

genehmigte Dissertation

Promotionsausschuss:

Vorsitzender:	Prof. Dr. Ulrich Szewzyk
Berichter:	Prof. Dr. Wolfgang Rotard
Berichterin:	Dr. Gabriele E. Schaumann
Berichter:	Prof. Dr. Martin Kaupenjohann

Tag der wissenschaftlichen Aussprache: 13.01.2006

Berlin 2006

D 83

“O povo unido jamais será vencido!”

dedicado ao

Movimento dos Trabalhadores Rurais Sem Terra (MST)

e a todos que ainda acreditam num melhor mundo

Table of Contents

Acknowledgements

First of all, I want to thank to my partner Uwe Hott and to my parents, who supported me during the whole time that I was working on this thesis. The encouragement and patience of my good friends Monika, Tanja, Basti, and Ursel additionally helped me to get through the difficult phases of this work.

I thank Dr. Gabriele Schaumann for the supervision of this dissertation. With her great knowledge, she always stood by my side, but she also gave me the freedom to develop my own ideas. Especially by her effort to extend the project for one more year, she guaranteed my financial situation. I am also thankful to the co-examiners Prof. Dr. Wolfgang Rotard and Prof. Dr. Martin Kaupenjohann, who helped me to improve the manuscript by their critical reading and their helpful advices. To Prof. Dr. Wolfgang Rotard, I am also indebted for giving me the possibility to use the laboratories of the Department of Environmental Chemistry and other facilities of the TU Berlin.

Because of many interesting discussions and helpful impulses, the soil chemistry group of the Department of Soil Science of the Institute for Ecology was very important for me. I am also indebted to my colleagues of the HUMUS group of the Department of Environmental Chemistry for their support. Jeannette Regnery and Katharina Knobel performed an enormous number of DSC measurements for this work and supported the realization of many experiments due to their exceptional commitment in the laboratory. Julia Bayer and Dörte Diehl proof-read parts of the manuscript and contributed to reduce the number of typing errors and to improve previously unclear phrasings.

Many NMR measurements of this study were carried out by Eleanor Hobley within the context of a student research project. Stephan Rosenkranz conducted a part of the DSC experiments for his diploma thesis. I am also grateful to Prof. Dr. Jörg Bachmann and Michael Klatt from the Institute of Soil Science of the TU Hannover for the use of the ESEM microscope and to Dr. Ruth Ellerbrock and Ralf Rath from the ZALF in Müncheberg for the use of the IR spectrometer. Karsten Täumer, Christine Ehrlicher, and Claudia Kuntz from the Department of Soil Science of the Institute for Ecology and Gabi Hedicke from the Department of Physical and Theoretical Chemistry of the Institute of Chemistry of the TU Berlin supported the work in the laboratory. I thank Dr. Sören Thiele-Bruhn, Dr. Friederike Lang, and Prof. Dr. Christian Siewert for the supply of the soil samples from Halle, Bad Lauchstädt, Bavaria, Baden-Württemberg, and Siberia. Special thanks goes to Michael Facklam, who often could solve problems concerning special applications of soil physical methods.

The work was funded by the German Research Association DFG (research group INTERURBAN, SCHA 849/4).

Abstract

Several ecologically relevant aspects of soil organic matter (SOM), like the sorption of organic compounds and the water uptake kinetics, can only be explained in terms of the macromolecular structure of the humic substances. It is known that the conformation of the macromolecular SOM network is distinctly affected by the water status in soil. But, the underlying processes, as the way of water binding and the resulting effects on the rigidity of the organic soil matrix, are still insufficiently understood.

This thesis focused on the characterization of the interactions between solid SOM and water. On the one hand, the hydration process of humous soil samples was studied. Especially, differences in the wetting process of water repellent and wettable samples and possible factors of influence for soil water repellency were investigated. On the other hand, the glass transition behavior of SOM, which sensitively reflects the way of water bonding, was examined for a set of 102 soil samples from different locations. The results of the wetting experiments as well as of the study of the glass transition behavior strongly support the macromolecular view of humic substances. In 52 out of the 102 soil samples, two types of glass transitions were detected: A classical glass transition can be observed only in water-free samples. The other transition type is strongly influenced by the moisture status in SOM and reveals a slowly reversing behavior, which contradicts the classical definition of glass transitions. The transition temperatures of this atypical transition ranged between 51 °C and 67 °C for all studied air-dried samples. According to the hydrogen bond-based crosslinking (HBCL) model, a crosslinking of the side chains of the organic substances by hydrogen bond water molecules may explain the comparable rigidity and with that the similar transition temperatures of SOM in air-dried samples. In addition to the water status, the atypical glass transition-like step transition is influenced by the C_{org} content, the profile depth, and by anthropogenic impacts to the soil. Due to aging effects, the time additionally represents an important factor. These aging effects may cause an increasing rigidity of the organic soil matrix in the course of time and are based on conformational changes of SOM, which are distinctly influenced by the effects of water molecules on the macromolecular structure.

Most probably, slow conformational changes occurring at the SOM surfaces are also responsible for the slow wetting process of water repellent samples, which may last up to three weeks. The results of this study indicate that the mechanisms causing water repellent behavior may differ from location to location. For one of the two studied anthropogenic sites, the occurrence of water repellent regions is correlated to low pH and high ionic strength in the soil solutions. The protonation of negatively charged functional groups and a more condensed SOM structure due to the high electrolyte contents may cause the lower wettability of these regions. For both locations, lower surface tensions were measured in aqueous extracts of actually water repellent samples than for actually wettable samples. Amphiphilic substances consequently are supposed to play an important part for the occurrence of water repellent spots in soil.

Zusammenfassung

Viele ökologisch wichtige Aspekte der organischen Bodensubstanz (OBS), wie die Sorption von organischen Verbindungen und die Wasseraufnahme-Kinetik, lassen sich nur mit Hilfe einer makromolekularen Betrachtungsweise der humosen Substanzen erklären. Es ist bekannt, dass die Konformation des makromolekularen OBS-Netzwerks stark vom Wasserstatus des Bodens beeinflusst wird. Die zugrunde liegenden Prozesse, wie die Art der Wasserbindung und die daraus resultierenden Effekte für die Starrheit der organischen Bodenmatrix, werden bisher jedoch nur unzureichend verstanden.

Im Mittelpunkt dieser Dissertation stand die Charakterisierung der Wechselwirkungen zwischen der festen OBS und Wasser. Einerseits wurde der Wasseraufnahmeprozess humoser Bodenproben untersucht. Dabei wurden vor allem Unterschiede des Benetzungsvorgangs zwischen wasserabweisenden und benetzbaren Proben und mögliche Einflussfaktoren für Benetzungshemmung im Boden betrachtet. Andererseits wurde für 102 Bodenproben von unterschiedlichen Standorten das Glasübergangsverhalten der OBS, das sehr genau die Art der Wasserbindung widerspiegelt, untersucht. Sowohl die Ergebnisse der Benetzungsversuche als auch die der Glasübergangsuntersuchungen stützen die makromolekulare Vorstellungsweise der humosen Substanzen. In 52 der 102 Bodenproben wurden zwei Arten von Glasübergängen festgestellt: Ein klassischer Glasübergang lässt sich nur in wasserfreien Proben beobachten. Der andere Übergangstyp ist stark vom Wasserstatus der OBS abhängig und zeichnet sich durch einen nur langsam reversierenden Charakter aus, was der klassischen Definition von Glasübergängen widerspricht. Die Übergangstemperaturen dieses untypischen Übergangs lagen für alle untersuchten luftgetrockneten Proben zwischen 51 °C und 67 °C. Gemäß des Wasserstoffbrückenbindungs-Modells (HBCL) kann eine Quervernetzung der Seitenketten der organischen Substanzen durch mittels Wasserstoffbrücken gebundene Wassermoleküle die vergleichbare Starrheit und damit die ähnlichen Übergangstemperaturen der OBS luftgetrockneter Proben erklären. Zusätzlich zum Wasserstatus beeinflussen der C_{org}-Gehalt, die Profiltiefe und anthropogene Bodenveränderungen den untypischen glasübergangsähnlichen Stufenübergang. Aufgrund von Alterungsprozessen stellt die Zeit einen weiteren wichtigen Faktor dar. Die Alterungsprozesse können eine zunehmende Starrheit der organischen Bodenmatrix im Verlauf der Zeit verursachen und beruhen auf Konformationsänderungen der OBS, die stark von den Effekten der Wassermoleküle auf die makromolekulare Struktur abhängen.

Höchstwahrscheinlich sind auch langsame Konformationsänderungen an den OBS-Oberflächen für den langsamen Benetzungsprozess von wasserabweisenden Proben, der bis zu drei Wochen dauern kann, verantwortlich. Die Ergebnisse dieser Arbeit zeigen, dass die Mechanismen, die für das wasserabweisende Verhalten verantwortlich sind, von Standort zu Standort variieren können. Für einen der beiden untersuchten anthropogen beeinflussten Standorte ist das Auftreten benetzungsgehemmter Bereiche mit niedrigen pH-Werten und hohen Leitfähigkeiten der Bodenlösung verbunden. Die Protonierung negativ geladener

funktioneller Gruppen und eine stärker kondensierte OBS-Struktur aufgrund der hohen Elektrolytgehalte können die schlechte Benetzbarkeit dieser Bereiche verursachen. Für beide Standorte wurden in wässrigen Extrakten von wasserabweisenden Proben geringere Oberflächenspannungen als für die benetzbaren Proben gemessen. Es kann folglich vermutet werden, dass amphiphile Substanzen für das Auftreten von benetzungsgehemmten Bereichen im Boden eine wichtige Rolle spielen.

1. General Introduction

1.1. Ecological relevance of soil organic matter

The important functions of soil organic matter (SOM) for ecologically relevant soil processes are a matter of common knowledge. Thus, the water and air balance of loam, silt, and clay soils is significantly improved by humic substances, which stabilize coarse pores in the aggregate structure (Scheffer and Schachtschabel 1992). Due to these stabilizing properties of SOM, field and air capacity are strongly influenced by the organic matter (OM) content of soils (Krahmer et al. 1995; Ronaldo de Macedo et al. 2002). The aggregate stability mainly depends on hydrophobic SOM components (Monreal et al. 1995; Piccolo and Mbagwu 1999) and is linked to a reduction of soil wettability because of increasing aggregate cohesion by the organic substances (Zhang and Hartge 1992; Chenu et al. 2000). Additionally, SOM plays an important part for the storage of nutrients in soil. In this context, especially the labile organic fraction providing easily mineralizable carbon and nitrogen represents an indicator for soil quality (Scheffer and Schachtschabel 1992; Gregorich et al. 1994; Haynes 2005). Sorption and transport processes of organic compounds are also pronouncedly affected by the organic substances in soil. A high number of specific sorption sites can be assumed at the surfaces and within the macromolecular matrix of SOM (Schulten and Leinweber 2000). However, the sorption behavior of the organic soil matrix cannot be described only in terms of fixed sorption sites. It reacts very sensitively on changes of the external conditions like the moisture status (Graber and Borisover 1998b) or previous exposure to solutions with high levels of sorbate concentration (Pignatello and Xia 2000). The degree of nonlinearity of sorption isotherms and of hysteresis effects between sorption and desorption is considered to be associated with diagenetically altered materials with small amounts of polar functional groups and with that low O/C ratios, which are often designated as “condensed” SOM structures (e.g., Huang and Weber Jr. 1997; Gunasekara and Xing 2003).

Despite the high importance of SOM, the humification mechanisms, the chemical structure, and physico-chemical properties of the humic substances, which form the basis for understanding the above mentioned processes, are still under debate. One widely accepted model of SOM is based on an aggregation of small amphiphilic molecules to a supramolecular structure (Wershaw 1999; Piccolo 2002), while the sorption behavior of SOM often is interpreted in terms of polymer models (LeBoeuf and Weber Jr. 1997; Graber and Borisover 1998a; Pignatello 2003). For the formation of humic substances, different mechanisms are discussed: One possible pathway is based on progressive oxidation and degradation of existing plant polymers, whereas another one involves that humic macromolecules are microbiologically synthesized from smaller molecules derived from plant precursors (Swift 1999).

1.2. Macromolecular structure of soil organic matter

Up to now, most efforts to elucidate the characteristics of humic substances and SOM are based on investigations of their molecular structure. Especially, modern liquid and solid state NMR techniques have yielded important information on the organic matter structure in whole soil samples and humic fractions and on SOM transformation processes (Kögel-Knabner 1997; Randall et al. 1997). However, there is still a gap in the knowledge of the macromolecular structure of the organic soil phase. But, only this macromolecular structure can explain distinct aspects of the SOM behavior. Thus, for the sorption of organic compounds to humic substances, a polymeric structure consisting of glassy and rubbery domains is proposed (LeBoeuf and Weber Jr. 1997; Xing and Pignatello 1997). The rubbery phase is supposed to account for linear sorption isotherms due to partitioning processes, while the glassy regions are linked with nonlinear sorption, competition, and hysteresis effects. The pronounced swelling by water (Scheffer and Schachtschabel 1992) as well as the gel properties of humic substances (Benedetti et al. 1996; Schaumann et al. 2000) also reflect the macromolecular SOM structure.

In the last years, scientists have commenced to analyze the polymeric nature of SOM. For this purpose, predominantly indirect approaches as the study of the structural conformation of dissolved humic substances were applied: Myeni et al. (1999) studied the macromolecular structure of humic substances in solution as a function of solution chemistry and deduce a more dense structure of humic substances in acidic than in alkaline soils. Conte and Piccolo (1999; 2000) examined the conformation of humic substances in solutions differing in composition by size-exclusion chromatography (SEC). They concluded from their results that humic substances rather behave as loosely bound self-associations of relatively small molecules than as macromolecular polymers. Contrary to their concepts of macromolecular structure, Swift (1999) supposes the flexible random-coil model for humic substances in solution on the basis of SEC and ultracentrifugation studies.

The analysis of sorption isotherms of organic compounds to humic substances represents another indirect method to describe the macromolecular properties of SOM. Based on the dual-mode or distributed reactivity model (LeBoeuf and Weber Jr. 1997; Xing and Pignatello 1997), which distinguishes between the sorption to rubbery flexible-chain regions and the sorption to more rigid glassy regions, a more comprehensive understanding of the polymeric structure is achieved by the study of additional sorbate effects. The observed linear or even exponential regions in the sorption isotherms for high sorbate concentrations indicate plasticization of the macromolecular system (Xia and Pignatello 2001; Pignatello 2003). This process is linked to swelling and to the transformation of glassy to rubbery domains or at least to domains with less glassy, i.e. more flexible behavior. Increased sorbate uptake and isotherm nonlinearity of SOM after previous equilibration at high concentrations of the sorbate is known as “conditioning effect”. This effect accounts for true hysteresis or isotherm non-singularity and can be explained by a pore deformation mechanism of the nanovoids in the glassy matrix (Lu and Pignatello 2002; Pignatello 2003). The disruption of polar contact

points in the SOM macromolecular complex by high solute activities represents an alternative explanation for the conditioning effect (Graber and Borisover 1998b). In contrast to the pore deformation mechanism, this concept does not require glassy domains in the polymeric soil matrix. However, the detection of glass transitions in humic substances (LeBoeuf and Weber Jr. 1997) as well as in selected whole soil samples (Schaumann and Antelmann 2000; DeLapp and LeBoeuf 2004) and in a peat (Schaumann and LeBoeuf 2005) supports the hypothesis of the coexistence of rubbery and glassy regions in SOM.

1.3. Interactions with water

Under field conditions, soils are permanently subjected to changes of the moisture conditions. Studies of the soil wettability indicate that the conformational structure of SOM is strongly influenced by the water content. Thus, drying is expected to result in an orientation of hydrophobic groups to the outside of the organic molecules or molecule associates, while polar functional groups orientate to the inside due to the formation of hydrogen bonds among themselves (Ma'shum and Farmer 1985; Valat et al. 1991; Roy et al. 2000). Remoistening conversely causes that the hydrophilic groups reorientate outwards shielding the hydrophobic groups from the aqueous phase. These changes of the conformational structure may be very slow, so that hysteresis effects have to be expected (Valat et al. 1991; Altfelder et al. 1999; Schaumann 2005). However, the underlying mechanisms, e.g., the way of water binding in the amorphous SOM matrix, are only insufficiently understood. First efforts to determine the bond strength of water in SOM were made by investigations of the freezing and melting behavior of the water in peat (McBrierty et al. 1996; Schaumann 2005). Since water molecules which are tightly bound to the soil matrix may not participate in the freezing process of bulk water, the magnitude of water bonding to SOM can be estimated by measuring the freezing enthalpies of the soil samples. ^{1}H NMR Relaxometry represents another promising method to determine the mobility and with that the degree of binding of water molecules in SOM (McBrierty et al. 1996; Todoruk et al. 2003b; Schaumann et al. 2004; Schaumann et al. 2005a). Especially, the characterization of the glass transition behavior of a peat sample as a function of its water status (Schaumann 2005; Schaumann and LeBoeuf 2005) yielded important information on the interactions of water molecules with the organic soil matrix. Schaumann and LeBoeuf (Schaumann 2005; Schaumann and LeBoeuf 2005) suggested the hydrogen bond-based crosslinking (HBCL) model, assuming an antiplasticization effect by crosslinks of water molecules in SOM for low moisture contents.

Since sorption of organic substances is distinctly affected by the water status in SOM (Unger et al. 1996; Altfelder et al. 1999; Berglöf et al. 2000; Borisover and Graber 2004), a more detailed knowledge of the interactions between the organic molecules or molecule associates and the water molecules would help to predict the fate of organic compounds in soil.

1.4. Objectives of this thesis

The main objective of this thesis was to describe the interactions between solid SOM and water. At first, the macroscopically observable hydration process of humous soil samples was studied. For the macromolecular SOM matrix, this process can be divided into the processes of wetting and swelling. The wetting process represents the first interactions of the water molecules with the pore surfaces. It can be very slow in water repellent soils, where the water molecules have to change the interfacial characteristics of the pore surfaces before they can penetrate into the solid organic phase. The subsequent swelling of the SOM network is based on the dissolution of SOM segments and the disruption of crosslinks by water molecules, resulting in a gel-like phase (Elias 1997). The study of the glass transition behavior of SOM, which represents the second part of this work, was intended to obtain more information on the macromolecular characteristics of SOM and the influence of water on this system. Above all, the question, whether glassiness can be considered a common characteristic of SOM, was in the focus of attention. For the verification of the polymer model, which describes humic substances as an amorphous system which can convert from the rubbery to the glassy state and vice versa (LeBoeuf and Weber Jr. 1997; Xing and Pignatello 1997), the detection of glass transitions in different humous soil samples is essential. Further support for the polymer model would result from the observation of aging processes (Cortés and Montserrat 1998) in the glassy SOM matrix. By studying the influence on the sample history on the glass transition behavior, it was examined, whether these aging processes may occur in SOM. Since the glass transition parameters reflect the matrix rigidity of the glassy state, they additionally represent a very sensitive indicator for the effects of water in the polymeric SOM network.

In order to characterize the differences in the hydration process of water repellent and wettable soil samples, water uptake kinetics were traced by direct gravimetric determination of the water contents in the course of hydration time. One of my fundamental assumptions was that water molecules are subjected to different types of bondings with SOM of water repellent and of wettable soils. To test this hypothesis, the degree of water bonding was characterized by the phase transition behavior of the soil water. Especially, the portion of non-freezable water served as an indicator for the amount of water bound to SOM. In addition, ^{1}H NMR Relaxometry measurements were performed in the course of hydration to monitor the mobility of the water molecules, which depends on the sizes of the water-filled pores, the interactions between pore walls and water molecules, and the dissolution of organic or inorganic substances during the hydration process. The combination of these methods was designed to identify differences in the water sorption process of water repellent and wettable soil samples as comprehensive as possible. The differentiation between the processes of wetting and swelling was another goal of the study of the water uptake kinetics by these methods. The results of these experiments are presented in Chapter 2.

In order to ascertain possible reasons for the differences in the wetting behavior, selected properties of sample pairs consisting of two samples which were taken directly side by side, but which distinctly differed in wettability were studied. It is commonly accepted that the

wetting characteristics of soils are distinctly affected by the moisture content (e.g., King 1981; Ritsema and Dekker 1998; Quyum et al. 2002). We hypothesized that the small-scale heterogeneity in soil wettability occurring every year during the summer months in the locations Buch and Tiergarten (see Chapter 1.5) do not depend only on the moisture contents. Instead, we assumed that there must be further intrinsic soil properties which differ between the water repellent and the wettable spots and which cause the differences in the degree of wettability. In order to examine, if a sole dependency of the actual wettability on the moisture contents really can be excluded, we carefully investigated the influence of the water status on the wettability of the studied sample pairs. For this purpose, the initially field-moist samples were subjected to different pretreatment methods, such as sample drying and equilibration in defined relative humidities. After the adjustment of the moisture states of the samples by these methods, it was tested, whether the differences in wettability within the sample pairs still remained. The persistence of the differences in wettability of the sample pairs was additionally examined by measuring the sample wettability in the course of a drying and remoistening cycle. To verify our hypothesis that other factors apart from the water status influence the wettability characteristics, stable SOM properties were characterized with respect to possible interrelations to the wetting behavior of the samples. Both, the solid SOM and soil solutions, which also reflect the SOM properties, were analyzed, because the soil wettability depends on the interfacial properties of the solid phase as well as of the liquid phase. Due to the known effects of pH and ionic strength on the conformation of humic substances in solution, we assumed that especially these solution parameters may also affect the molecular conformation at the SOM surfaces and consequently alter its wetting characteristics. The results of this investigation of the properties of the actually water repellent and actually wettable samples are summarized in Chapter 3.

To examine the hypothesis that glassiness is a typical characteristic of SOM, 102 soil samples of different locations were investigated concerning their glass transition behavior. In order to detect factors of influence for the glass transition parameters, samples from different soil horizons and with different C_{org} contents and types of anthropogenic impacts were incorporated into the study. Possible contributions to the glass transition behavior of selected SOM fractions of the samples, as e.g., humic and fulvic acids and a black carbon-like fraction, were also studied. Due to the highly condensed structure and the nonideal sorption behavior of carbonaceous substances (Chiou et al. 2000; Cornelissen et al. 2004), we hypothesized that the glass transition intensity depends on the content of this SOM fraction. The influence of the water status, however, was in the center of our interest. Accordingly, the transferability of the HBCL model, suggested for a peat sample by Schaumann and LeBoeuf (Schaumann 2005; Schaumann and LeBoeuf 2005), to various soil samples with low to moderate C_{org} contents was examined. On the basis of this model, a comparable water status in soil samples is expected to result in a similar degree of SOM crosslinking by hydrogen bonds of water molecules and with that in a similar matrix rigidity. Assuming a more or less constant energy required for the disruption of the water crosslinks, the transition temperatures, at which this disruption occurs, are supposed to be similar for SOM with comparable water states.

Chapter 4 contains a description of all the Differential Scanning Calorimetry (DSC) measurements performed to characterize the glass transition behavior of the different soil samples and SOM fractions as well as a comprehensive discussion of the results.

Besides the effects of the moisture content and the way of water bonding in the organic soil matrix, the influence of the time after a change of the moisture conditions was investigated. In the course of time, two processes which affect the glass transition behavior may occur: On the one hand, the binding of water molecules within the SOM is expected to increase in strength. On the other hand, below the transition temperature, aging processes of the amorphous organic matrix linked with structural relaxation may proceed, if SOM can be characterized by the same models as synthetic polymers or inorganic glasses. The structural relaxation processes are a consequence of the non-equilibrium nature of the glassy state of amorphous systems (Struik 1978; McKenna and Simon 2002). They are reflected by reductions in segmental mobility, enthalpy, and free volume and result in increasing glass temperatures and the occurrence of annealing peaks in DSC thermograms (Moynihan et al. 1974; Cortés and Montserrat 1998; Hutchinson 1998). In order to examine, if aging effects can be observed for SOM, DSC measurements were conducted after different times of sample storage at temperatures below their transition temperatures. For the differentiation between the effects of water within the SOM matrix and real structural relaxation of the organic substances, the soil samples were stored at different moisture conditions. The results of these experiments are presented in Chapter 5.

1.5. Soil samples

The anthropogenic locations Tiergarten and Buch, which were intensively investigated within the scope of the research group INTERURBAN, were in the center of interest of this work. The Tiergarten is an inner-city park in Berlin, which has been created between the 17th and the 20th century. The location Buch represents a former sewage field in the north of Berlin, which was used for more than 100 years until 1985. Both locations reveal a small-scale heterogeneity of all soil properties. The Tiergarten is characterized by different anthropogenic source materials, as e.g., construction waste, whereas partially elevated C_{org} contents play an important role in the location Buch. In the studies of Schaumann et al. (2005a) and Täumer et al. (2005), a detailed description of the soil properties of these two sites is given.

In order to incorporate further soils with various properties, samples of agricultural sites, of natural forest locations and from different climatic zones in Siberia containing various landscapes additionally were selected for this work. In the forest location Chorin in the north-east of Berlin, the interactions between water and organic matter were investigated by a cooperation of scientists working on this topic (Ellerbrock et al. 2005; Schaumann et al. 2005a). In addition to this well characterized site, four spruce forest locations in Bavaria and Baden-Württemberg serving as Level II monitoring plots under EU legislation were studied (Kölling 2000). The use of the soil samples from Siberia (Siewert 2001) yielded the

possibility to extend the examinations of this study to many soil types of different climatic zones. The tillage samples came from the well studied fertilized and non-fertilized plots of the “Static Fertilization Experiments” in Halle and Bad Lauchstädt in Sachsen-Anhalt (Leinweber et al. 1992; Merbach et al. 2000; Thiele-Bruhn et al. 2004).

The DSC experiments performed in order to analyze the effects of the sample history and of the water status additionally were carried out with a peat sample from the Warnowtal in Mecklenburg. Due to its high OM content, more pronounced effects were assumed for this sample in comparison with the mineral soil samples.

The comparison of the results of this work for all these different soils aimed at the attainment of a detailed understanding of SOM behavior with special respect to its dependency on the water status.

2. Hydration kinetics of wettable and water repellent soil samples

2.1. Abstract

The hydration kinetics of soil organic matter (SOM) are an important factor of influence for transport and sorption processes in soil. Nevertheless, our knowledge about wetting and swelling processes, which control the hydration kinetics, is limited. In this study, three independent methods were applied to observe the hydration process of actually water repellent and wettable soil samples, whereby the NMR results are already published in a separate article. Direct gravimetric measurements of the water uptake as well the analyses by ^{1}H NMR Relaxometry have shown that the wetting of water repellent soils may last up to three weeks. This period of time is distinctly longer than the WDPT of the samples, which consequently only reflect the first wetting step of the soil surface occurring within a time scale of hours. A comparison between the water uptake kinetics of the untreated soil samples and of organic-free reference samples indicated that the reduction of the wetting rate in water repellent samples is caused by the SOM phase. By means of repeated ^{1}H NMR Relaxometry measurements, which reflect the portions of water in different pore types, it was shown that the wetting process represents a slow redistribution of water molecules from coarse to fine pore types. The phase transition characteristics of the soil water, which were examined by Differential Scanning Calorimetry (DSC), point to stronger bond strengths of water molecules to the solid phase of water repellent than of wettable soil samples. Thus, a decreased freezing enthalpy and lower freezing and melting temperatures were observed for a water repellent sample than for a wettable sample, which was taken next to the water repellent sample and consequently revealed similar soil properties. But, these differences in the phase transition characteristics of water repellent and wettable samples slowly disappeared within several days, after the moisture contents of the samples had been adjusted. Thus, the smaller portions of freezable water in field-moist water repellent soil samples may be a consequence of their usually low water contents.

2.2. Introduction

Under field conditions, soil moisture contents frequently change. Many studies have shown that the water content, the hydration time, and the way of water bonding strongly influence the sorption of organic substances in SOM (Unger et al. 1996; Altfelder et al. 1999; Berglöf et al. 2000; Borisover and Graber 2004; Schaumann et al. 2004). Additionally, the soil moisture kinetics undoubtedly are very important for plant growth. Nevertheless, many aspects of hydration and drying processes are still not understood.

The water vapor uptake of isolated humic and fulvic acids often was analyzed (Shatemirov et al. 1972; Chen and Schnitzer 1976; Chiou et al. 1988). In a relative humidity (RH) of 90 %, Chen and Schnitzer (1976) determined a water content of 23 % for humic acids and of 51 % for fulvic acids at 25 °C. Chiou et al. (1988) calculated for the water vapor sorption of a

humic acid a comparable limiting water content of 25 % at 23 °C. These moisture contents are related to dry mass like all moisture contents in this thesis, if nothing else is stated. However, there is a lack of studies dealing with the hydration of SOM in unfractionated soil samples. It can be assumed that the wetting and swelling processes differ between humic fractions and the complete undisturbed organic soil phase, because within the large macromolecules and molecular associates of solid SOM, the different humic substances are combined with each other. In the distinctly smaller humic and fulvic acid molecules (Scheffer and Schachtschabel 1992; Piccolo 2002), the network structure may be controlled by other types of bondings and by another degree of crosslinking than in the whole SOM. But, the characteristics of this network structure are responsible for the degree of swelling and with that for the hydration kinetics. If the uptake of water from the vapor phase to whole soil samples was studied, mainly high-organic-content soils as peat and muck were used (Orchiston 1953; Rutherford and Chiou 1992; Robens and Wenzig 1996). Based on isotherms of water vapor uptake, Rutherford and Chiou (1992) determined saturation water capacities of 37 % for the SOM of a peat sample and 39 % for the SOM of a muck sample. The studies which deal with the water vapor sorption of mineral soils usually focus on the adsorption of water molecules to the mineral soil matrix (Orchiston 1953; Sharma et al. 1969; Stawinski 1983; Chiou and Shoup 1985; Rhue et al. 1988).

The above mentioned studies describe the gravimetric water uptake from the gas phase. But, under field conditions, the water uptake from the liquid phase may be the dominating process in soil. Presumably, the reached water contents of humous substances are distinctly higher, if the water is supplied via the liquid phase instead of the gas phase. Thus, for solid SOM under field conditions, limiting water contents between 300 % and 500 % are quoted (Scheffer and Schachtschabel 1992). The differences in the water adsorption process between the water uptake via the gas phase and via the liquid phase can be explained by different interfacial tensions between soil and water on the one hand and soil and air which contains gaseous water molecules on the other hand. Additionally, a complete sample wetting and possible swelling processes of the SOM may occur only by water supply via the liquid phase. The lack of studies analyzing the uptake of liquid water into SOM of mineral soils probably is based on the impossibility to transfer common methods to examine sorption and swelling processes of pure materials to SOM, which often amounts to contents below 10 % in mineral soil samples. The different organic matter (OM) contents of mineral soils and peat also cause that the methods which were used to determine the degree of swelling of peat samples by measuring their volumetric expansion (Baes and Bloom 1988; Lyon and Rhodes 1993) are not transferable to SOM in mineral soil samples.

The goal of this study was to analyze the differences in the hydration process between actually water repellent and actually wettable mineral soil samples. Miyamoto et al. (1972) also aimed to detect characteristics of the water adsorption which reflect the soil wettability. But, they did not find differences uniquely related to repellency in the amount of adsorbed water, the shape of the adsorption isotherms, the heat of adsorption, and the integral free

energy of adsorption. Thus, they concluded that the effects of wettability and repellency on the water uptake process may occur at the portion which is beyond the vapor adsorption. Based on this experience and in order to reproduce the moisture conditions in the field, we supplied the water via the liquid phase to the soil samples and compared it to the water uptake from the vapor phase. Since it is known that hydration and drying processes in soil may last up to three weeks (Waksmundzki and Staszczuk 1983; Altfelder et al. 1999; Schaumann et al. 2004), we traced the water uptake of the samples as a function of time during a period of three weeks. For this purpose, three independent methods were applied: Direct gravimetric determination of the water contents, ^{1}H NMR Relaxometry, and Differential Scanning Calorimetry (DSC) analyses of the phase transitions of the soil water.

We assumed that in water repellent soil samples, not only the first wetting of the SOM surfaces, but the whole hydration process of the organic soil matrix proceeds with a smaller rate than in wettable samples, if the water is supplied via the liquid phase. Contrary to liquid water molecules, gaseous water molecules may penetrate into SOM without applying the wetting enthalpy, which would cause that no differences can be observed between the water vapor sorption of wettable and water repellent soils. By measuring the gravimetric water contents in the course of hydration time for the water supply via the liquid phase and via the gas phase, this hypothesis was investigated. In order to ascertain, if the observed hydration differences between the samples can be attributed to differences in the SOM phase, organic-free reference samples were incorporated into the study.

Since the degree of wettability and swelling determines the way of water bonding arising after soil moistening (Schaumann et al. 2004; Schaumann et al. 2005a), water in water repellent soils should be bound differently than in wettable soils. Probably, in addition to the bulk water, a part of the water in water repellent soils is enclosed in fine pores (Berezin et al. 1973; Pfeifer et al. 1985), bound as gel water in SOM (Quinn et al. 1988; Tsereteli and Smirnova 1992), or as hydrate water (Nishinari et al. 1997; Ping et al. 2001). DSC measurements of the freezing, melting, and evaporation processes in the soil samples and ^{1}H NMR Relaxometry analyses (Schaumann et al. 2005a) were performed to examine, if the bond strengths of sorbed water molecules really differ between water repellent and wettable soil samples. Especially, the portions of unfreezable water in the samples were used as an indicator for the mean bond strength of the soil water (Quinn et al. 1988; McBrierty et al. 1996; Nishinari et al. 1997). NMR measurements additionally were carried out, because the ^{1}H NMR relaxation times reflect the mobility of water molecules within the pore system of the soil samples and with that the degree of interactions between the sorbed water and the solid soil phase. In order to examine, if differences in the water bonding depend on different moisture contents of water repellent and wettable samples, the DSC and NMR measurements also were performed at several points of time after adjusting the water contents of the samples.

Previous studies have shown that wetting as well as swelling kinetics of soil samples can be observed by ^{1}H NMR relaxation measurements (Todoruk et al. 2003a; Schaumann et al. 2005a). The swelling process is linked with a shift of the peak positions in the relaxation time

distributions, while the wetting process is reflected by slow changes of the water portions between different ranges of relaxation times (Schaumann et al. 2004; Schaumann et al. 2005a). By ^{1}H NMR Relaxometry, a differentiation of the wetting kinetics between wettable and water repellent samples is possible: For wettable samples, the wetting of all pore types occurs directly after sample moistening, whereas for water repellent samples, the time constants of the first-order wetting process amount up to several days (Todoruk et al. 2003b; Schaumann et al. 2005a). The time constants of the first-order swelling process derived from ^{1}H NMR relaxation (Schaumann et al. 2004; Schaumann et al. 2005a) are of the same size of order as the time constants of the wetting process of water repellent samples. In this study, the question, if swelling processes occur besides the wetting processes in the analyzed soil samples should be answered by the evaluation of the changes in the NMR relaxation time spectra in the course of sample hydration.

2.3. Experimental Section

2.3.1. Soil samples

The soil samples were taken in the inner-city park Tiergarten, which has been created between the 17th and the 20th century. This location reveals a high small-scale heterogeneity of soil properties. Especially, the wettability changes within few centimeters from easily wettable regions to spots with strong water repellency. A further description of this site is given by Schaumann et al. (2005a) and in Chapter 3.3.2. From the humous upper layer (10 - 30 cm) of this location, four samples T1-T4 with comparable C_{org} contents were taken directly side by side (maximal 1 m distance between them). The samples T1 and T3 were strongly water repellent, while the samples T2 and T4 were easily wettable. Tab. 2.1 summarizes the soil properties of these samples. The samples were used in the field-moist as well as in the air-dried state. Before the measurements, the air-dried samples were equilibrated at least for three weeks in a defined relative humidity of 31 % over saturated $CaCl_2$ solution. Additionally, subsamples were ashed for 2 h at 550 °C and used as organic-free reference samples.

Tab. 2.1. Characterization of the soil samples (WDPT: water drop penetration time, OM: organic matter content). The soil texture does not vary between the four samples.

	T1	T2	T3	T4
wettability behavior	water repellent	wettable	water repellent	wettable
WDPT (actual repellency)	3:18 h	0 s	> 5 h	0 s
grav. water content [%] (field-moist)	12.2	30.2	13.0	29.8
OM [%]	7.6	8.8	7.7	7.2
pH	3.7	5.0	3.7	4.9
sand [%]	85			
silt [%]	11			
clay [%]	4			

In order to study the water uptake process, specific amounts of water were added to the soil samples. By means of a micro-syringe, small water droplets were distributed within the whole samples. With this method, a homogeneous wetting without disturbing the water uptake process by stirring the samples was achieved.

2.3.2. Gravimetric water uptake

For analyzing the water uptake process of the soil samples T1 and T2, two methods were applied. By one method, the water sorption of the air-dried samples via the gas phase was studied. For this purpose, water-saturated air was routed through a closed perspex sample chamber (99 % relative humidity). Square plastic containers (3 cm x 3 cm, 0.5 cm height) containing (1.5 ± 0.2) g of the soil samples in 3 mm layers were placed into the sample chamber. The other method operated with a water supply via the liquid phase. A ceramic plate (2 bar air entry value, standard flow, Soilmoisture, Santa Barbara, CA, USA) was placed into a water saturated sand bed. By circular perspex containers (4 cm diameter, 1 cm height) with paper filters at their bottoms, which contained (2.5 ± 0.8) g of the air-dried soil samples in 3 mm layers, a close contact to the ceramic plate was ensured. Different from the common use of ceramic plates in pF measurement equipments, the water was supplied under atmospheric pressure to the samples. For both methods, the gravimetric water contents of the samples were determined at several points of time in the course of sample hydration at 20 °C. Two measurement replications were carried out for each sample.

2.3.3. Phase transitions in the course of water uptake

The processes of freezing, melting, and water evaporation were analyzed for the samples T1 and T2 in the field-moist state and after adjusting specific moisture contents in these samples. On the one hand, sample T1 was moistened to the field-moist water content of sample T2 (30.2 %). On the other hand, both samples T1 and T2 were moistened to a distinctly higher moisture content of 55.0 %. All these three moistened samples were stored for three weeks in a climatic chamber at 20 °C. During this period of time, subsamples were taken at several points of time and used for the phase transition measurements, which were performed with two replications.

The phase transitions were analyzed with the Mettler Toledo DSC 822e (Mettler Toledo, Germany) with an intracooler and nitrogen as purge gas (80 mL min^{-1}). 20 to 30 mg of the samples were placed into a 40 µL standard aluminum crucible. The DSC measurements of the freezing and melting processes were carried out in closed crucibles, while before the evaporation measurements, holes were punched into the lids of the crucibles. For analyzing the freezing and melting, the samples were cooled from 25 °C to -30 °C with a rate of 2 K min^{-1} and after that heated to 15 °C with the same rate. This small rate was used in order to minimize kinetic effects, which strongly influence the freezing and melting peaks in DSC thermograms. The water evaporation from out of the samples was measured by heating from

25 °C to 180 °C with a rate of 10 K min^{-1}. The evaluation of the phase transitions was performed by the STAR^e software (Mettler Toledo). For a further characterization of the peaks, Origin 6.1 (OriginLab, Northampton, MA, USA) was used.

In order to examine, which thermal events in the DSC thermograms are linked with a mass loss of the samples, thermogravimetry (TG) measurements additionally were conducted with a Mettler Toledo STGA 851e thermogravimetric system (Mettler Toledo, Switzerland) under dry air (200 mL min^{-1}). 0.5 to 0.6 g of the sample were placed into a ceramics crucible. An crucible filled with Al_2O_3 was used as reference. The sample was heated with 5 K min^{-1} from 25 °C to 950 °C. In the resulting thermograms, the proportional weight loss (DTG signal) is plotted as a function of temperature. The evaluation of the TG curves was performed with the Thermal Advantage V4.0 software (TA Instruments, Germany).

2.3.4. NMR study of the wetting kinetics

The NMR study has already been published by Schaumann et al. (2005a). The following paragraph contains a summary of the experiments which is necessary to understand the discussion in this thesis.

In the course of sample hydration, the distribution of the water molecules within the pore volume was analyzed by ^{1}H NMR Relaxometry. The field-moist samples T3 and T4 were filled into NMR containers with a circular cross-section (3 cm diameter, 4.5 cm height). Directly before starting with the measurements, the samples were moistened in these containers to a moisture content of 54 %. Within the next 20 days, the samples were stored at 20 °C, and at several points of time, they were subjected to NMR measurements. The measurements were carried out with a 2 MHz Relaxometer (Maran 2, Resonance Instruments, Witney, UK). The transversal relaxation time T_2 was measured by the CPMG (Carr-Purcell-Meiboom-Gill) pulse sequence (Meiboom and Gill 1958) with an interecho spacing t of 150 µs. For each relaxation decay curve, 64 scans were recorded. The NMR measurements were performed with two replications for each sample.

The proton relaxation time in a pore system is composed by the surface relaxation time T_S within the distance l of the pore walls and the bulk relaxation time T_B (Hinedi et al. 1997):

$$\frac{1}{T} = \frac{\lambda \cdot S}{T_S \cdot V} + \frac{1}{T_B} \qquad (2.1)$$

where V and S are the volume and the surface area of the water filled pores.

The NMR data evaluation was performed with the WinDXP software (Resonance Instruments, Witney, UK). A sum of 256 exponential decay functions was fitted by an inversion algorithm to the measured relaxation decays. By choosing a weight factor of 20, which considers the signal to noise ratio, a compromise between a sufficient peak separation and a physically reasonable water distribution was achieved (Schaumann et al. 2005a). The fitting procedure results in a distribution of relaxation times, indicating the amplitudes for all the 256

relaxation times. Each amplitude is proportional to the amount of water relaxing with the corresponding relaxation time, and the sum of all amplitudes is proportional to the total amount of water in the sample. In order to be able to quote the portions of water belonging to distinct relaxation times, the relaxation time distributions were normalized to the sum of all amplitudes, i.e. to the total amount of water. According to the evaluation method of Schaumann et al. (2005a), the distributions then were divided into four regions, which were assigned to different pore types (type I: 0 - 15 ms, type II: 15 - 90 ms, type III: 90 - 600 ms, type IV: > 600 ms). These pore types represent different pore sizes and different bond strengths of the water molecules in the pores. Based on the surface relaxivities given by Hinedi et al. (1997) for silica and assuming a cylindrical pore system, Schaumann et al. (2005a) estimated that pore type I should mainly consist of intraparticle micropores < 0.5 nm and interparticle mesopores < 180 nm. The pore type IV represents the free water in macro-pores. Due to the influence of the characteristics of the internal pore surfaces (l) and the pore geometry (V, S), it is not possible to assign unambiguous pore sizes to the measured relaxation times, but the development of the water distribution in the different pore types can be observed in the course of hydration time. The proportion of water belonging to one of these pore types was calculated by adding all amplitudes within the corresponding range of the relaxation time distribution.

2.4. Results und Discussion

2.4.1. Gravimetric water uptake

The water uptake in the course of time for the air-dried soil samples T1 and T2 and for their air-dried organic-free references is shown in Fig. 2.1. The curve progression of the water uptake via the gas phase is comparable to that of a loess observed by Waksmundzki and Staszczuk (1983). For both, the water supply via the liquid phase and via the gas phase, the untreated soil samples reached higher water contents than their reference samples. For the untreated soil samples, the hydration process via the liquid phase was slow and resulted in water contents above 80 %. Contrary to that, the hydration process via the gas phase was fast and resulted in water contents between 3 and 4 % for the untreated samples, indicating an incomplete sample wetting.

It is not possible to calculate plausible water contents for the SOM phase of the samples by assuming that the mineral phase of each sample sorbed the same content of water as the ashed reference sample. This approach results in negative values for the SOM moisture contents for all points of time. Most probably, the sample ashing at 550 °C causes changes at the mineral surfaces (Kaiser and Guggenberger 2003) with the consequence of an increased water uptake in comparison with the mineral compounds in the untreated samples. Additionally, new pores between the mineral particles are created by ashing their organic coatings, and these new pores may absorb a comparable amount of water as the SOM coatings of the untreated samples. Thus, the water uptake by the organic substances of the samples only can be

estimated by assuming that all the water was sorbed by the SOM phase. Then, for the water supply via the liquid phase, the final moisture contents of SOM would be (1130 ± 30) % for T1 and (1500 ± 300) for T2. For the water supply via the gas phase, the final moisture contents would be (43 ± 4) % for T1 and (35 ± 1) % for T2. These values are comparable to the limiting moisture contents determined by Rutherford and Chiou (1992) for the water vapor sorption to SOM of peat and muck samples, and they are between the calculated values for fulvic and humic acids (Chen and Schnitzer 1976; Chiou et al. 1988). Consequently, our results do not confirm the hypothesis of pronounced differences between the water uptake of isolated humic fractions and solid SOM in unfractionated soil samples for the water vapor sorption. However, they support the assumption of distinctly higher water contents for the water uptake from the liquid phase in comparison with the water uptake via the gas phase.

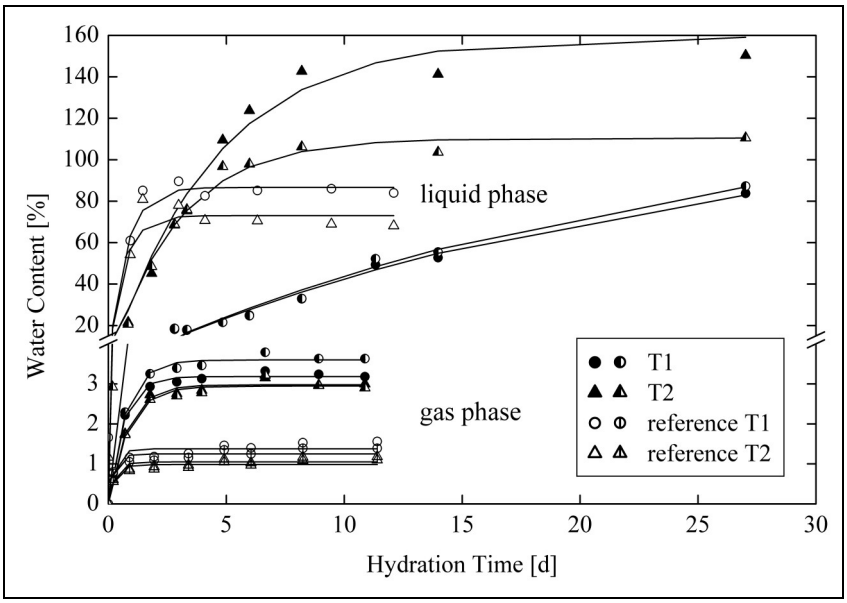

Fig. 2.1. Water uptake of the air-dried samples T1 and T2 and their organic-free references (two replications for each sample). Shortly after starting the experiment, the water contents of all samples which were moistened via the liquid phase proceed above the axis break, while the water contents of all samples which were moistened via the gas phase remain below the axis break.

In order to examine, if the hydration process can be described by first-order kinetics, exponential functions were fitted to the curve progressions of the water contents *Q*:

$$\Theta = A \cdot \left(1 - e^{-t/\tau}\right) \tag{2.2}$$

Tab. 2.2 lists the final water contents *A* and the time constants *t* for the studied samples. For the water supply via the liquid phase, the water uptake process was significantly slower for the water repellent sample T1 than for the wettable sample T2. Contrary to the other samples, the hydration process was not completed after three weeks for the sample T1 (Fig. 2.1). The water uptake via the gas phase revealed no rate difference between the samples T1 and T2.

For both moistening methods, the hydration rates were smaller for the untreated samples T1 and T2 than for their reference samples.

The water uptake process of the untreated samples via the liquid phase cannot be described as a sum of the mineral and the organic phase assuming that the time constant of the mineral phase is similar to that of the reference sample. On the one hand, the fitting results indicate a dependency among the fitting parameters, if a sum of two exponential functions is used to describe the data points of the water uptake of T1 and T2 from the liquid phase. On the other hand, non of the calculated time constants does agree with the time constants of the reference samples, if a sum of two exponential functions nevertheless is fitted to the data. This also may be based on alterations of the mineral soil matrix due to sample ashing.

Tab. 2.2. Final water contents *A* and time constants *t* of the exponential functions fitted to the water contents as functions of hydration time. The errors were calculated on the basis of the difference between the measurement replications.

	via liquid phase		via gas phase	
	A	*t* [d]	*A*	*t* [d]
T1	124 ± 9	23 ± 1	3.4 ± 0.4	0.7 ± 0.1
T2	140 ± 50	4 ± 2	3.0 ± 0.1	0.8 ± 0.1
T1 reference	87 ± 3	0.7 ± 0.1	1.3 ± 0.1	0.3 ± 0.1
T2 reference	73 ± 4	0.6 ± 0.2	1.0 ± 0.1	0.3 ± 0.1

In all, the results of the gravimetric water uptake experiments indicate a very slow wetting as rate-limiting process in the water repellent sample T1 in comparison with the wettable sample T2. It can be assumed that this slow wetting process is linked to the SOM, because for the organic-free reference samples, the hydration proceeds with a significantly faster rate, which does not differ between the reference samples of T1 and T2. For the water supply via the gas phase, the fast hydration rates, which are comparable for all the samples, point to the absence of a wetting process of SOM by this moistening method, which is in accordance with the assumptions of Miyamoto et al. (1972). Either, the gaseous water molecules can penetrate into the SOM structure without applying the wetting enthalpy. Or, the organic soil matrix mainly remains dry, and only the mineral surfaces are wetted, if the water is supplied via vapor intrusion. Moreover, differences in the water diffusion rates between the water sorption via the gas and via the liquid phase cannot be excluded due to slightly different sizes of the sample layers and different degrees of compactness as well as an effective relative humidity below 100 % for the water uptake from the gas phase.

2.4.2. Phase transitions in the course of water uptake

Fig. 2.2 shows all phase transitions of the field-moist and moistened T1 and T2 samples. For a better comparability, the DSC heat flows are standardized to the amounts of water in the samples. The main differences between the field-moist samples are the lower transition temperatures of all phase transitions in the water repellent sample T1 (0.5 °C, 0.9 °C, and

36 °C onset temperature difference to T2 for freezing, melting, and evaporation, respectively) and the additional peak at 145 °C after the main evaporation peak for T1. Thermogravimetry measurements have shown that this additional peak is connected to a weight loss (Fig. 2.3), pointing to the evaporation of a small amount of water at a higher temperature than the main water portion of this sample. However, further studies examining, if the TG weight loss at this temperature is really caused by water, have to be carried out in order to determine unambiguously the origin of the peak. The temperature differences of this peak between the DSC and the TG measurements (peak maximum at (145 ± 1) °C in the DSC thermogram and at (133 ± 1) °C in the TG thermogram) may be caused by the different heating rates.

The peak areas of the freezing and melting processes represent another difference between the field-moist samples: They are distinctly smaller for T1, indicating that a part of the water of this sample is unfreezable due to tight bondings (Quinn et al. 1988; McBrierty et al. 1996; Nishinari et al. 1997).

With increasing water content, the freezing exotherm becomes broader and shows a composite structure in the form of resolved component peaks for both samples (Fig. 2.2, left), probably caused by different degrees of mobility of the water molecules. Surprisingly, this composite structure occurs for the freezing and not for the melting peak, which contradicts observations for peat samples (McBrierty et al. 1996; Schaumann 2005). After moistening, the melting temperature, the enthalpy, and the curve progression of the melting process of the sample T1 approach to the melting of the sample T2. For the evaluation of the freezing temperatures, the melting peaks are more suitable than the freezing peaks, because during the freezing, the DSC temperature protocol counteracts the heat evolution of the exothermic freezing process, resulting in non-reproducible temperatures in the samples. In addition, the absorbed water in the soil samples may cause a supercooling resulting in a depression of the freezing temperature (Quinn et al. 1988; McBrierty et al. 1996). The occurrence of the melting peaks above 0 °C is in accordance with the results for peat samples by McBrierty et al. (1996) and Schaumann (2005). Schaumann (2005) proposed the formation of a glassy amorphous phase of water and peat during the DSC cooling, which then may serve as a melting barrier in the heating cycle.

The main evaporation peak of T1 shifts to the peak of T2 after moistening the sample (Fig. 2.2, right). With increasing amounts of water in T1, the area of the additional peak at 145 °C of this sample decreases. For T1 and T2, the curve progression of the evaporation endotherm differs between the field-moist and the 30.2 % water content samples on the one hand and the 55.0 % water content samples on the other hand: The sharper peak form for the higher water content is linked with a higher evaporation rate and a higher portion of water which evaporates above 100 °C.

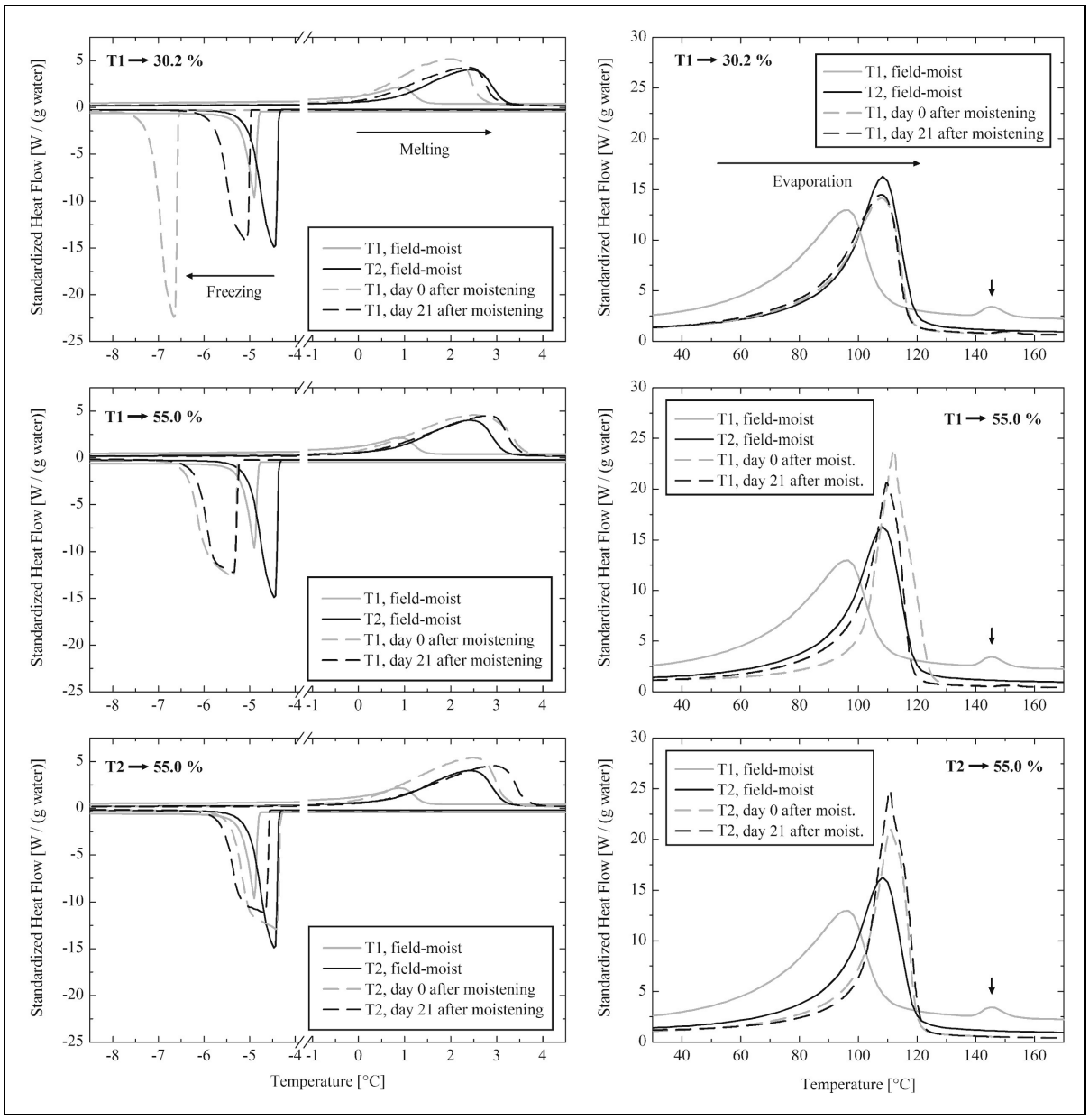

Fig. 2.2. Freezing and melting process (left) and water evaporation (right) of T1 after moistening to water contents of 30.2 % (top) and 55.0 % (middle) and of T2 after moistening to a water content of 55.0 % (bottom). In all graphs, the field-moist T1 and T2 samples are included for comparison. The arrow to the evaporation curve of the field-moist T1 sample indicates an additional evaporation peak.

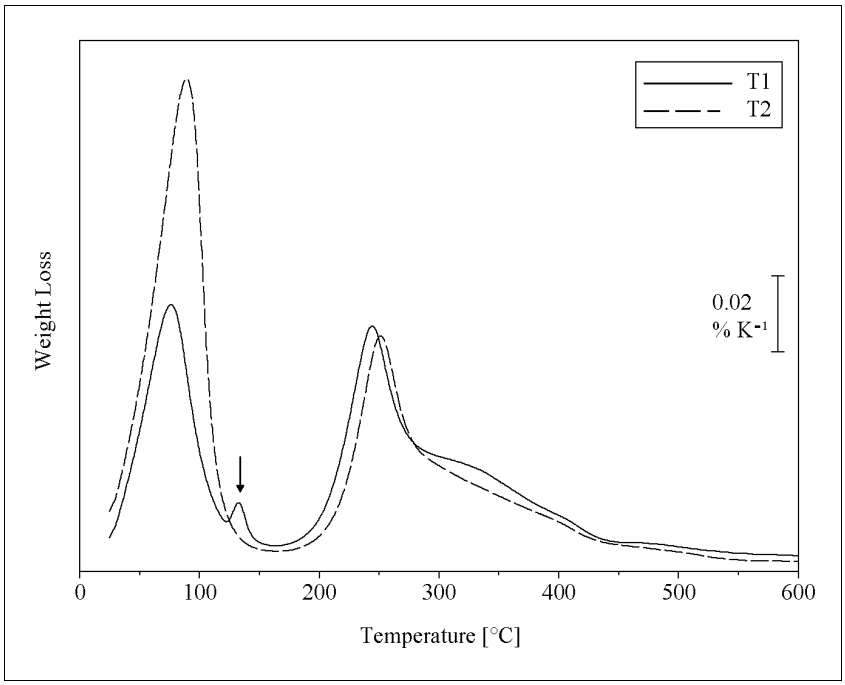

Fig. 2.3. Thermogravimetry of the air-dried samples T1 and T2. The arrow to the thermogram of the T1 sample indicates an additional peak at (133 ± 1) °C.

Fig. 2.4 shows that all freezing enthalpies of soil water are smaller than the heat of fusion of free water, which is 333.5 J g^{-1} (Landoldt-Börnstein 1982). Because of a higher proportion of unfreezable water, the water repellent samples exhibit smaller enthalpies than the wettable samples. By the higher proportions of unfreezable water, the hypothesized stronger bondings of the water molecules in water repellent samples than in wettable samples are supported. For the moistened samples, the freezing enthalpies are higher than for the field-moist samples indicating a higher amount of free or loosely bound water just after sample moistening. The studies of McBrierty et al. (1996) and Schaumann (2005) show linear correlations between water contents and freezing enthalpies for individual peat samples, for which the water contents were changed. These observations agree with the assumption that the deviation of the water repellent and the freshly moistened samples from the linear trend (Fig. 2.4) is based on the different water states in these samples.

The water content of (1.3 ± 0.6) % (related to wet sample mass) which is linked to freezing and melting enthalpies of 0 J g^{-1}, corresponds to the intersection of the two regression lines (Fig. 2.4). This water content may serve as a measure for the amount of unfreezable water in the field-moist samples from the locations Tiergarten and Buch (see Chapter 3.3.2).

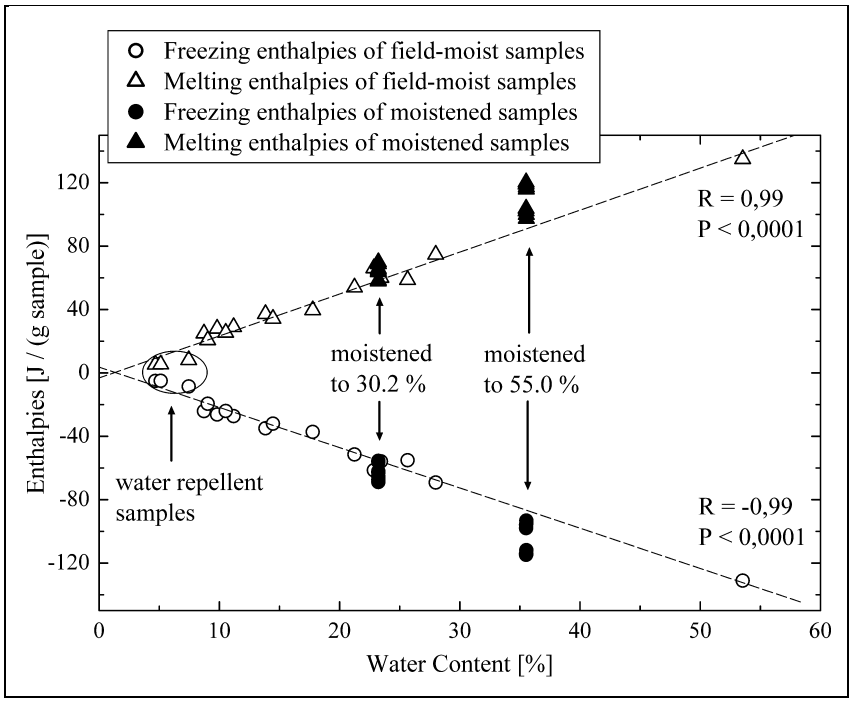

Fig. 2.4. Freezing and melting enthalpies of samples from the locations Tiergarten and Buch (Chapter 3.3.2; Täumer et al. 2005) as a function of the water content (related to wet sample mass). Additionally to the field-moist samples, the moistened T1 and T2 samples are included in the graph (15 min, 2 days, 7 days, and 21 days after moistening). All field-moist water repellent samples are edged with a circle. The linear regressions were performed only for the field-moist samples.

After the samples had been moistened, the standardized freezing enthalpies decreased in the course of time (Fig. 2.5), which may be caused by a slow bonding of the added water molecules to the soil matrix. Due to the higher water contents after moistening, the small original enthalpies of the field-moist samples were not reached again. The comparison with a sand-water mixture (Fig. 2.5) indicates that the organic matter in the studied sandy soils most probably is responsible for the decreased freezing enthalpies linked to bound water. The curve progressions of the enthalpies after sample moistening (Fig. 2.5) as well as of the onset temperatures, the peak heights, and the peak symmetry characteristics (degree of fronting or tailing) of all phase transitions (not shown) reveal irregularities between 2 and 7 days, probably based on a change of the of bonding status of the water in the soil samples. For the samples which had been moistened to 55.0 % water content, these irregularities are more pronounced than for the T1 sample moistened to 30.2 % water content.

The differences of the standardized freezing enthalpies also can be interpreted in another way: In the field-moist state, the smaller freezing enthalpy of the water molecules in the water repellent sample T1 than in the wettable sample T2 can be based on higher salt concentrations in the soil water of T1 as a consequence of its lower water content. According to this explanation, the dilution of the soil solutions by the abrupt increase of the water contents in both samples after water addition may have caused the risen freezing enthalpies. Then, in the course of hydration time, a slow dissolution process of additional ions could have been the

reason for the slowly decreasing standardized enthalpies. On the basis of our present results, different salt concentrations as well as different bond strengths of the water molecules may cause the differences in the freezing enthalpies of the soil samples. Future studies including ^{1}H solid-state NMR to elucidate the way of water bonding to the soil matrix are necessary in order to differentiate between these two possible factors of influence.

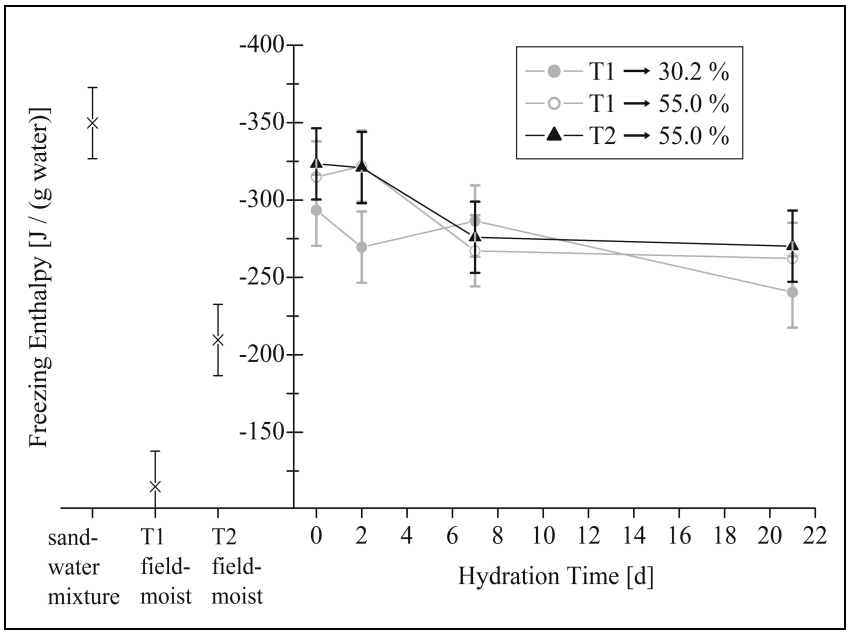

Fig. 2.5. Standardized freezing enthalpies of the moistened samples T1 and T2 in the course of hydration, of the field-moist samples T1 and T2, and of a quartz sand-water mixture (19.0 % water content related to dry sample mass). The errors were calculated on the basis of the difference between the measurement replications.

After 2 days of hydration time, the curve progressions of the freezing enthalpies of both samples moistened to 55.0 % water content are comparable. The same was observed for the peak heights and the onset temperatures of the phase transitions (not shown). Consequently, the adjustment of the water contents in the samples T1 and T2 causes that the phase transition characteristics of the samples approach each other. If it is assumed that the phase transitions mainly reflect the bond strength of the water molecules in the samples and that the salt concentration represents only a minor factor of influence, the adjustment of the water contents results in comparable mobility of the water molecules due to a similar degree of interactions with the solid soil phase.

In summary, the phase transitions of the soil water point to the existence of different bond strengths of water molecules in the soil samples. A part of the soil water probably is bound very tightly to the SOM, so that it is unfreezable. In the field-moist state, this water proportion is higher for T1 than for T2. The hypothesis that the mean bond strength of water molecules is higher in the water repellent sample T1 than in the wettable sample T2 also is supported by the additional evaporation peak at 145 °C and the lower freezing and melting temperatures (Berezin et al. 1973; Pfeifer et al. 1985; Nishinari et al. 1997; McBrierty et al. 1999; Ping et

al. 2001). In this connection, Ping et al. (2001) divided the freezable water into bulk-like water and freezable-bound water, which crystallizes at lower temperatures than the bulk-like water. By adjusting the water contents of the samples T1 and T2, the differences in the phase transition characteristics could be compensated within 21 days. Consequently, the different bond strengths of the water molecules are most probably based on the different water contents and not on the different wettability properties of the field-moist samples. After moistening the samples, the added water has a higher mobility than the water which has been in the samples before. The composite structure of the freezing exotherms after sample moistening may reflect these two degrees of water mobility. The subsequent decrease of the freezing enthalpy in the course of hydration indicates a slow bonding process of the additional water molecules to the soil matrix. This process does not differ between the samples T1 and T2. Thus, the decreasing freezing enthalpies during sample hydration probably do not reflect the wetting process, but possibly are based on a slow swelling process of SOM, which may occur in both samples irrespective of their wetting properties (Schaumann et al. 2005a).

2.4.3. NMR study of the wetting kinetics

Contrary to the wettable sample T4, the NMR relaxation time distribution of the water repellent sample T3 shows a high portion of free water (type IV) directly after moistening (Fig. 2.6, Schaumann et al. 2005a). In the sample T3, the remaining water apart from the bulk water peak reveals relaxation times which are on average smaller than for the sample T4 (for the relaxation time range below 200 ms, mean relaxation time of (7 ± 2) ms for T3 and (32 ± 2) ms for T4). This may reflect stronger mean bond strengths of the water molecules which were already existent in the field-moist samples before moistening in the water repellent sample than in the wettable sample, as also indicated by the phase transition characteristics. Thus, the NMR results support the assumption that the differences in the standardized freezing enthalpies between the field-moist samples may be based on different degrees of water bonding to the solid phase and not on different salt concentrations. Otherwise, the concentration of paramagnetic substances reducing the relaxation times also has to be significantly higher in the water repellent sample T3 than in the wettable sample T4. However, differences in the pore size distribution or the composition of the mineral matrix likewise can explain the different mean relaxation times apart from the free water.

Compared with the wettable sample T4, the NMR relaxation time distributions of the water repellent sample T3 strongly changed after the sample moistening (Fig. 2.6, Schaumann et al. 2005a). 15 min after adding the water to T3, free water represented the main portion, whereas after a hydration time of three weeks, the main portion of water has shifted to the pore types I-III. On the other hand, the distributions of T4 show only a very small shifting to smaller relaxation times in the course of hydration (Schaumann et al. 2005a).

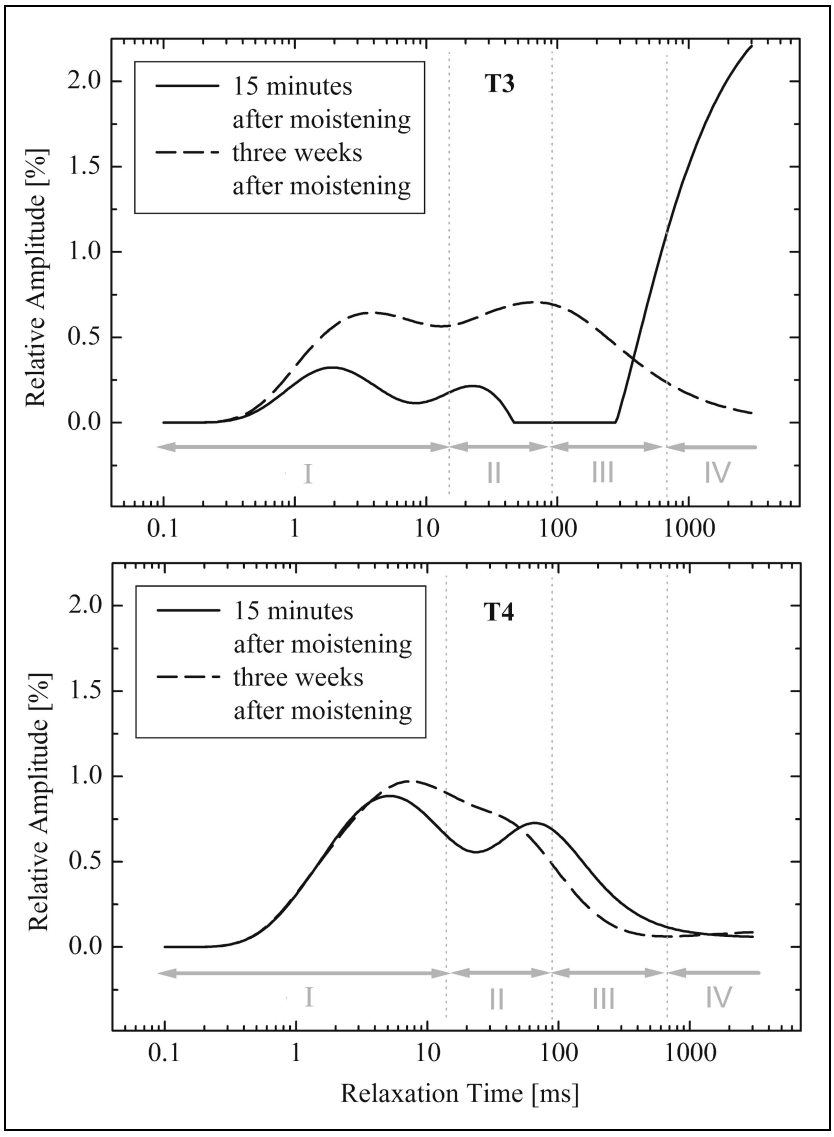

Fig. 2.6. ^{1}H NMR relaxation time distributions of the samples T3 and T4 recorded 15 min and three weeks after moistening the samples to 54 % water content (Schaumann et al. 2005a). Below the distributions, the relaxation time ranges assigned to the four pore types are indicated.

For both samples, the peak positions did not move significantly during the hydration process. By the NMR measurements, consequently no swelling process of SOM, linked with changes of the pore sizes, the thickness of the layer l where surface relaxation is the dominating process, or the mobility of the water molecules in the bulk phase, was observed (Schaumann et al. 2005a).

Fig. 2.7 shows the percentages of water in the pore types as a function of hydration time. Different from the water repellent sample T3, no significant changes of the water distribution in the pore types occurred after moistening the wettable sample T4. According to Schaumann et al. (2005a), the changes of the amounts of water in the different pore types of the sample T3 can be fitted by exponential functions of the form:

$$y = A_1 \cdot \left(1 - e^{-t/\tau_1}\right) + A_2 \cdot e^{-t/\tau_2} \tag{2.3}$$

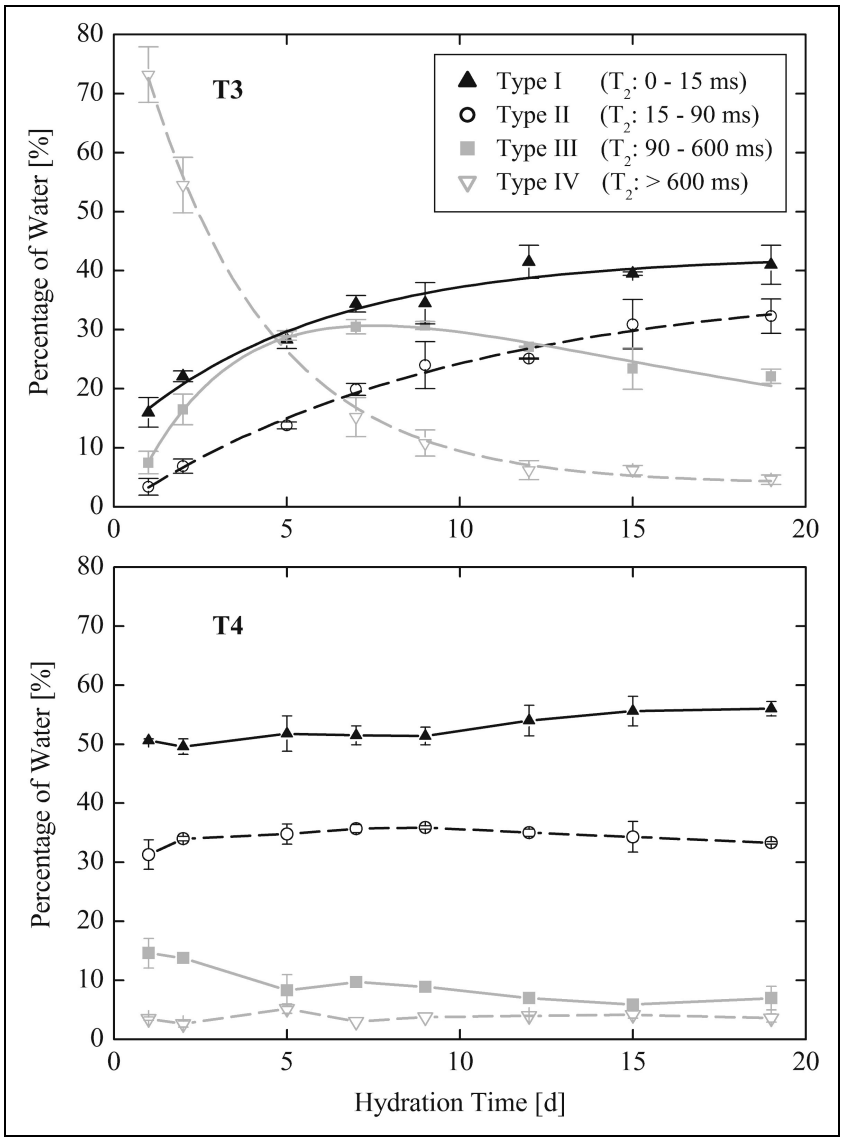

Fig. 2.7. Percentages of water in the different pore types in the course of hydration time for the samples T3 and T4 (Schaumann et al. 2005a). For the sample T3, the water portions as a function of hydration time were fitted by exponential functions (one exponential function for the pore types I, II, and IV, a sum of two exponential functions for pore type III). For the sample T4, the data points are connected by straight lines. The errors were calculated on the basis of the difference between the measurement replications.

After moistening, the water percentages in pore types I and II increase with time constants t_1 of (6 ± 1) d and (10 ± 2) d, respectively (Schaumann et al. 2005a). The water portion in pore type IV decreases with a time constant t_2 of (3.6 ± 0.3) d (Schaumann et al. 2005a). The curve progression of the water percentage in pore type III can be described by a sum of two exponential functions with t_1 of (3.5 ± 0.9) d for the increase and t_2 of (16 ± 4) d for the decrease (Schaumann et al. 2005a). Thus, the free bulk water (type IV) slowly moves to the smaller pores of type I and II. The medium-sized pores of type III act as an intermediate storage for the water in this process. The time constant of the initial increase of the amount of water in this pore type corresponds to the time constant of the decrease of the bulk water. The

wetting process of the water repellent sample consequently represents a slow redistribution process of water between the different pore types, beginning in the coarse and ending in the fine pores (Schaumann et al. 2005a).

In order to gain a more comprehensive understanding of the wetting process, the NMR results of the samples T3 and T4 were compared to the results for the freezing enthalpies of the samples T1 and T2. Because of the direct proximity of the samples in the field and their similar properties (Tab. 2.1), a comparability of the water repellent samples T1 and T3 as well as of the wettable samples T2 and T4 can be assumed.

By means of the freezing enthalpies of the soil water (Fig. 2.5) and the heat of fusion of free water of 333.5 J g^{-1} (Landoldt-Börnstein 1982), the portion of unfreezable water was determined and related to the dry mass of the samples. In both samples T1 and T2, the proportion of unfreezable water abruptly decreases after sample moistening (from (65 ± 3) % to (5 ± 3) % in T1 and from (36 ± 3) % to (2 ± 3) % in T2). In the course of hydration, the amount of unfreezable water increases from (0.02 ± 0.01) to (0.11 ± 0.01) g / (g dry mass) in the water repellent sample T1 and from (0.01 ± 0.01) to (0.11 ± 0.01) g / (g dry mass) in the wettable sample T2.

For both the water repellent and the wettable samples, the development of the amount of unfreezable water and of the amount of water in pore type I during the hydration process show differences (Fig. 2.8). While the portion of water in pore type I gradually increased after moistening the water repellent sample, the amount of unfreezable water abruptly rose between 2 to 7 days of hydration time (Fig. 2.8, top). In the wettable sample, the water immediately wetted the pores of type I, so that the amount of water in these pores did not change any more in the subsequent time. The portion of unfreezable water, however, only reached a constant value after 2 days of hydration time (Fig. 2.8, bottom). These divergences of the changes of the portions of unfreezable water in the course of time from the changes of the portions of water in pore type I show that the amount of unfreezable water reflects the wetting process only indistinctly. For the water repellent sample, the slow increase of water in pore type I represents a direct measure for the alterations of the surface properties of the inner pore walls. Due to hydrophobic properties of the pore walls, at first, the water only penetrated into the coarse pores. As a result of the contact with water, the surface properties have changed gradually, allowing the water to penetrate slowly into finer pores. At the same time, the proportion of unfreezable water increased. But, the differences between the development of the freezing and the NMR data indicate that the unfreezability of a part of the soil water cannot be explained solely by its inclusion in fine pores.

In the wettable and the water repellent samples, the amounts of water in pore type I were higher for all points of time than the amounts of unfreezable water (Fig. 2.8). The presented differences even may be too small, because of a possible overestimation of the percentage of unfreezable water by the used method (Kuntz and Kauzmann 1974; Quinn et al. 1988). The overestimation may occur, because the heat of fusion of freezable water in hydrated systems is not constant, and the value of 333.5 J g^{-1} for pure water only represents the upper limit

(Kuntz and Kauzmann 1974). If a smaller heat of fusion is assumed for the freezable soil water due to its interactions with the solid soil phase and particularly due to dissolved salts and DOM, the calculated amounts of unfreezable water would become smaller and consequently the differences to the amounts of water in pore type I would be higher. A part of the difference between the unfreezable water and the water in pore type I also can be attributed to the use of the different samples. However, the soil properties of both water repellent and both wettable samples are so similar (Tab. 2.1), that their influence most probably can be neglected.

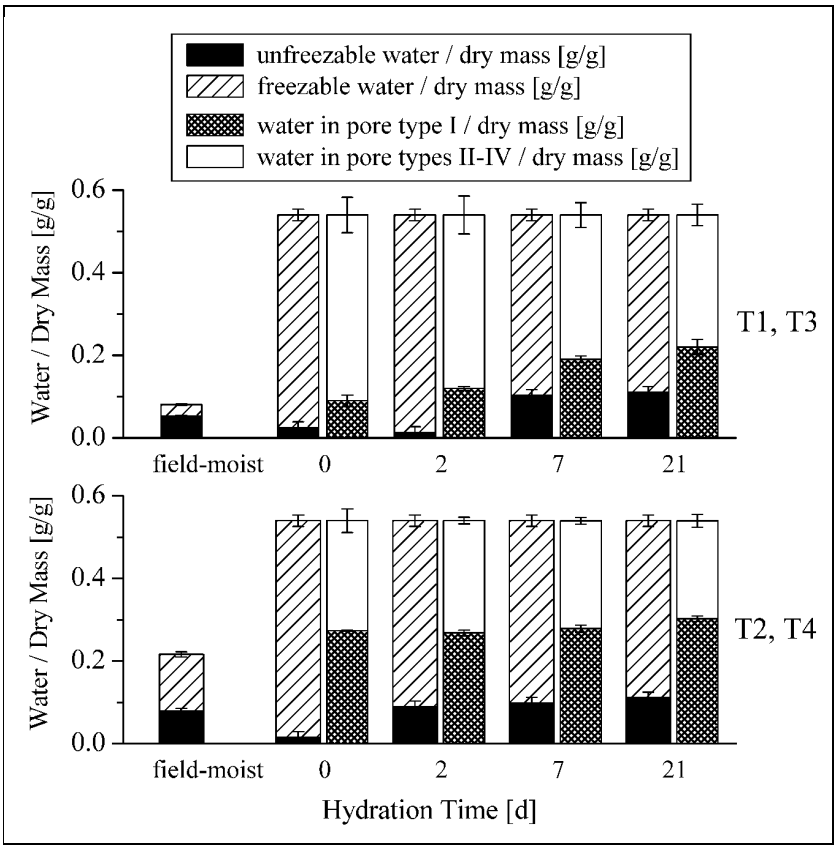

Fig. 2.8. Comparison of the amounts of unfreezable water and of water in pore type I in the course of hydration for the water repellent samples T1 and T3 and the wettable samples T2 and T4 after moistening them to 54 % or 55 % for the NMR and the DSC measurements, respectively. The errors were calculated on the basis of the difference between the measurement replications.

Contrary to the assumptions deduced from the comparable development of the freezing enthalpies of the wettable and the water repellent samples in the course of hydration, no changes of the pore sizes, characteristic for swelling processes, could be detected by the NMR measurements. But, the relaxation distributions showed differences in the water distribution in different pore types as a function of hydration time between the samples T3 and T4, indicating that the wetting process represents a redistribution of water molecules between different pore types (Schaumann et al. 2005a). According to the NMR results, initially, the walls of the pore types I-III of water repellent samples reveal hydrophobic characteristics.

After moistening the samples, water molecules can penetrate gradually into finer pores and with that alter their surface tensions. This slow change of the wetting behavior of the pore walls can be explained with water-induced conformational changes of SOM, as the reorientation of hydrophobic and hydrophilic molecule groups (Ma'shum and Farmer 1985; Valat et al. 1991; Roy et al. 2000). The development of non-freezable water proceeds simultaneously to the penetration of water into the small pore types. Possibly, the inclusion of water molecules in fine pores is partially responsible for the increase of unfreezable water in the course of the hydration process (Berezin et al. 1973; Pfeifer et al. 1985). But, other mechanisms, as chemical bonding of water to the solid soil matrix, also can contribute to a decreased mobility and consequently to a non-freezable status of a part of the water molecules (Quinn et al. 1988; Tsereteli and Smirnova 1992; Nishinari et al. 1997; Ping et al. 2001). The existence of different mechanisms causing unfreezability of soil water may be the reason for the differences partially occurring in the course of hydration between the development of unfreezable water and the development of the amount of water in small pore types (Fig. 2.8).

For the studied water repellent samples, the measured time constants of the gravimetric water uptake and of the redistribution of water molecules from medium-sized (type III) to small sized pores (types I and II), measured by NMR, are comparable. They indicate that the wetting process may last two to three weeks. Consequently, the distinctly lower WDPT (Tab. 2.1) reflect only the first wetting step of the outer soil surfaces.

2.5. Conclusions

The hydration process of soil samples was characterized by three independent methods. The results indicate that the water uptake mainly is influenced by SOM and that the reached water contents of the organic matrix are comparable for whole soil samples and isolated humic fractions. A differentiation between water repellent and wettable soil samples only is possible by direct measurements of the gravimetric water uptake, if the water is supplied via the liquid phase. Both, the gravimetric measurements and the ^{1}H NMR relaxation analyses yield in first-order wetting kinetics of water repellent soils, which last up to three weeks (Schaumann et al. 2005a). Differences in the bond strength of water molecules in wettable and water repellent soil samples, as indicated by the phase transition characteristics, are most probably a result of the different moisture contents under field conditions. According to the results of this study, the portions of unfreezable water, the freezing and melting temperatures, and the temperature ranges of the evaporation process of water repellent and wettable soil samples approach each other after adjusting their water contents.

For modeling transport and sorption processes, the hydration kinetics, which may be very slow in water repellent soils, have to be taken into account. In some cases, equilibrium conditions may be achieved only after several weeks after precipitation or desiccation events, and not just after some hours, as indicated by the WDPT measurements.

3. Properties of soil organic matter and aqueous extracts of actually water repellent and wettable soil samples

3.1. Abstract

The occurrence of water repellent spots can inhibit a homogeneous wetting progress in soil. Although the wettability is an important factor for sorption and transport processes, the knowledge about the reasons for water repellent behavior and its effects on other soil properties is still insufficient. In this study, water repellent and wettable soil samples from two urban locations were compared. It was examined to which extent differences in the actual water repellency of closely neighboring spots are associated to variable factors like the water content or to stable properties of soil organic matter (SOM). In order to analyze the interrelations between the moisture status and the wettability behavior, soil samples were either subjected to drying-remoistening cycles or pre-conditioned under various conditions. For the characterization of stable SOM properties, the soil samples were investigated by ESEM (Environmental Scanning Electron Microscope) and FT-IR spectroscopy. Beside the investigation of solid soil samples, selected properties of aqueous soil extracts were measured. The results of this study indicate that the water content is not the only factor responsible for the differences in actual water repellency. For different locations, the wettability behavior probably is based on different mechanisms. For one of the examined sites, differences in actual repellency of closely neighboring samples were interrelated with differences in pH and the ionic strength of the soil solutions. For both locations, amphiphilic substances probably are an important factor of influence for the wettability behavior. Additionally, the results suggest that the time which proceeds after a change of the moisture status in soil is an important factor for water repellency.

3.2. Introduction

Water repellency is a problem in many soils. Therefore, a great number of studies, which deal with various aspects related to this subject, exist. Nevertheless, for many locations, the causes for water repellent behavior are still not understood.

The water content is one of the main influencing factors for the current water repellency (e.g., King 1981; Ritsema and Dekker 1998; Quyum et al. 2002). The relationship between the wettability and the water content is either described with the conception of a maximal water repellency at a critical water content (e.g., King 1981; de Jonge et al. 1999; Bachmann and van der Ploeg 2002) or by a soil moisture threshold with water repellent behavior below and wettable behavior above it (Dekker and Ritsema 2000; Ritsema and Dekker 2000). Additionally to the dependence of the wettability on the water content, an influence of the time after a change of the moisture status has been reported (Doerr et al. 2000). It was observed that water repellency is not necessarily re-established just after the soil gets dry (Doerr and Thomas 2000). Todoruk et al. (2003a) and Schaumann et al. (2005a) observed an

increase of wettability with increasing residence time of water by H-NMR Relaxometry studies. The change of the wettability characteristics in the course of time can be explained by conformational re-arrangements (Ma'shum and Farmer 1985; Valat et al. 1991; Roy et al. 2000). The process of wetting is slow in water repellent soils. H-NMR Relaxometry studies point to a first-order re-distribution of water (Todoruk et al. 2003a; Schaumann et al. 2005a) with activation energies in the order of magnitude of chemical reactions (Todoruk et al. 2003a). Todoruk et al. (2003a) suggested ester hydrolysis as a possible chemical transformation in the course of wetting.

Despite the dynamics of water content in field conditions, distinct regions of water repellency can often be observed over a long period of time (Ritsema and Dekker 2000). This suggests that the wettability additionally depends on stable properties of the solid soil organic matter (e.g., DeBano 1981; Wallis and Horne 1992; Doerr et al. 2000). By analyses of soil extracts prepared with various organic solvents, aliphatic hydrocarbons and amphiphilic substances (mainly long-chain fatty acids, n-alkanes, and cycloalkanes) were related to hydrophobicity (e.g., Hudson et al. 1994; Roy et al. 1999; Franco et al. 2000). The extraction procedures applied in these studies, however, may change the composition, the structure, and the properties of the organic substances. Especially, the macromolecular structure of SOM is expected to be severely affected by the extraction procedures. To avoid such limitations, Capriel et al. (1995) studied the SOM directly in the soil matrix with Diffuse Reflectance Infrared Fourier Transform Spectroscopy (DRIFT). They found a close relation between the content of aliphatic hydrocarbons and the degree of soil water repellency.

Beyond these factors, soil properties like the pH and the ionic strength may affect the wettability behavior. The amount of polar functional groups is responsible for the wettability of SOM (Tschapek 1984; Valat et al. 1991; Almendros et al. 1992; Rutherford and Chiou 1992). Therefore, it can be assumed that a protonation of the negatively charged carboxyl and phenolic groups result in a decrease of the wettability. Steenhuis et al. (2001), who tested the wettability of more than 3000 soil samples from New York State, found an interrelation between low pH and water repellency. Additionally, the positive effect of the application of lime on water repellent soils was often reported (e.g., Jackson and Gillingham 1985; Blackwell 1997). Ritsema and Dekker (1998) also found a correlation between low pH and water repellent zones in a Typic Psammaquent. They however explained these findings with the former application of manure, which was transported only through the major flow pathways to the wettable regions. Until now, it remains ambiguous, whether a low pH is a cause or a consequence of water repellency.

A high ionic strength in the soil solution can cause that charged functional groups of the SOM approach to each other. Possibly, because of the associated change of molecular conformation, hydrophobic molecule groups are exposed to the surface to a higher extent. An aggregation of the humic substances due to bridges by polyvalent cations may also result in a lower wettability. Tarchitzky et al. (2000) explained the role of polyvalent cations for water repellency with the enhanced formation of coatings on mineral surfaces due to high

concentrations of polyvalent cations, resulting in a reduction of the hydrophilic reactivity of the mineral surfaces. Bartoli and Philippy (1990) reported a disruption of hydrophobic Al-organic matter associates and dissolution in solutions with high Na^+ or H^+ contents with the consequence of an increase of soil wettability. The conclusions of this study do not agree with the correlation between solution properties and soil wettability which was described in the above mentioned works, but they also show the importance of pH and ion concentrations to organic matter aggregation and the concomitant wettability behavior of the soil.

Under field conditions, wettability also depends on the interfacial properties of the soil solution (Chen and Schnitzer 1978; Tschapek 1984). Chen and Schnitzer (1978) analyzed the surface tensions of aqueous solutions of fulvic and humic acids in dependence on the pH and proposed a possible mechanism for the reduction of water repellency in the field by liming: Humic acids which effectively reduce the surface tension of water are soluble only at pH > 6.5. In addition, the surface tension of fulvic and humic acid solutions decreases with increasing pH. The lower surface tension of soil solutions at high pH may result in an increased infiltration into the soil.

The above mentioned studies imply that both the solid soil matrix and the soil solution may severely affect the wettability in the field. Soil pH and ionic composition are specified as important factors of influence, but responsible mechanisms could only rarely be identified (Tschapek 1984; Wallis and Horne 1992). Despite the high number and diversity of detailed studies on the phenomenon of soil water repellency, there is still a lack of studies explaining the occurrence of stable water repellent regions on the one hand and dynamics and heterogeneity of water repellency in field and laboratory on the other hand.

In two anthropogenically influenced locations in Berlin, a high heterogeneity in actual water repellency can be observed for long periods of the year (Täumer et al. 2005). This heterogeneity expresses itself by a close neighborhood of actually wettable and water repellent spots as illustrated in Fig. 3.1. Soil texture does not correlate with the water repellency and is not heterogeneous. By statistical evaluation of 864 samples from one of the two locations, no distinct critical water content could be identified, below which most of the samples became water repellent (Täumer et al. 2005). Therefore, Täumer et al. (2005) developed a model that correlates the occurrence of actual water repellency with the water content and the amount of SOM. While the combination of water content and SOM content allowed to distinguish between actually repellent and actually wettable samples in this location, the degree of water repellency could not be related to water and SOM quantity.

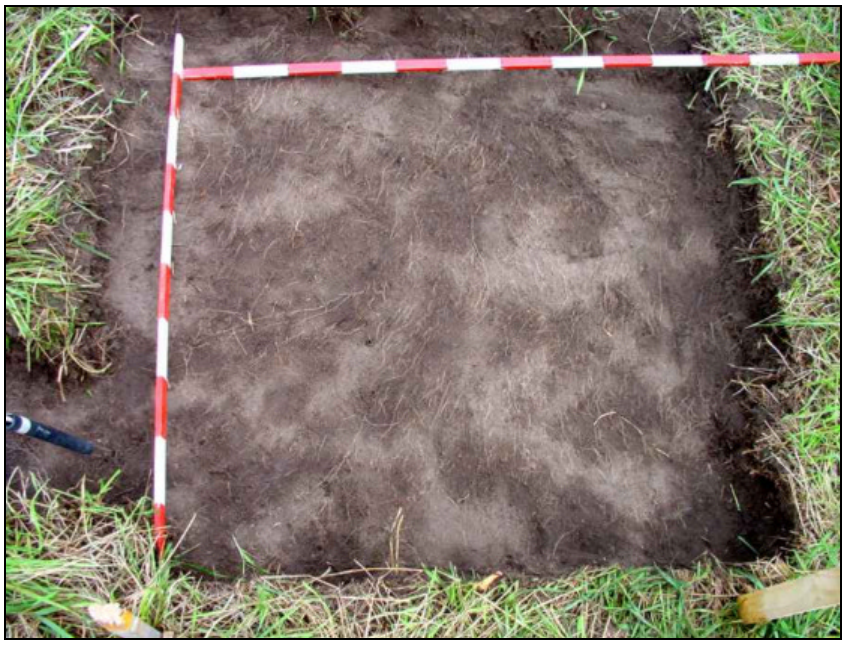

Fig. 3.1. Typical moisture pattern, which is related to spatially variable water repellency, at the location Buch (15 cm deep soil profile, each mark of the tape: 10 cm). The photo is taken by Karsten Täumer, department of Soil Science, Institute for Ecology, TU Berlin.

The aim of this study was to elucidate possible reasons for the occurrence of the heterogeneity of actual water repellency at the two Berlin locations. As the spatial heterogeneity of the investigated sites implies that each location has a high diversity of soil properties, the influence of spatial heterogeneity was minimized by comparing samples of closely neighboring spots with comparable soil properties, but severely differing actual wettability. In the first part of the study, relations between water repellency and water content were closely investigated to examine the hypothesis that the differences in actual wettability behavior are caused by differences in the actual water content. An exclusive dependence of water repellency on the moisture status would mean that the soil can reversibly change from water repellent to wettable behavior and vice versa. As a result, the samples would be identical with respect to their wettability behavior. Possible hysteresis effects of the water repellency were investigated by a drying-remoistening cycle.

The relationship between stable SOM properties and soil wettability was examined in the second part of the study. Therefore, structural and physicochemical properties of the solid SOM of water repellent and wettable samples were characterized by FT-IR spectroscopy and ESEM (Environmental Scanning Electron Microscope) observations. In order to characterize soil solution properties, which also reflect the SOM properties and the wettability behavior, DOC content, UV/VIS absorption, surface tension, molecular size distribution, and general solution parameters as pH, electrical conductivity, and anion composition were measured in aqueous soil extracts of the samples.

3.3. Materials and Methods

3.3.1. Determination of soil wettability

The wettability of the soil samples was determined by the water drop penetration time (WDPT) method. Three water drops were placed on the surface of the soil sample, and the WDPT was determined by measuring the time that is necessary for the water droplets to infiltrate into the soil. For the determination of WDPT > 3 min, the samples were placed in a cooled incubator at 20 °C in order to minimize evaporation. For a better identification of the point of time, when the droplets penetrated into the soil, they were observed by magnified photographs, which were taken automatically in short time intervals by a digital camera. The time intervals were increased from 1 to 10 min with increasing measuring time.

3.3.2. Soil samples

The soil samples were taken from the humous upper layer (10 - 20 cm) of the research locations Tiergarten and Buch of the DFG research group INTERURBAN. The Tiergarten is an inner-city park in Berlin, which has been created between the 17th and the 20th century. In Buch, an ancient sewage field, which was used for more than 100 years until 1985, is being investigated by the research group.

Because of the high variability of soil properties in the field, sample pairs of actually wettable and water repellent samples, which were located directly side by side (maximal 20 cm distance), were compared. Despite the direct proximity of the two samples of each pair, they differed distinctly in water content and wettability, as can be seen in Fig. 3.1 for the location Buch. The dark soil regions represent easily wettable spots with high water contents, while the light regions are related to low water contents and water repellency.

A total of eight sample pairs from the location Tiergarten and seven sample pairs from the location Buch were investigated. Due to the thorough examination of the selected pairs of wettable and water repellent samples, the measured data were evaluated by quoting the proportion of sample pairs which show the examined characteristic, but we consider the significance of statistical assessments low for the seven to eight sample pairs. In this contribution, most results are shown exemplarily for one representative sample pair of each site. In the following text, the depicted sample pairs are designated T1 and B1, related to the locations Tiergarten and Buch, respectively. A characterization of these soil samples is given in Tab. 3.1. For practical reasons, we refer in the text to the actually water repellent and the actually wettable samples as “water repellent” and “wettable”, respectively.

In order to avoid artifacts caused by further changes in the soil moisture status, all experiments with the exception of the FT-IR-measurements were performed directly after the samples were taken from the field.

Tab. 3.1. Properties of the soil samples of the sample pairs T1 and B1.

	sample pair T1		sample pair B1	
	water repellent	wettable	water repellent	wettable
WDPT (actual repellency)	(10 ± 1) h	(0 ± 0.1) s	(9 ± 1) h	(0.3 ± 0.1) s
grav. water content [%] (field-moist)	10.4 ± 0.1	28.1 ± 0.1	8.9 ± 0.1	17.5 ± 0.1
C_{org} [%]	4.4 ± 0.4	5.3 ± 0.1	4.2 ± 0.1	3.8 ± 0.1
pH	4.2 ± 0.1	4.8 ± 0.1	5.6 ± 0.1	4.7 ± 0.1
sand [%]	85.1		94.3	
silt [%]	10.6		5.4	
clay [%]	4.3		0.3	

3.3.3. Influence of the moisture status on the wettability

In order to examine to which extent the wettability depends on the moisture status of soil samples, the WDPT were determined in the field-moist status, after storing the samples for three month at 7 °C, after drying them for 24 h at 35 °C, and after conditioning them over saturated $CaCl_2$ (31 % relative humidity, 20 °C) and NaCl solutions (76 % relative humidity, 20 °C), until an equilibrium water content was reached.

Additionally to the investigation of the different sample pretreatments, the field-moist sample pairs were subjected to a drying-remoistening cycle. First, the samples were dried for 12 days over a saturated $CaCl_2$ solution (31 % relative humidity, 20 °C). At several points of time, the water content and the WDPT were determined for each sample. After this drying, the samples were remoistened for 8 days via the gas phase. For this purpose, a water saturated air stream was routed through a closed sample chamber (99 % relative humidity, 20 °C). In the course of this remoistening, the water contents and WDPT were measured several times.

It is known that high atmospheric relative humidity can result in an increase of water repellency (Doerr et al. 2002). Therefore, the used remoistening method via the gas phase needs not necessarily to reverse the effects of the previous drying process. However, by moistening via the liquid phase, it is not possible to separate the water which is already absorbed in the soil from free water: The measured water content in a sample remains constant in the course of time, although it can take a long time, before a sudden wetting, which is accompanied by a reduction of the contact angle to 0, occurs. The sample moistening via the liquid phase would be an alternative to the gas phase, if the wetting progress can be observed, as it is possible e.g. by H-NMR Relaxation studies. The moistening via the gas phase is the only straightforward possibility to observe the progress of wettability change of water repellent soils, because the gas molecules can penetrate into the solid soil matrix, and the gravimetric water content corresponds to the water absorbed in the sample.

3.3.4. Characterization of the solid SOM

To describe the morphology of the organic particles and coatings on mineral surfaces, ESEM (Environmental Scanning Electron Microscope) investigations were carried out. Due to the possibility to observe moist samples under this microscope, it was used to examine, whether morphological differences of SOM between the field-moist wettable and water repellent soil samples can be identified. In the Institute of Soil Science of the TU Hannover, a Quanta 200 ESEM (FEI, Germany) was used with a pressure of 800 Pa and an acceleration voltage of 15 kV. Two different magnifications (4000 and 7000) were applied to compare the structure of SOM particles between the samples. Each sample was carefully scanned by the microscope, and approximately 100 close-ups were examined.

To characterize the molecular structure of the SOM of wettable and water repellent soil samples, IR spectra were recorded. A FTS 135 FT-IR spectrometer (Bio-Rad, Germany) from the ZALF in Müncheberg was used in the absorption mode. With the Bio-Rad Win IR Foundation tm software, the absorbance for the wave numbers between 450 and 4000 cm^{-1} with a resolution of 1 cm^{-1} was analyzed. For each sample, 16 scans were performed. To remove the water, which overlaps with the aliphatic C-H signal in the IR spectra, the samples were oven dried for 24 h at 105 °C. To obtain reference samples without organic material, parts of the samples were gently heated for 7 h at 450 °C. From the soil samples, KBr disks (13 mm) were pressed with 9 tons under vacuum, using 0.5 mg of soil and 80 mg of KBr after intensive mixing in an agate mortar.

In the IR spectra, the C-H band between 2800 and 3030 cm^{-1} is caused by asymmetric and symmetric stretching vibrations of aliphatic C-H bonds in methyl, methylene, and methine units. The C=O value is composed of the bands of the dissociated carboxyl groups (1600 - 1640 cm^{-1}) and the protonated carboxyl groups (1710 - 1740 cm^{-1}). For the quantitative evaluation, the heights and the areas of the different peaks were determined, whereby the construction of the baseline for the C-H band was adopted from Capriel et al. (1995). For the other peaks, a horizontal baseline through the lowest point of the spectrum was applied. According to Capriel et al. (1995), the ratio of the C-H band to the content of organic carbon in the sample was determined to estimate the degree of water repellency. But distinct from Capriel et al. (1995), who used the peak area to calculate this ratio, the peak height also was evaluated as suggested by Ellerbrock and Gerke (2004), because it was assumed that the peak areas are stronger influenced by overlapping neighbor peaks. Another difference of the evaluation are the limits for the integration of the C-H band (from 2800 to 3030 cm^{-1} in this study and from 2800 to 3000 cm^{-1} in the study of Capriel et al. (1995)). Additionally to the CH/C_{org} ratio, the CH/CO ratio was calculated as an alternative indicator for water repellency.

3.3.5. Characterization of the soil extracts

Besides the characterization of the solid SOM, the extractability of the organic substances in water and the properties of the obtained soil extracts were analyzed for six sample pairs from

the Tiergarten and six sample pairs from Buch. Therefore, the field-moist soil samples were shaken with water (1:5 mass ratio of dry soil to water) for 12 h with a horizontal shaker, and the extracts were filtered to 0.45 µm. The measurements described below were carried out with two replications of extraction.

For appraising the total amount of DOM, the content of non-purgeable organic carbon (NPOC) was measured in the extracts with the TOC-5000 Analyzer (Shimadzu, Germany). To characterize the extracted organic matter, UV/VIS spectra were recorded with the UV Spectrophotometer UV-160 (Shimadzu, Germany). The surface tension and the molecular size distribution in the extracts were measured to characterize colloidal properties of the solutions. The surface tension measurement was performed with a K10ST tensiometer (Krüss, Germany; DuNouy ring method) in a thermostatic device maintained at 23 °C. With the platinum ring, a lamella was pulled up for 30 min, before measuring the surface tension.

The molecular size distribution was analyzed by LC-OCD, a size exclusion chromatograph from DOC-Labor Dr. Huber (Germany) with online OC and an UV detection. A standard phosphate buffer (1.25 gL^{-1} Na_2HPO_4, 2.5 gL^{-1} NaH_2PO_4) was used as mobile phase. A polymeric gel (TSW HW 40 (S), Toso Haas, Stuttgart, Germany) served as stationary phase. The retention time is inversely proportional to the decadic logarithm of the molecular weight of the organic molecules or molecule associates. The calibration of the molecular weights was done with polyethylenglycol (PEG) standards. Because of different molecule shapes and densities, the DOM molecules in the measured soil extracts may not necessarily have exactly the same size and molecular weight as the PEG molecules which appear at the same time in the detector. It is possible to assign a range of molecular sizes to each peak in the chromatograms and to identify differences in molecular weight between the samples rather than the absolute molecular weight.

In addition, the pH, the electrical conductivity, and the concentrations of the anions fluoride, chloride, nitrate, phosphate, and sulfate were measured as general solution parameters. The analysis of anions was done with DX-120 Ion Analyzer (Dionex, Germany).

3.4. Results

3.4.1. Influence of the moisture status on the wettability

Fig. 3.2 shows the WDPT after the different sample treatments exemplarily for one sample pair from the location Buch and one sample pair from the Tiergarten. The WDPT of the wettable samples remain at 0 s or increase up to maximal 25 min after all sample treatments including drying. The initially water repellent samples remain water repellent with WDPT > 1 h after all investigated treatments with the exception of the storage at 7 °C. Thus, after all the treatments, the initially water repellent samples still reveal higher WDPT than the wettable samples, but the difference between the WDPT of the water repellent and the wettable samples decrease for both sample pairs. All tested sample treatments with the

exception of the 35 °C drying of the water repellent sample from Buch result in a decrease of the WDPT of the water repellent samples. Only shock-freezing with liquid nitrogen and subsequent storage at -18 °C does not change the water repellency significantly (data not shown). The remaining differences in the wettability after the different sample treatments indicate a general difference between the initially wettable and repellent samples, which most probably is not governed by the water content.

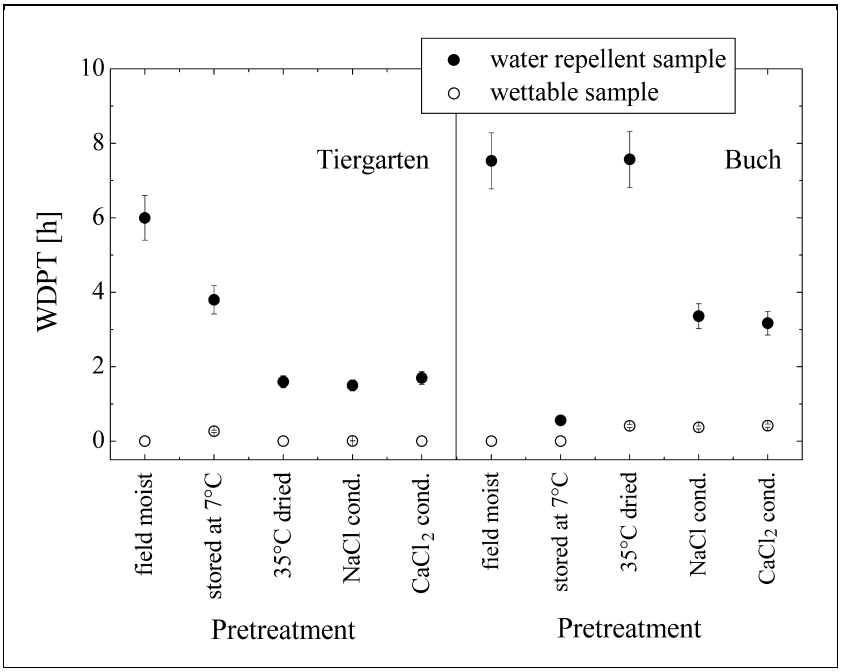

Fig. 3.2. WDPT in the field-moist status, after sample storing for three month at 7 °C, after drying at 35 °C, and after conditioning over saturated NaCl and $CaCl_2$ solutions for a Tiergarten and a Buch sample pair.

Tab. 3.2 summarizes for eight sample pairs from the Tiergarten and seven sample pairs from Buch, for how many pairs the WDPT of the water repellent sample remains higher than the WDPT of the initially wettable sample after the different sample pretreatments. With one exception, the WDPT of the initially water repellent sample remains higher than for the corresponding wettable sample after the different sample pre-conditioning methods. But storing the field-moist samples partially results in an adaptation of the WDPT (3 out of all 15 pairs) or even in a higher WDPT for the initially wettable sample than for the initially water repellent sample (2 out of the 15 pairs). All the tested sample treatments lead to a decrease of the WDPT of the water repellent samples and to no shifting or a small increase of the WDPT of the wettable samples. Exceptions of these directions of the WDPT shifting are only observed for three out of the 30 samples after the 35 °C drying and for only one sample after the storage at 7 °C. Therefore, for most sample pairs, the different conditioning methods and the sample storing cause that the WDPT of the wettable and the water repellent sample approach each other, but the samples remain different.

Tab. 3.2. Number of sample pairs for which the WDPT of the water repellent sample remains higher than the WDPT of the initially wettable sample after different sample pretreatments (a total of eight sample pairs from the Tiergarten and seven sample pairs from Buch).

Location	$WDPT_{repell.} > WDPT_{wett.}$	three month stored at 7 °C	dried at 35 °C	conditioned over saturated NaCl	conditioned over saturated $CaCl_2$
Tiergarten	true	6	8	8	8
	false	2	0	0	0
Buch	true	4	7	6	7
	false	3	0	1	0

Fig. 3.3 shows the water contents as a function of time in the course of a drying and remoistening cycle of the sample pairs T1 and B1. For all points of time, the water content of the wettable sample remains higher than the water content of the water repellent sample of the pair T1. But after 8 days of drying, an approach of the water contents of the two samples has occurred ((1.9 ± 0.2) % for the wettable sample and (1.4 ± 0.1) % for the water repellent sample). At the end of the remoistening, the water contents of both samples slightly decline. The latter may be due to a slight deviation of the relative humidity in the sample chamber from the target value. Different from the T1 pair, already after 2 days of drying, the water contents of the B1 samples do not differ any more. After 5 days, an equilibrium water content was reached in the samples ((1.2 ± 0.1) % in the water repellent and (1.3 ± 0.1) % in the wettable sample). During the following remoistening, the water contents also remain indistinguishable. For all the samples, the water contents at the end of the remoistening do not reach the initial water contents, which were measured before the drying cycle. These smaller water contents at the end of the experiment are due to the remoistening method via the gas phase that results in lower water contents than moistening via the liquid phase, which causes higher water contents in the field.

For the water repellent sample of the pair B1, the experiment was aborted after two weeks due to inaccuracies of the adjusted relative humidity. The other samples indicate that at this point of time, equilibrium water contents were reached. A repetition of the experiment for this sample was not considered as useful, because the storage time of soil samples also can influence their wettability behavior (Doerr et al. 2000).

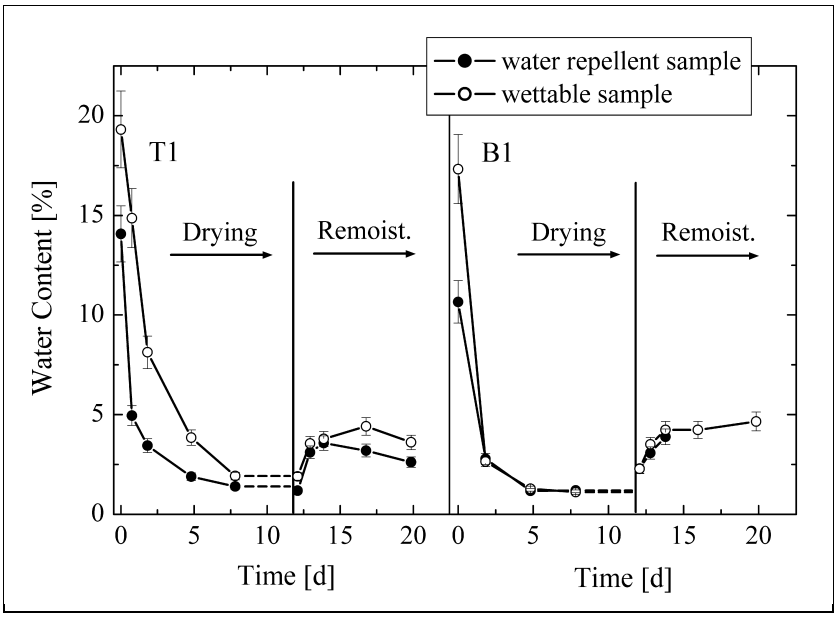

Fig. 3.3. Water contents in the course of drying and remoistening by vapor intrusion of the sample pairs T1 and B1. The errors were determined on the basis of multiple measurement repetitions for one sample.

In Fig. 3.4, the WDPT is shown as a function of the water content for the sample pairs T1 and B1. The WDPT of the water repellent sample of the pair T1 is higher than the WDPT of the corresponding wettable sample for most water contents during the drying-remoistening cycle. Corresponding to the expectations, the WDPT of both samples increase during the drying progress. At the end of drying, large increases of the WDPT of the water repellent sample (change of 2.6 h) are related to very small decreases of the water content (reduction of 0.7 % in 7 days). The water repellency during the remoistening progress is higher than it was at the accordant water contents during the drying progress. However, the WDPT of the initially wettable sample does not change significantly in the course of the remoistening cycle.

For the sample pair B1, the initially water repellent sample revealed a higher WDPT than the initially wettable sample for all water contents in the first two weeks of the experiment. The sample drying causes an increase of the water repellency up to a maximal WDPT of (6.1 ± 0.6) h for the water repellent and (4.0 ± 0.4) h for the wettable sample. For both samples, this WDPT maximum arises at a water content between 2 and 3 %. Further drying reduces the water repellency. At the end of the drying cycle, very small changes of the water content (changes in 3 days below 0.2 %) are accompanied by distinct decreases of the WDPT (reduction of 23 min in the water repellent sample and of 45 min in the wettable sample). For both samples, the water repellency during the subsequent remoistening is lower than it was at the accordant water contents during the drying process. Only the last two data points of the water repellent sample make an exception. These data points show that WDPT changes can occur without significant changes of the water content in the course of time. The maxima of water repellency at water contents between 2 and 3 % are also marginally existent in the remoistening cycle.

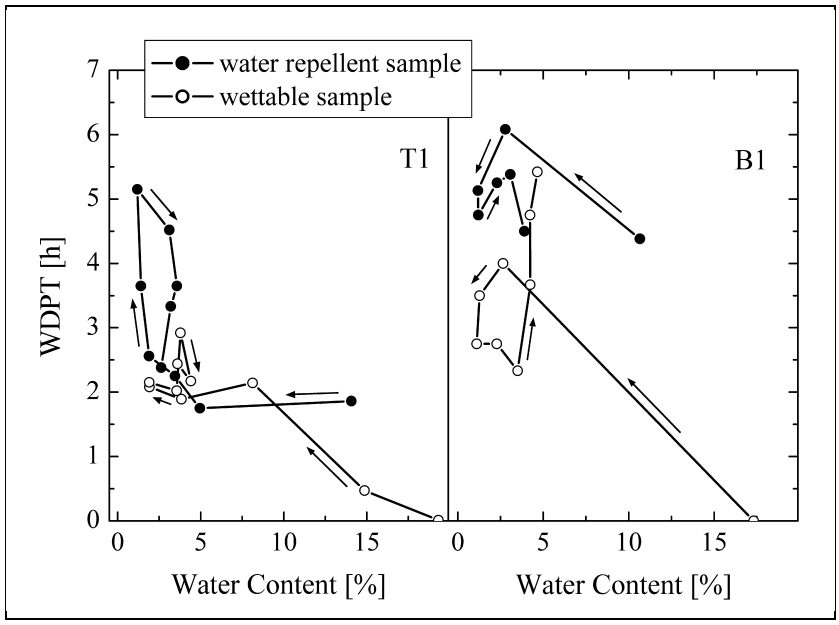

Fig. 3.4. WDPT as a function of water content in the course of drying and remoistening by vapor intrusion of the sample pairs T1 and B1.

The relationship between the water content and the WDPT shows hysteresis effects with different responses of the sample pairs on the drying-remoistening cycle: Remoistening resulted in a lower degree of water repellency for the sample pair B1 and in a stronger water repellency for the sample pair T1. The drying-remoistening cycles show that beside the reached water content, the time must be taken into account as an important factor of influence for the soil wettability. In contrast to the T1 samples, the shape of the WDPT hysteresis curves of the sample pair B1 point at the similarity between the water repellent and the wettable sample. For both sample pairs, the WDPT curves seem to approach each other. It is important to note that, if at all, this approach only appears after a number of days. From these results, we conclude that the water content is not the only factor controlling repellency behavior. Beside the time, SOM properties may be hypothesized to be responsible.

3.4.2. Solid SOM

Exemplarily, two ESEM pictures with the magnification 4000 of the field-moist sample pair T1 are shown in Fig. 3.5. The comparison of approximately 100 close-ups of the two samples resulted in the conclusion that no significant differences of the superior structure of the organic matter can be observed between the samples by using the ESEM. In the wettable and the water repellent sample, particles which contain only organic matter, pure mineral particles, and mineral particles with organic coatings were identified. There is a great variation of the sizes and shapes of the particles and the pores between them in both samples, what only was ascertainable, because many parts of the samples were observed with the microscope.

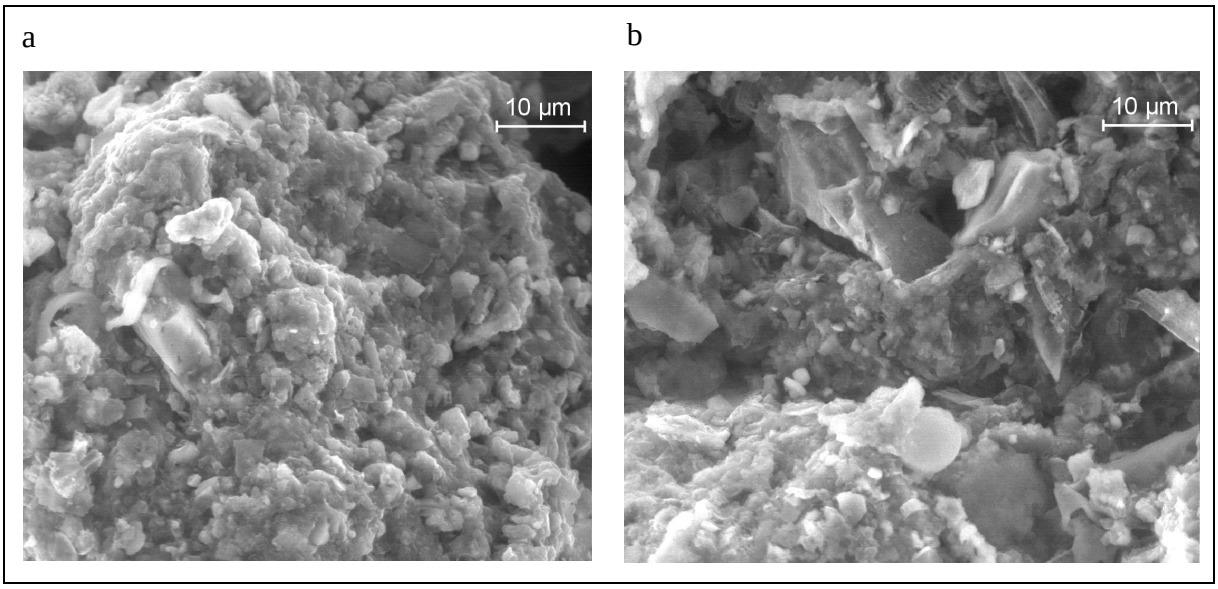

Fig. 3.5. Environmental Scanning Electron Microscope (ESEM) photographs of the water repellent (a) and the wettable (b) sample of the sample pair T1 (magnification 4000).

The FT-IR spectra of the sample pairs T1 and B1 are displayed in Fig. 3.6. For the pair T1, the sizes of all bands are larger for the water repellent sample than for the wettable one. If the peak heights are considered, the CH/CO quotient is 0.106 ± 0.002 for the water repellent sample (0.032 ± 0.007, if the peak areas are considered). For the wettable sample, no CH peak was detected. This points to the absence of aliphatic hydrocarbons which are related to water repellent behavior. Due to the lack of a CH peak, the CH/CO ratio and the CH/C_{org} ratio result in 0 for the wettable sample. For the water repellent sample, the CH/C_{org} ratio is $(0.03 \pm 0.01)\ mg^{-1}$, if the peak height is considered ($(2.2 \pm 0.6)\ mg^{-1}$, if the peak area is considered).

Compared to the sample pair T1, there are only small differences in the peak sizes between the two samples of the pair B1. The CH band was detectable for both samples of the pair B1. For the water repellent sample, the CH/CO quotient is 0.200 ± 0.002 for the peak high evaluation and 0.060 ± 0.006 for the peak area evaluation. For the wettable sample, it is 0.163 ± 0.001 for the peak high evaluation and 0.064 ± 0.006 for the peak area evaluation. This means that by considering the peak heights, the CH/CO ratio is marginally higher for the water repellent sample, whereas there is no difference of the ratio, if the peak areas are considered. The CH/C_{org} ratio of the water repellent sample is $(0.07 \pm 0.02)\ mg^{-1}$ for the peak height evaluation and $(5.3 \pm 1.5)\ mg^{-1}$ for the peak area evaluation. For the wettable sample, it is also $(0.07 \pm 0.02)\ mg^{-1}$ for the peak height evaluation and $(6.2 \pm 1.9)\ mg^{-1}$ for the peak area evaluation. Thus, regardless of the way of peak evaluation, this ratio shows no difference between the two samples.

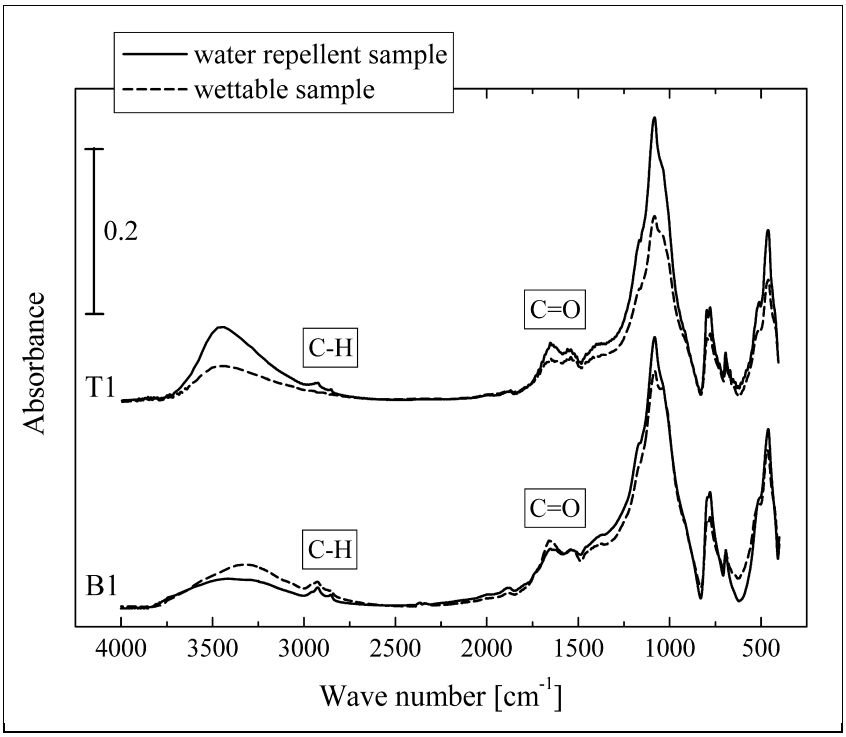

Fig. 3.6. Fourier-transform infrared (FT-IR) spectra of the sample pairs T1 and B1.

3.4.3. Soil extracts

The results of the characterization of the soil extracts are summarized in Tab. 3.3 for the sample pairs T1 and B1. The DOC release, referred to the content of SOM, is comparable for the wettable and the water repellent samples of these pairs. Nevertheless, other properties of the soil extracts differ.

Tab. 3.3. Properties of the soil extracts (LC-OCD main peak see Fig. 3.7: fraction between 1.5 and 20 kg mol^{-1}). The errors were determined by means of extraction repetitions.

	sample pair T1		sample pair B1	
	water repellent	wettable	water repellent	wettable
DOC / SOM [mg g^{-1}]	0.45 ± 0.01	0.38 ± 0.03	1.04 ± 0.03	0.93 ± 0.02
absorption $_{254\,nm}$ / DOC [L cm^{-1} g^{-1})]	47 ± 12	60 ± 17	46 ± 6	47 ± 5
surface tension [mN m^{-1}]	59.0 ± 0.5	64.7 ± 0.5	67.9 ± 0.5	71.5 ± 0.5
LC-OCD main peak position [kg mol^{-1}]	2.3 ± 0.1	3.8 ± 0.2	4.2 ± 0.1	4.3 ± 0.1
pH	4.7 ± 0.1	5.6 ± 0.2	5.3 ± 0.1	5.1 ± 0.4
conductivity [µS cm^{-1}]	134 ± 14	76 ± 1	97 ± 5	105 ± 18
chloride [mg L^{-1}]	1.1 ± 0.1	1.3 ± 0.1	1.6 ± 0.7	2.0 ± 0.6
nitrate [mg L^{-1}]	12 ± 5	10 ± 1	11 ± 2	16 ± 4
phosphate [mg L^{-1}]	n.d.	n.d.	6 ± 1	8 ± 2
sulfate [mg L^{-1}]	33 ± 10	11 ± 1	24 ± 6	20 ± 6

In order to identify possible parameters of influence for the wettability, we proceeded in the following way: For each investigated parameter, a hypothesis on the relation of this parameter between water repellent and wettable samples was formulated. The hypotheses and the corresponding numbers of sample pairs to which the hypotheses apply are summarized in Tab. 3.4.

Tab. 3.4. Number of the sample pairs for which the formulated hypotheses apply. The numbers in front of the slashes correspond to significant differences which are larger than the error bars of the two samples of each pair. The numbers behind the slashes correspond to differences which are smaller than the error bars. (UV absorption: UV absorption at 254 nm, related to the DOC content; mol. size: molecular size, determined by the main peak position in the size exclusion chromatograms of the LC-OCD; EC: electrical conductivity).

Formulated hypothesis	Tiergarten		Buch	
	true	false	true	false
UV absorption $_{repell.}$ < UV absorption $_{wett.}$	2 / 4	-	0 / 4	0 / 2
surface tension $_{repell.}$ < surface tension $_{wett.}$	3 / 1	2 / 0	6 / 0	-
mol. size $_{repell.}$ < mol. size $_{wett.}$	6 / 0	-	2 / 2	0 / 2
pH $_{repell.}$ < pH $_{wett.}$	5 / 0	0 / 1	-	1 / 5
EC $_{repell.}$ > EC $_{wett.}$	4 / 1	1 / 0	2 / 2	0 / 2
sulfate $_{repell.}$ > sulfate $_{wett.}$	5 / 0	0 / 1	5 / 1	-

A trend of the UV absorption at 254 nm, related to the DOC content, can be recognized for the samples from the Tiergarten. The relative UV absorption is lower for the water repellent than for the corresponding wettable samples. Although only for two out of six sample pairs the difference of the relative UV absorption is greater than the error bars, a general difference in UV absorption can be assumed due to its identification in all the six sample pairs. In contrast to the Tiergarten samples, for the sample pairs from Buch no significant difference of the relative UV absorption between wettable and water repellent samples could be observed.

For 10 out of 12 sample pairs from both locations, the surface tension of the extracts is lower for the water repellent sample than for the corresponding wettable sample.

In Fig. 3.7, a size exclusion chromatogram of the LC-OCD is shown for the sample pair T1. The position of the main peak, which occurs approximately after 50 min, was compared for the different soil samples. The peak position was determined on the basis of the peak maximum. For all the sample pairs of the Tiergarten, a difference of the peak position was measured, indicating smaller molecules of this size fraction in the water repellent samples than in the wettable samples. For the sample pairs from the location Buch, no difference in the peak positions could be observed (significant difference only for two out of the six sample pairs from Buch), but the retention times of the peaks more likely point at smaller molecular weights for the water repellent samples, too.

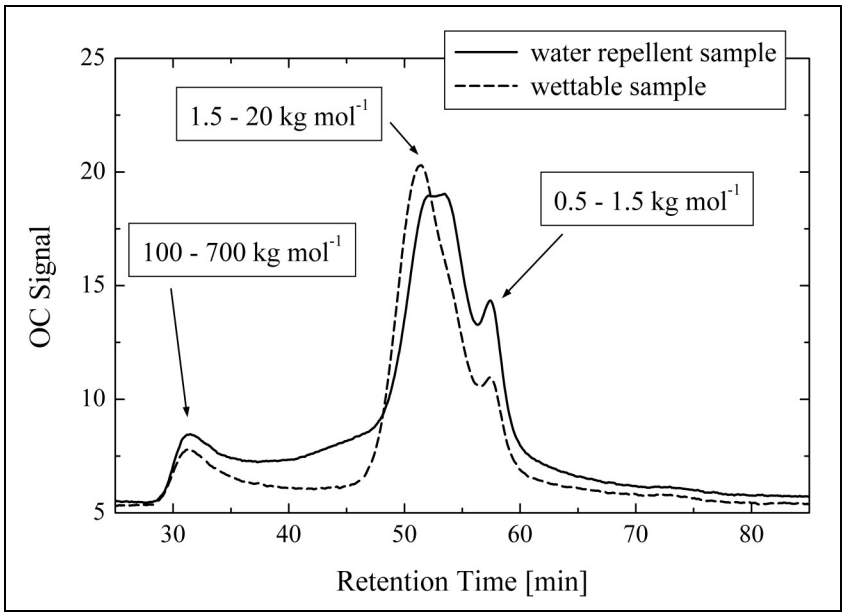

Fig. 3.7. Size exclusion (LC-OCD) chromatograms of the sample pair T1 (molecular mass calibration done with polyethylenglycol standards).

In order to calculate the molecular sizes, the density based on the hydrated volume of the organic molecules must be known. De Wit et al. (1993) rated the density of hydrated humic material from 0.7 to 1.7 kg L^{-1}, Birkett et al. (1997) calculated and measured densities of dissolved humic and fulvic acids between 1.2 and 2.1 kg L^{-1}. Assuming a density of 1 kg L^{-1} and a spherical geometry, the molecular radius basing on the main peak position ((53.48 ± 0.01) min; (2.30 ± 0.01) kg mol^{-1}) results in (9.71 ± 0.01) nm for the water repellent sample from the T1 sample pair. For the wettable sample, the peak position ((51.4 ± 0.2) min; (3.8 ± 0.2) kg mol^{-1}) results in a predominate molecular radius of (11.5 ± 0.2) nm. The main molecular radii of the B1 pair take values of (11.9 ± 0.1) nm for the water repellent sample and (12.0 ± 0.1) nm for the wettable one, so that they do not differ distinctly. The magnitude of all the calculated radii agrees with the radii of dissolved humic material which were determined by Cameron et al. (1972), Summers and Roberts (1988), de Wit et al. (1993), Birkett et al. (1997), and Wagoner and Christman (1998).

For five out of six sample pairs from the Tiergarten, the pH in the extracts of the water repellent samples is lower than for the wettable samples. Contrary to the Tiergarten samples, there is no significant pH difference between the water repellent and the wettable samples from the location Buch. For five out of six pairs from the Tiergarten, the electrical conductivity of the water repellent is higher than of the corresponding wettable samples. For two out of the six pairs, the difference between the samples of one pair differed by one size of order. For the sample pairs from Buch, no general difference in the conductivity between the wettable and the water repellent samples was identified.

In order to examine, whether the interrelation between the wettability on the one hand and pH and electrical conductivity on the other hand is characteristic for the whole Tiergarten location in contrast to the Buch location, all 145 samples which were taken from both locations within

three years were regarded with respect to pH and conductivity. The resulting box plots based on the frequency distributions are shown in Fig. 3.8. For the location Tiergarten, the water repellent samples have a lower pH and a higher conductivity than the wettable samples on the base of 25 % percentiles. Consequently, the observed interrelations between pH and conductivity and the wettability behavior, which were observed for the sample pairs from the Tiergarten, can also be found in the overall location. Fig. 3.8 further supports the observation that in Buch, such correlations do not apply.

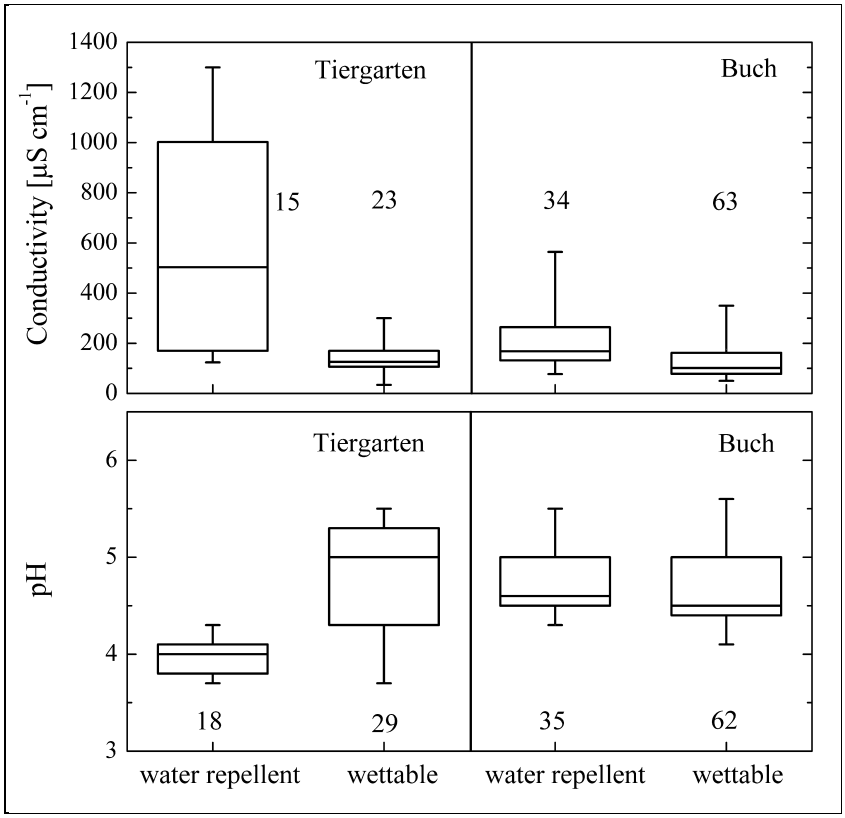

Fig. 3.8. Box plots of the electrical conductivity and the pH for all samples taken from the locations Tiergarten and Buch. Each box shows the median and ranges from the 25 to the 75 percentile, the whiskers range from the 5 to the 95 percentile. Sample with WDPT > 5 s are classified as water repellent, samples with WDPT £ 5 s are classified as wettable. The number of considered samples is indicated for each box.

The sulfate concentrations in the extracts of the water repellent samples are higher than in the extracts of the corresponding wettable samples for 11 out of all 12 sample pairs. For the other anions, no significant differences between the water repellent and the wettable samples could be observed. The composition of the cations, which only was measured in the extracts of selected sample pairs of the two locations (not shown), does not change noticeably with varying ionic strength. For both locations, calcium is the cation with the highest concentration.

3.5. Discussion

An important question of this study was to which extent the heterogeneity in actual water repellency in the field is related to variable factors as the water content, and to which extent differences in stable SOM properties may be the reason. Therefore, the changeable SOM characteristics, which mostly depend on the water status, and the stable SOM properties will be discussed separately with respect to their relations to the soil wettability behavior.

The results of the investigation of the different soil pretreatment methods indicate that the higher degree of water repellency of the initially water repellent samples than of the corresponding wettable samples is independent of different water states. Additionally, the drying and remoistening experiments show that for different water contents, the WDPT of the water repellent samples remain higher than for the wettable samples. These differences in the degree of water repellency remain, although the absolute WDPT of each sample changes in the course of drying and remoistening, resulting in strong water repellency even for the initially wettable samples (Fig. 3.4). This indicates that the soil wettability behavior of the examined sample pairs is partly governed by the water content as expected, but it depends on additional factors beside the water content. At the end of the drying-remoistening cycle, the influence of the proceeding time after a change of the water status may become apparent. The comparable WDPT of the initially water repellent and the initially wettable samples after two weeks in the saturated water atmosphere may serve as a sign that after longer waiting times, the samples possibly become similar.

In contrast to the description of the interrelation between water repellency and water content by King (1981), de Jonge et al. (1999), and Bachmann and van der Ploeg (2002), a maximal degree of water repellency at a certain water content could not be identified in this study. Only for the sample pair B1, such a critical water content may exist around 2 % (Fig. 3.4). For the sample pairs T1 and B1, the relationship between the water content and the WDPT shows hysteresis effects. A decrease of soil water repellency by increasing numbers of wetting and drying cycles, which was observed by Quyum et al. (2002), also points at hysteresis effects. Doerr and Thomas (2000) investigated the development of water repellency during a moistening-drying cycle. Like Quyum et al. (2002), they moistened the soil samples via the liquid phase, so that higher water contents than in our study were reached. For the samples which could be wetted by the added water, the water repellent behavior disappeared and could not be restored by the following sample drying. The hysteretic behavior of the WDPT which was observed for the Tiergarten and the Buch samples can be explained by slow conformational changes at the surface of the SOM caused by the drying, like the orientation of hydrophobic and hydrophilic molecule groups (Ma'shum and Farmer 1985; Valat et al. 1991; Roy et al. 2000). These processes possibly cannot invert during one week, because they proceed with slower kinetics than the remoistening process. Sorption experiments of Altfelder et al. (1999) also point at a rehydration time about two to three weeks which was explained by a slow reorientation process of polar and hydrophobic groups of humic structures.

Neither the macroscopic structure observed by ESEM nor the molecular structure analyzed by FT-IR spectroscopy can explain the different wettability behavior of the samples of the pairs T1 and B1. For the sample pair B1, the CH/CO ratio only shows a difference, if the peak heights of the IR spectra are evaluated, and if the peak areas or the CH/C_{org} ratio are considered, no differentiation between the two samples is possible either. In the wettable sample of the pair T1, no aliphatic hydrocarbons could be detected, but the C-H band also is very small for the water repellent sample. The resulting CH/C_{org} ratio is by a factor of 10 smaller than the mean CH/C_{org} ratio determined by Capriel et al. (1995) for arable soils. Therefore, it cannot be concluded that this small difference of the samples of the pair T1 is solely responsible for the different wettability behavior. Other characteristics, like the conformation of the organic molecules, probably contribute to the water repellency in the examined soil samples.

It cannot be excluded that the soil pH and the amount of ions are related to the occurrence of the water repellent spots in the Tiergarten. This possibility is supported by the significant correlation between the wettability on the one hand and pH and electrical conductivity on the other hand for the overall location. An aggregation of SOM due to low pH and high electrolyte content may result in a lower wettability. Particularly the protonation of negatively charged functional groups is assumed to be responsible for the interrelation between pH and wettability behavior. The formation of Ca^{2+} bridges may be an important factor that can explain water repellent behavior due to a high ionic strength.

We could not observe an interrelation between the pH or the ionic strength and the water repellency for the sample pairs from the Buch site. This points at the assumption that different mechanisms are related to water repellency, depending on the characteristics of the locations. The development of the WDPT of the sample pair B1 during the drying-remoistening cycle furthermore may indicate less pronounced differences of the intrinsic SOM qualities than for the samples from the Tiergarten.

Up to now, the reason for the pH and ionic strength differences of the Tiergarten sample pairs remains uncertain. The lower electrical conductivity in the extracts of the water repellent samples cannot be explained by the lower pH in these extracts, compared to the extracts of the corresponding wettable samples. Due to their high concentrations in the extracts, sulfate and nitrate seem to be the relevant anions for the conductivity.

The ionic strength, characterized by pH, electrical conductivity, and the ion concentrations, may also be responsible for the differences in the molecular masses of the dissolved molecules between the water repellent and the wettable samples of the Tiergarten site. A low pH and a high ion concentration result in coiling and intramolecular contraction of the DOM molecules (Birkett et al. 1998; Rice et al. 2000). Consequently, the sizes of molecules or molecule aggregates, measured with size exclusion chromatography, might be smaller than in extracts with lower electrolyte concentrations. This explanation was also given by Dittmar and Kattner (2003) who compared DOM size exclusion chromatograms of waters with varying salinity. Perminova et al. (1998) likewise reported an influence of the charge density

and the hydrophobicity of the organic analyte on the molecular size, measured by size exclusion chromatography. They assumed an overestimation of the sizes of negatively charged organic molecules and an underestimation of hydrophobic substances because of electrostatic and hydrophobic interactions of the DOM molecules with the gel in the column. These effects may contribute to the apparent differences in molecular sizes, measured for the sample pairs from the Tiergarten site. The protonation of organic acids in the extracts of the water repellent samples, which have a low pH, and hydrophobic regions in the DOM molecules could lead to an underestimation of the molecular sizes.

An interrelation between the pH and the UV absorption of the soil extracts from the Tiergarten site also is possible. The lower UV absorption in the extracts of the water repellent samples suggests that the DOM of the water repellent samples contains a minor amount of conjugated p systems than the DOM of the wettable samples. Due to protonation, the number of electrons which could serve for conjugated systems decreases, and a smaller specific UV absorption in the extracts of the water repellent samples may be the consequence.

For the sample pairs from the Buch location, the above described effects of pH and ionic strength cannot exist, because no significant differences in pH and electrolyte content were observed. This may be the reason that no differences of the molecular weights and the UV absorption of the organic molecules were found between the extracts of the water repellent and the wettable samples from Buch.

For both locations, the main differences in the soil extracts of the water repellent and the wettable samples are expressed by the surface tension and the sulfate concentration. The higher sulfate contents of the water repellent samples can be a consequence of the limited water flow in these regions. In a rewetted peat soil, a temporary gypsum precipitations was observed, which probably was related to the abrupt change in the water flow, resulting in non-equilibrium conditions (Regnery 2003).

The relation between the pH and the surface tension of the soil extracts of the Tiergarten samples is against the theory, which predicts a higher solubility and a higher interfacial activity of humic acids with increasing pH (Chen and Schnitzer 1978). The effect of the pH on the wettability may be suppressed by another effect. For both locations, the lower surface tension of the extracts of the water repellent samples points at a different DOM composition between the water repellent and wettable samples: The greater interfacial activity of the dissolved organic molecules of the water repellent samples can either be caused by a greater amount or by a higher efficiency (stronger surfactant characteristics) of amphiphilic compounds. Probably, a greater content of amphiphilic molecules at the surface of the solid SOM of the water repellent samples is responsible for the higher amount of such molecules in the soil extracts. If the water repellent and the wettable samples differ only in the structural composition at the surface of SOM, these differences are possibly not reflected by the IR absorbance spectra which characterize the bulk solid phase.

For the sample pairs from the Tiergarten, an influence of the molecular conformation of the DOM on the surface tension of the soil extracts is improbable, but cannot be excluded. For humic substances, the conformation in solution is characterized by the formation of condensed coils or long stretched chain molecules (Swift 1999) and gel properties (Benedetti et al. 1996), connected with shrinkage and swelling. These conformational arrangements of DOM molecules are mainly controlled by the concentration of electrolytes in the solution. For the samples from the Tiergarten, the higher electrolyte contents in the water extracts of the water repellent samples may influence the interfacial characteristics: The reduction of electrostatic repulsion along with the lower solubility of the hydrophobic parts of the amphiphilic organic molecules can enable an increase of the adsorption of these surfactant molecules at the interface between air and water, resulting in a decrease of the surface tension (Tajima 1971; Carale et al. 1994; Mitra and Dungan 1997).

It is noteworthy that for both studied locations, the surface tension in the extracts of the soil samples which show strong resistance to wetting with water in the laboratory is lower than for the samples which are easily wettable. On the one hand, this means that the water repellent soil regions may help themselves due to the solubilization of organic molecules which lower the surface tension of the soil solution with the consequence of a better wettability. On the other hand, the dissolved amphiphilic molecules can hydrophobize the SOM of wettable soil regions by adsorbing to polar functional groups with their polar groups. For the overall locations, it may be assumed that the wettabilities of the different regions approach each other.

An important result of the drying-remoistening cycles and the dependence of wettability on the different soil pretreatment methods is that the time after a change of the moisture status must be taken into account as an influencing factor for water repellency. After rainfall events and during dry periods, the possibility of a gradual change of soil wettability in the course of time must be considered in models that predict the water infiltration in the field. As the results which show the influence of time were achieved for very small water contents, in further experiments, the influence of time on the wettability behavior needs to be carefully investigated at higher soil moistures.

3.6. Conclusions

Although the moisture status of the studied soil samples significantly influences the degree of their wettability, the occurrence of water repellent and wettable spots at the investigated locations is not based exclusively on the water status. The actually wettable samples may become repellent, and the actually repellent samples may become wettable, but the samples remain different. Soil water repellency probably is related to SOM properties, even though it cannot be explained in terms of structural composition of SOM. For the municipal park Tiergarten, the pointwise water repellent behavior may be interrelated to low pH and high ionic strength. Because this possible interrelation could not be observed in the former sewage

field Buch, it is assumed that the mechanisms that cause water repellency may differ from site to site. But in both sites, amphiphilic substances are considered to be an important factor for the wettability behavior. The results of this study additionally suggest that the time that proceeds after a change of the moisture status influences the soil wettability.

4. Is glassiness a common characteristic of soil organic matter?

4.1. Abstract

Until now, glass transitions were detected in isolated humic and fulvic acids as well as in distinct soil samples with usually high C_{org} contents. The results of this study indicate that glassiness has to be considered a common characteristic of soil organic matter (SOM). However, two types of glassiness were observed in various soil types. Additionally to a typical glass transition with low intensity, a slowly reversing glass transition-like step transition with significantly higher intensity was detected in 52 out of 102 tested soil samples. The intensity of this transition type is correlated to the organic matter content of the samples. The transition behavior additionally depends on characteristics of the locations and changes within soil profiles. Relations to particulate organic matter (POM), mineral-associated organic matter (MOM), and the thermostable fraction of the soil samples were not significant.

A surprising result of the study is that the step transition temperatures of all analyzed air-dried soil samples range between 51 °C and 67 °C in closed systems, pointing to a superordinate mechanism which controls the matrix rigidity of the organic molecules. This may be represented by the formation of hydrogen bond-based crosslinks between water molecules and SOM suggested in a previous study. Thus, glassiness in SOM may be caused by physical and physicochemical mechanisms.

4.2. Introduction

Macromolecular characteristics of natural organic matter (NOM) are important for sorption and transport of organic compounds in soil. Sorption models suggested by Xing and Pignatello (1997) and LeBoeuf and Weber (1997) are based on the coexistence of glassy domains with rigid and condensed structure and rubbery domains with fluid-like properties in NOM. Glassy domains are related to nonlinear isotherms and sorption-desorption hysteresis due to a hole filling mechanism, whereas rubbery domains are proposed to account for linear sorption (LeBoeuf and Weber Jr. 1997; Xing and Pignatello 1997). Among others, humic acids, humins, and carbonaceous substances such as charcoal or soot, which are collectively termed black carbon (BC), can represent SOM fractions with nonideal sorption behavior (LeBoeuf and Weber Jr. 1997; Xing and Pignatello 1997; Chiou et al. 2000; Cornelissen et al. 2004). Generally, the rigidity of a macromolecular structure is reflected by the glass transition temperature T_g (McKenna 1989; Höhne et al. 1996). This interrelation can be illustrated by the glass transition temperatures of 72 °C for lignin (LeBoeuf and Weber Jr. 2000a), 225 °C for cellulose (Akim 1978), and 355 °C for coal (Lucht et al. 1987).

Glass transitions are characteristic for amorphous systems in a “frozen” non-equilibrium state. When a glassy polymer is heated through its glass transition region, it exhibits a significant change in heat capacity and the coefficient of thermal expansion due to a sudden increase in

side chain mobility (McKenna 1989; Elias 1997). The transition intensity is characterized by the change in heat capacity (*DC*). As the glassy state is not a thermodynamical equilibrium state, glassy matrixes undergo structural relaxation or aging processes (Cortés and Montserrat 1998). The glass transition is thus strongly influenced by the thermal history of the sample (Höhne et al. 1996; Cortés and Montserrat 1998; Hutchinson 1998). After sample storage below T_g or slow cooling, glass transitions reveal the shape of a peak rather than of a step (Moynihan et al. 1974; Cortés and Montserrat 1998; Hutchinson 1998). This peak is called annealing peak or enthalpic overshoot. Wide distributions of structural relaxation times result in broad glass transition regions with weakly pronounced or no annealing peaks (Cortés and Montserrat 1998; Hutchinson 1998). Thus, broad step-like glass transitions are expected for heterogeneous amorphous materials such as NOM.

Glass transitions have been discovered with DSC in humic and fulvic acids (LeBoeuf and Weber Jr. 1997) and in a small number of whole soil samples, sediments, and peat (Schaumann and Antelmann 2000; DeLapp and LeBoeuf 2004; Schaumann and LeBoeuf 2005). While weakly pronounced glass transitions were detected in dry samples in open systems (e.g., DeLapp and LeBoeuf 2004; Schaumann and LeBoeuf 2005), well pronounced transitions were observed in air-dried samples, if the pans were hermetically sealed (Schaumann and Antelmann 2000; Schaumann and LeBoeuf 2005). The latter disappear in a second DSC run directly following the first one, but reappear after some days of storage. Due to their only slowly reversing character, the transitions do not fully match classical glass transition behavior (Seyler 1994), although they are accompanied by matrix softening (Schaumann and LeBoeuf 2005; Schaumann et al. 2005b). To distinguish them from the classical type, they are called glass transition-like step transitions. These transitions are an important part of the glass transition behavior of NOM.

Both transition mechanisms are differently linked with OM glassiness. While aromatic structures are made responsible for increased glassiness in NOM in the classical glass transition (e.g., LeBoeuf and Weber Jr. 2000a, 2000b; Xing 2001), the hydrogen bond-based crosslinking model (HBCL) suggested by Schaumann and LeBoeuf makes water bridges between individual structural units responsible for the glassiness of air-dried SOM (Schaumann 2005; Schaumann and LeBoeuf 2005). Although needing verification by spectroscopic methods (Schaumann 2005; Schaumann and LeBoeuf 2005), the model is in accordance with the mechanism assumed for antiplasticizing properties of water in the literature (e.g., Illinger 1977; Guo 1993) and provides explanations for the disappearance of the transition in a second heating run and for the lower T_g and *DC* in open systems (Schaumann and LeBoeuf 2005).

Although identified in some soil samples (DeLapp and LeBoeuf 2004; Schaumann and LeBoeuf 2005), it is still uncertain, whether glass transition behavior is representative of SOM. Furthermore, it is unknown, which properties of the organic substances control temperature and intensity of the transitions. The SOM content as well as structural properties such as crosslinking density (McKenna 1989; LeBoeuf and Weber Jr. 2000a; Lu and Pignatello 2004), degree of decomposition (LeBoeuf and Weber Jr. 2000a), and degree of

swelling (LeBoeuf and Weber Jr. 1997; Schaumann and LeBoeuf 2005), may represent important factors of influence. Water has been found to act as plasticizer in humic substances (LeBoeuf and Weber Jr. 1997) and in a whole soil sample (Schaumann and Antelmann 2000). Results of Schaumann and LeBoeuf (2005), however, suggest an additional antiplasticizing function of water in a peat sample at water contents below 12 %.

The objective of this study was to examine to which extent glass transition behavior represents a common characteristic of SOM. Soil samples from various locations were investigated with respect to their glass transition behavior and the influence of amount and quality of SOM. We investigated possible contributions of individual SOM fractions, including humic acids, fulvic acids, particulate organic matter (POM), and mineral-associated organic matter (MOM).

4.3. Experimental Section

4.3.1. Samples

The soil samples represent pooled samples from four locations and a higher number of individual samples from two heterogeneous sites (Tab. 4.1). For the forest locations F and C, samples from different soil horizons were investigated with respect to the influence of the profile depth on the glass transition behavior. With the samples from Siberia (S), samples from a number of natural landscapes were incorporated. These were compared to samples from locations subjected to anthropogenic impacts. In addition to agricultural samples (A), samples from the inner-city park Tiergarten (T) and the former sewage field Berlin-Buch (B) were analyzed. These two locations are characterized by a small-scale heterogeneity of all soil properties, and therefore, a large number of individual samples instead of pooled samples was investigated.

All soil samples were air-dried and equilibrated for at least three weeks at 20 °C in a defined relative humidity (RH) of 76 %. Subsamples were ashed at 550 °C for 2 h before the measurements. The organic matter (OM) content was determined by the loss on ignition. To investigate the contribution of OM to the step transitions, additional subsamples were oxidized gently by wet-chemical methods to avoid thermal alteration of the mineral matrix (Kaiser and Guggenberger 2003). These wet-chemical oxidations were performed with H_2SO_4 (97 %), H_2O_2 (30 %), or bromine. The soil samples were brought into contact with the oxidants for 9 days under stirring (at 50 °C for H_2O_2 and 20 °C for H_2SO_4 and bromine). The remaining bromine then was destroyed by sodium thiosulfate. After filtration, the oxidized samples were washed with distilled water, dried at 105 °C, and equilibrated in 76 % RH. The oxidation with H_2O_2 and bromine was carried out with all Siberia samples, one Chorin sample, and one Buch sample. Due to the poor result (destruction of 19 % OM related to the loss on ignition), the H_2SO_4 oxidation was performed only with one Buch sample.

Tab. 4.1. Characterization of the soil samples (Q: water content on dry mass basis) and references for comprehensive descriptions of the locations.

Sample group	Description of the locations	Locations	Soil type	Soil texture	Horizon	OM content [%]	Θ [%] of air-dried samples
F: forest soils, 11 samples (1)	4 spruce forest locations (F1-F4) in Bavaria and Baden-Württemberg, Germany (Level II monitoring plots under EU legislation)	F1 (Flossenbürg)	Podzol	sandy loam	O_f O_h A_h B_h	74.0 37.1 14.3 14.6	4.7 ± 0.1 3.3 ± 0.1 1.5 ± 0.1 2.2 ± 0.1
		F2 (Rothenkirchen)	Cambisol	clay	O_f O_h A_h	92.4 79.7 71.2	5.6 ± 0.1 5.7 ± 0.1 6.2 ± 0.1
		F3 (Sonthofen)	Cambisol	clay	O_{fh} A_h	86.4 10.4	6.2 ± 0.1 1.3 ± 0.1
		F4 (Ochsenhausen)	Luvisol	loam	L O_h	73.9 42.3	5.2 ± 0.1 3.4 ± 0.1
C: Chorin, 6 samples (2,3)	beech forest in biosphere reserve Schorfheide-Chorin of a terminal moraine landscape 75 km north-eastern from Berlin	Chorin	Cambisol	sand	O_f A_{h1} A_{h2} $(B_v)A_h$ $B_v(A_h)$ B_v	37.8 10.4 3.8 3.0 2.3 1.1	0.9 ± 0.1 0.6 ± 0.1 0.3 ± 0.1 0.3 ± 0.1 0.2 ± 0.1 0.2 ± 0.1
S: Siberia, 15 samples (4)	9 sites in different climatic zones of Siberia	southern taiga	4 Luvisols	loam	O A_h	50 - 67 7 - 25	4.1 - 6.3 0.4 - 3.0
		forest steppe	3 Chernozems	loam	A_h	10 - 17	1.5 - 3.0
		mountain forest steppe	1 Luvisol	loam	A_h	11.8	1.5 ± 0.6
		steppe	4 Chernozems	loam	A_h	7 - 15	0.9 - 1.8
A: agricultural soils, 4 samples (5-7)	fertilized and non-fertilized plots of "Static Fertilization Experiments" in Halle and Bad Lauchstädt in Sachsen-Anhalt, Germany	Halle	Phaeozem, used for tillage since 1878	silt	A_p (0-30 cm)	1.9 (non-fertilized), 2.9 (fertilized)	0.8 ± 0.1 1.0 ± 0.1
		Bad Lauchstädt	Chernozem, used for tillage since 1902	silty clay loam	A_p (0-20 cm)	27.4 (non-fertilized), 41.0 (fertilized)	2.0 ± 0.1 2.1 ± 0.1
T: Tiergarten, 23 samples (3,8)	inner-city park Tiergarten in Berlin	Tiergarten	heterogeneous anthropogenic soil with construction waste, etc.	sand	upper 10 cm	4 - 23	0.4 - 2.3
B: Buch, 43 samples (8,9)	former sewage field in the north of Berlin (used until 1985)	Buch	anthropogenic soil with partially elevated C_{org} contents	sand	upper 10 cm	3 - 32	0.9 - 1.6

References in Tab. 4.1:

1: Kölling 2000; 2: Ellerbrock et al. 2005; 3: Schaumann et al. 2005a; 4: Siewert 2001; 5: Merbach et al. 2000; 6: Leinweber et al. 1992; 7: Thiele-Bruhn et al. 2004; 8: Chapter 3.3.2 of this thesis; 9: Täumer et al. 2005

For one Chorin sample and two Tiergarten samples, humic fractions were isolated according to the IHSS method (Swift 1996). Different from this method, the demineralization of the humin fraction was omitted because of the expected extreme sample alteration by HF treatment. For three samples of the location F1 and one Chorin sample, POM and MOM fractions were separated according to the method described by Cambardella and Elliott (1992). Before DSC measurement, all oxidized and fractionated samples were stored for at least three weeks in 76 % RH at 20 °C.

4.3.2. Thermogravimetry

Thermogravimetry (TG) was conducted with a Mettler Toledo STGA 851e thermogravimetric system (Mettler Toledo, Switzerland) under dry air at a flow rate of 200 mL min^{-1}. 0.2 to 1 g of the sample were placed into a ceramics crucible with an Al_2O_3 filled crucible used as a reference. The sample was heated with 5 K min^{-1} from 25 °C to 950 °C. In the resulting thermograms, the first derivative of the sample weight (DTG) and the differential thermal analysis (DTA) signal are plotted as a function of temperature. TG measurements were carried out for one Chorin sample, all Siberia samples, 14 Tiergarten, and 38 Buch samples.

4.3.3. DSC experiments

The samples were analyzed with the TA Instruments Q1000 DSC (TA Instruments, Germany) with a Refrigerated Cooling System (RCS) and nitrogen as purge gas (50 mL min^{-1}). Heat flow and temperature calibration was performed with indium at 10 K min^{-1}. In hermetically sealed standard aluminum pans, 2 to 20 mg of the samples were heated from -50 °C to 110 °C with a heating rate of 10 K min^{-1}. Further DSC measurements were carried out in pans in which three holes were punched. In these open pans, the air-dried samples were thermally pretreated for 30 min at 110 °C to remove all water before the DSC scans.

Samples were additionally investigated with temperature-modulated DSC (MDSC). For these MDSC measurements between -50 °C and 110 °C, the heating rate of 2.5 K min^{-1} was modulated by a sinusoidal oscillation with 90 s modulation period and ± 2 °C temperature amplitude. By means of Fourier transformation, the total heat flow can be divided into a reversing and a non-reversing heat flow. In this way, a differentiation between fast processes (reversing heat flow) and slow processes (non-reversing heat flow) is possible. Classical glass transitions reveal reversing characteristics, and structural relaxation and evaporation are non-reversing processes (Hutchinson 1998; Young and LeBoeuf 2000).

DSC data analysis was performed with the Thermal Advantage V4.0 software (TA Instruments). The DSC thermograms exhibit more or less pronounced curvatures attributed to unavoidable water evaporation. To diminish this curvilinearity, the thermogram of an immediately following second DSC run was subtracted, if it was free of thermal events. Glass transitions and glass transition-like step transitions are reflected by a step in the thermogram, which can be accompanied by an annealing peak. We assign the symbols T_g and T_g^* to the transition temperatures of the classical glass transition and the glass transition-like step transition, the asterisk (*) indicating the only slowly reversing behavior of the latter (see introduction). For the evaluation of step transitions in the baseline-corrected thermograms, three tangent lines are applied (Fig. 4.1). The transition temperature (T_g^* or T_g) is defined as the temperature at the half height of the central tangent line. The change of the heat capacity *DC* as a measure for the transition intensity is calculated from the difference between the first and the third tangent line at the transition temperature and is related to the sample mass.

All measurements were executed with three replications. By variation of the evaluation limits, maximum errors of evaluation were derived. Additionally, 95 % confidence intervals were determined for T_g, T_g^*, and *DC*. The errors of the data given in the text correspond to the higher value of the respective evaluation error – confidence interval pair.

4.4. Results and Discussion

Fig. 4.1 shows DSC thermograms of the horizons of the haplic Podzol profile of the forest location F1. The shape of the thermograms is representative of all thermograms of the air-dried samples for which step transitions were observed. As no thermal events were detected below 0 °C, only the temperature range above 0 °C is displayed in the graphs. In accordance with the findings of Schaumann and LeBoeuf (2005), the step transitions were only detected in hermetically sealed pans and disappeared or decreased significantly in immediately following second DSC scans. Due to their only slowly reversing character, these transitions are attributed to glass transition-like step transitions. TMA measurements carried out by Schaumann et al. (2005b) for selected soil samples of groups discussed in this work show increased softening around T_g^* for all investigated samples and thus indicate a decrease in matrix rigidity related with the transitions (Schaumann et al. 2005b).

Because of the lack of thermal events, the DSC thermograms of scans carried out immediately following the first ones were applied for baseline correction. For most samples, the thermogram of the second heating run reveals a comparable curvature as the first one, but shows no step transition. In some cases, part of the endothermic peak persists in the second runs (O_f and O_h horizons in Fig. 4.1, O_h horizon from the forest location F4 in Fig. 4.2, and POM and MOM fractions of the O_h horizon in Fig. 4.9). However, these thermograms do not reveal a step and are thus judged appropriate for baseline correction in order to improve the evaluability of T_g^* and *DC*. Consequently, after subtracting the second from the first runs, the

resulting overshoot peaks may be smaller than in the original thermograms, but *DC* is unaffected. The nature of this persistent endothermic peak will be described in chapter 5.

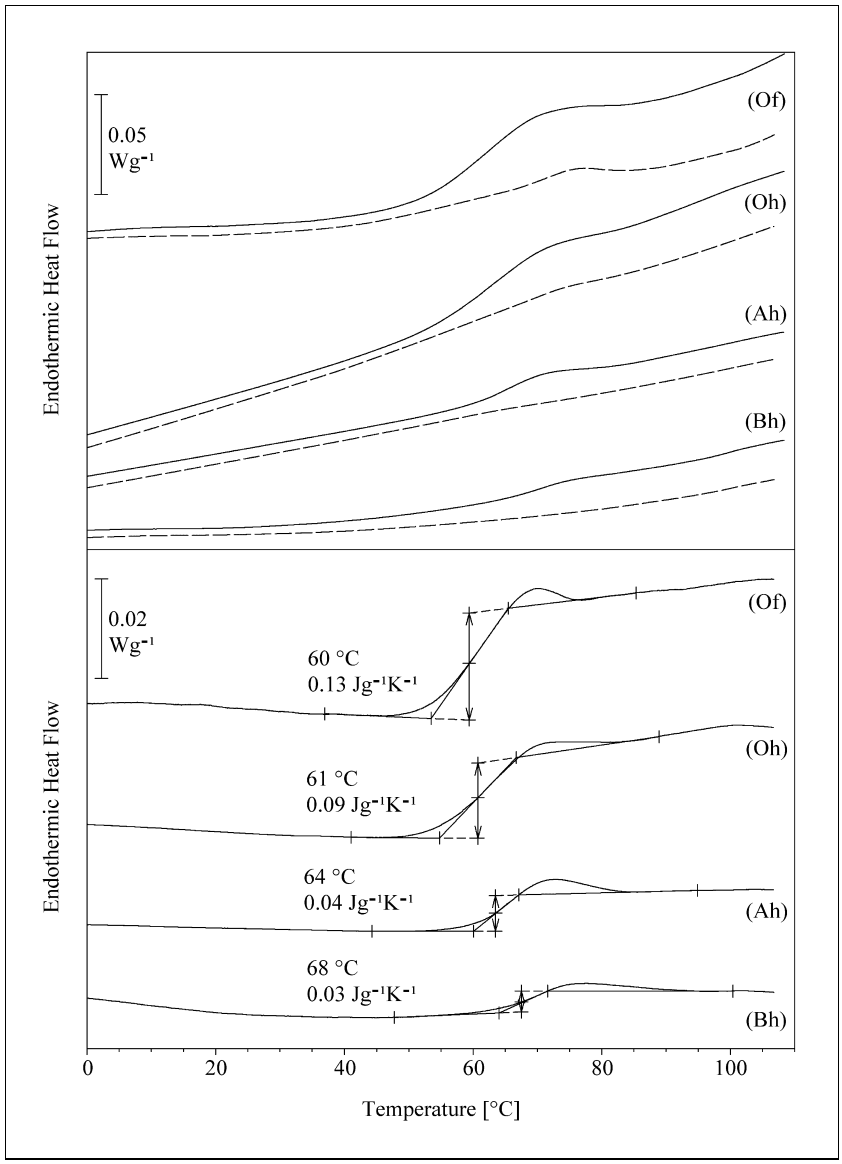

Fig. 4.1. DSC thermograms of air-dried samples of the different horizons of the forest location F1. The upper graph shows the original DSC curves (first run: solid line, second run: dashed line). The graph below shows the DSC curves after baseline correction (subtraction of the second run from the first run).

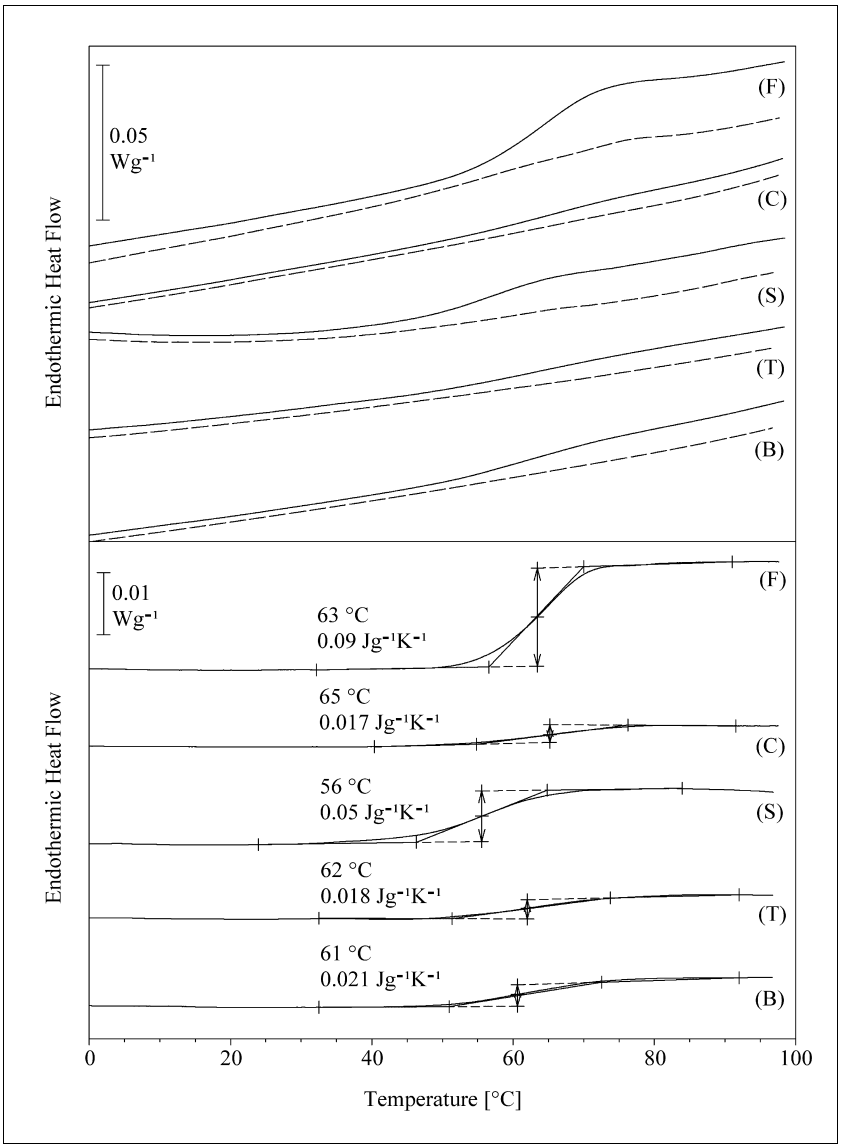

Fig. 4.2. DSC baseline corrections for air-dried samples of the different sample groups (F: O_h horizon of the forest location F4, C: A_{h1} horizon of the location Chorin, S: A_h horizon of the southern taiga, T: Tiergarten sample, B: Buch sample). The upper graph shows the original DSC curves (first run: solid line, second run: dashed line). The graph below shows the DSC curves after baseline correction (subtraction of the second run from the first run).

Only for some measurements, the curve progressions of the first and the second run were not parallel in the whole temperature range. Especially for the temperatures above 100 °C, evaporation of water may cause different curvatures of the consecutive runs. In Fig. 4.3, two DSC thermograms yielding transition regions, which are difficult to evaluate due to the non-parallel curve progressions of the subsequent runs, are shown exemplarily. Nevertheless, the comparison of both runs indicate a step transition. Differences in curvature between first and second run cause remaining curvatures in the resulting difference curves (Fig. 4.3). In such curved thermograms, the choice of the limits for the evaluation of the step transitions is difficult and influences the results for T_g^* and *DC*. In these cases, the DSC measurements were repeated.

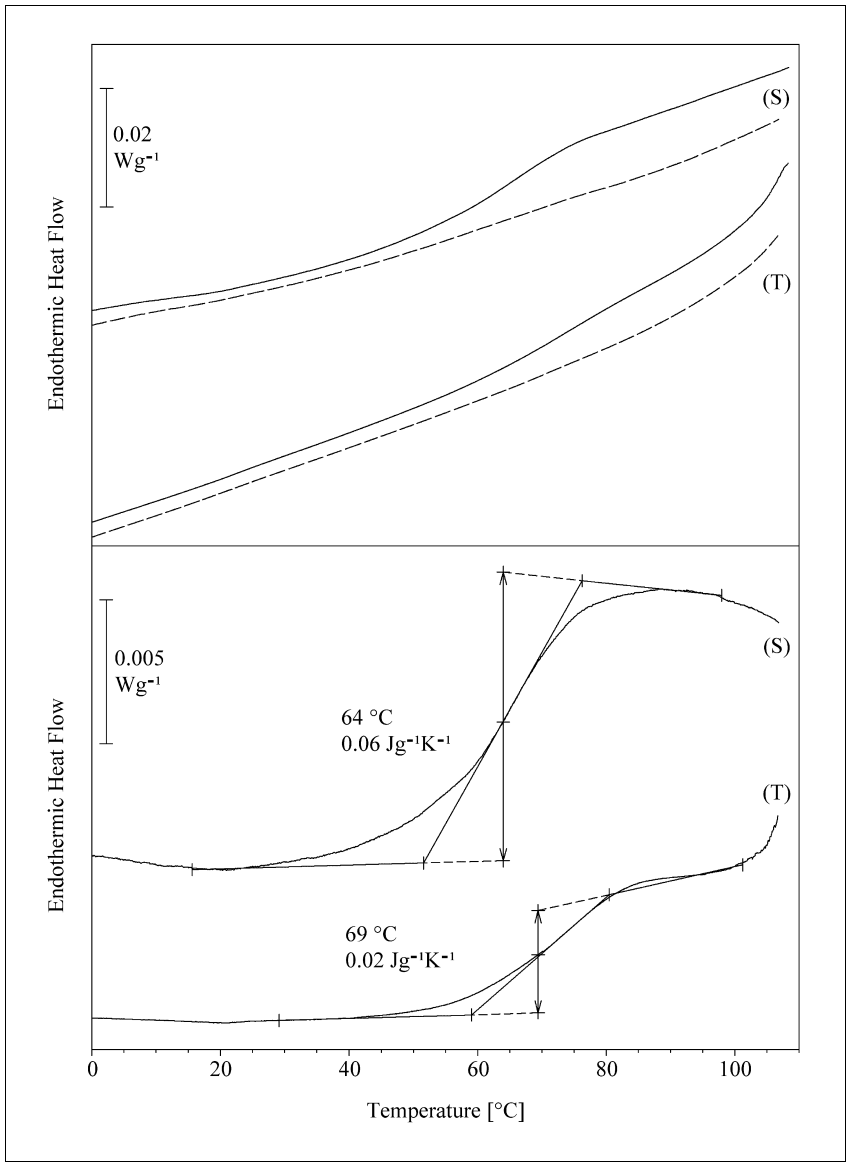

Fig. 4.3. DSC thermograms, which are difficult to evaluate, of an air-dried A_h sample of the southern taiga in Siberia (S) and an air-dried sample from the Tiergarten (T). The upper graph shows the original DSC curves (first run: solid line, second run: dashed line). The graph below shows the DSC curves after baseline correction (subtraction of the second run from the first run).

For the MDSC measurements (Fig. 4.4), it is difficult to decide whether the transitions in the total heat flow represent a step transition or rather solely an endothermic peak. However, the reversing and the non-reversing heat flow show a step transition, which is accompanied by a distinct enthalpic overshoot peak in the non-reversing heat flow (Fig. 4.4). The transition intensity of all investigated samples is divided into contributions of the reversing and the non-reversing heat flows. For the O_h horizon of the forest location F1, the contributions of both heat flows to *DC* are comparable.

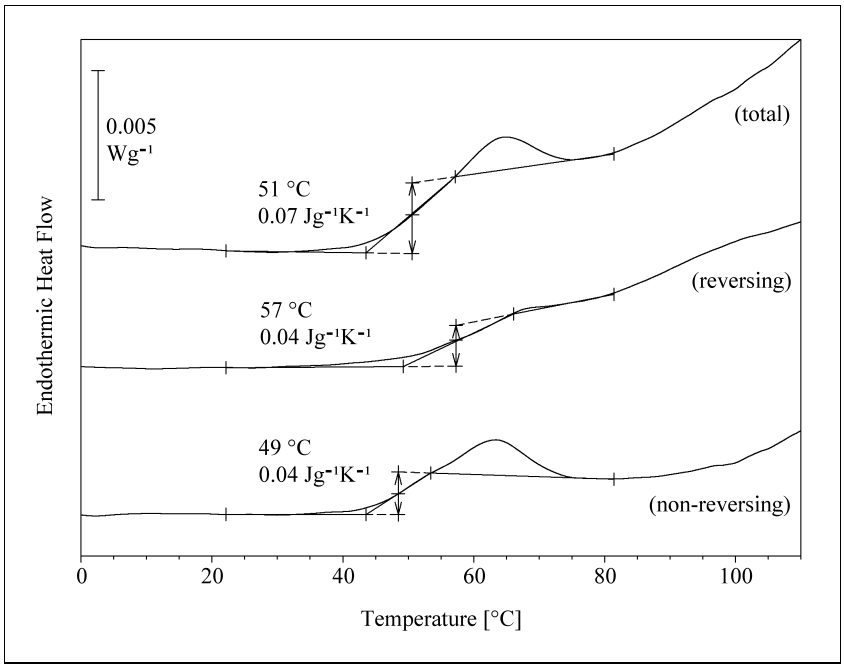

Fig. 4.4. Representative MDSC thermogram of the air-dried O_h sample of the forest location F1.

In water-free samples, the transitions become reversible, shift to significantly lower temperatures and decrease in intensity and broadness (Fig. 4.6). These transitions correspond to the classical type. Because of their low intensity, it was not possible to evaluate them quantitatively. This work thus focuses on the more intensive non-reversing transition type.

Tab. 4.2 gives an overview of the transition parameters of all samples. In addition to *DC* related to the whole sample, DC_{OM}, which is related to the mass of SOM, is specified. T_g^* ranges between 51 °C and 67 °C for all analyzed samples, giving additional support to the assumption of a superordinate factor controlling matrix rigidity like the postulated water bridges (Schaumann and LeBoeuf 2005).

In all air-dried samples of the forest locations F, step transitions were detected between 59 °C and 67 °C with *DC* between 0.02 and 0.20 J g^{-1} K^{-1}. 13 out of the 15 samples from Siberia also reveal step transitions (T_g^* between 51 °C and 59 °C and *DC* between 0.02 and 0.11 J g^{-1} K^{-1}). For the forest location Chorin, step transitions of decreasing intensity with increasing soil depth were observed in the upper four horizons.

In the forest locations of the sample groups F1, F3, and F4, T_g^* slightly increases with soil depth. Within the F2, Siberia, and Chorin profiles, no significant variation of T_g^* was measured. The differences in T_g^* development with soil depth underline the overlay of the different mechanisms affecting matrix rigidity. The higher T_g^* values of the deeper soil layers of the F1, F3, and F4 samples may be related to a more condensed structure of the organic substances due to decomposition processes, which is in accordance with the following studies: Thermogravimetric analysis, pyrolysis-GC/MS, and CPMAS ^{13}C NMR studies (Cuypers et al. 2002) suggest that humified SOM is more condensed than the original

material. Additionally, pyrolysis-mass spectrometry measurements (Schulten and Leinweber 1996) point to progressive crosslinking of lignin building blocks, alkylaromatics, lipids, and N-containing compounds by aryl-alkyl combinations with increasing SOM turnover. X-ray diffraction (Xing and Chen 1999) also indicates more condensed aromatic structures in deeper soil horizons. Furthermore, Kögel-Knabner (1997) showed an increasing rigidity of the alkyl chains with increasing depth in forest soils by means of the ^{13}C NMR dipolar dephasing technique.

Tab. 4.2. Characteristics of observed step transitions in the analyzed samples (n.d: not detectable).

Sample group	location, horizon (or OM range)	samples with a step transition (whole sample number)	T_g^* (° C)	DC (J g^{-1} K^{-1}) related to sample mass	DC_{OM} (J g^{-1} K^{-1}) related to OM mass
F	F1, O_f	1 (1)	60 ± 1	0.14 ± 0.02	0.19 ± 0.03
	F1, O_h	1 (1)	61 ± 1	0.07 ± 0.02	0.18 ± 0.07
	F1, A_h	1 (1)	63 ± 1	0.04 ± 0.01	0.30 ± 0.03
	F1, B_h	1 (1)	67 ± 1	0.04 ± 0.01	0.31 ± 0.02
	F2, O_f	1 (1)	60 ± 1	0.20 ± 0.01	0.21 ± 0.01
	F2, O_h	1 (1)	60 ± 1	0.18 ± 0.02	0.23 ± 0.03
	F2, A_h	1 (1)	59 ± 1	0.13 ± 0.01	0.18 ± 0.02
	F3, O_{fh}	1 (1)	61 ± 1	0.19 ± 0.04	0.22 ± 0.05
	F3, A_h	1 (1)	65 ± 3	0.02 ± 0.01	0.20 ± 0.05
	F4, L	1 (1)	61 ± 1	0.13 ± 0.01	0.17 ± 0.01
	F4, O_h	1 (1)	63 ± 2	0.09 ± 0.01	0.21 ± 0.02
C	Chorin, O_f	1 (1)	67 ± 2	0.10 ± 0.04	0.26 ± 0.09
	Chorin, A_{h1}	1 (1)	66 ± 2	0.02 ± 0.01	0.20 ± 0.04
	Chorin, A_{h2}	1 (1)	65 ± 3	0.01 ± 0.01	0.28 ± 0.01
	Chorin, $(B_v)A_h$	1 (1)	64 ± 1	0.01 ± 0.01	0.34 ± 0.05
	Chorin, $B_v(A_h)$	0 (1)	n.d.	n.d.	n.d.
	Chorin, B_v	0 (1)	n.d.	n.d.	n.d.
S	southern taiga, O	3 (3)	55 ± 1	0.11 ± 0.01	0.19 ± 0.02
	southern taiga, A_h	3 (4)	56 ± 3	0.04 ± 0.01	0.23 ± 0.06
	forest steppe, A_h	2 (3)	59 ± 4	0.03 ± 0.01	0.21 ± 0.05
	mountain forest steppe, A_h	1 (1)	58 ± 2	0.04 ± 0.01	0.36 ± 0.04
	steppe, A_h	4 (4)	51 ± 1	0.02 ± 0.01	0.18 ± 0.04
A	Halle, A_p	0 (2)	n.d.	n.d.	n.d.
	Bad Lauchstädt, A_p	0 (2)	n.d.	n.d.	n.d.
T	Tiergarten, OM < 7.6	0 (4)	n.d.	n.d.	n.d.
	Tiergarten, OM ≥ 7.6	6 (19)	63 ± 1	0.014 ± 0.001	0.13 ± 0.01
B	Buch, OM < 5.8	0 (7)	n.d.	n.d.	n.d.
	Buch, OM ≥ 5.8	18 (36)	62 ± 3	0.014 ± 0.002	0.13 ± 0.01

While DC decreases with soil depth in all studied soil profiles, DC_{OM} does not correlate with the profile depth in a uniform way. For the natural sample groups F, C, and S, DC_{OM} is higher than for the anthropogenic T and B samples. Different from the natural locations, only a low number of samples from the anthropogenic locations Tiergarten, Buch, Halle, and Bad

Lauchstädt revealed step transitions. The transition characteristics of the Tiergarten and Buch samples reflect the high heterogeneity of these sites. Glass transition-like step transitions were identified in only 6 out of 23 Tiergarten samples and 18 out of 42 Buch samples, and only in samples with OM contents above (7.6 ± 0.1) % and (5.8 ± 0.1) %, respectively. Due to the small number of step transitions and their low intensity, it is not possible to correlate the transition characteristics to other soil properties of these heterogeneous sites. The absence of transitions may be either due to low detectability or to T_g^* below or above the investigated temperature range. The latter would suggest linear or nonlinear sorption isotherms, respectively.

Fig. 4.5 illustrates the interrelation between *DC* and the OM content for all samples revealing glass transition-like step transitions. Despite the variance of data, the OM contents and *DC* values correlate significantly ($P < 0.0001$). For the classical glass transitions in the water-free samples, no correlation between *DC* and OM content was detected, probably due to their low intensity ranging in the limits of detectability.

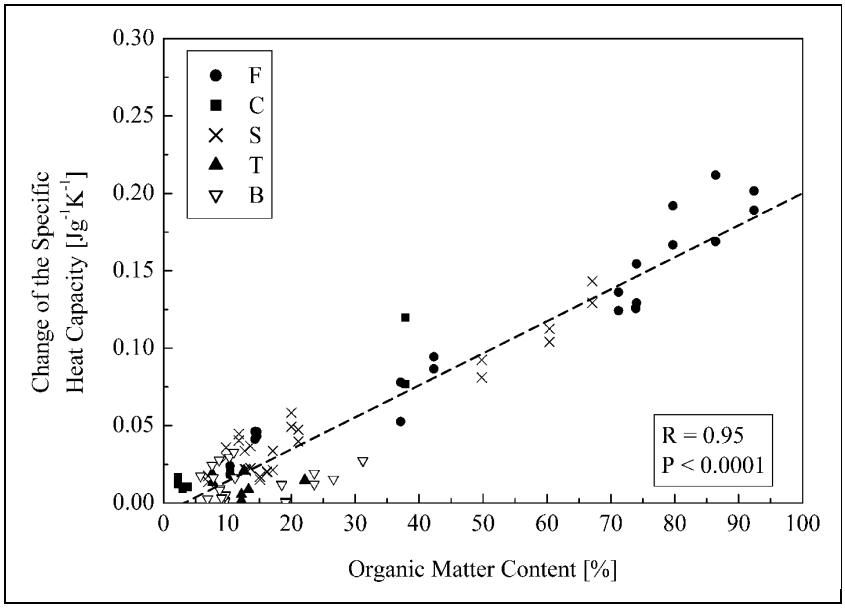

Fig. 4.5. Change of the heat capacity *DC* as a function of OM content for the air-dried samples. The figure contains a linear regression line calculated for the whole sample collective.

To further test the hypothesis that OM is involved in the step transitions, the samples were treated by different methods to remove OM. The oxidants H_2SO_4, H_2O_2, and bromine destroyed less organic material than the dry combustion. For most samples, the degree of efficiency increased in the order H_2SO_4, bromine, and H_2O_2. On average, the removal of OM amounts to (37 ± 10) % for bromine and (55 ± 20) % for H_2O_2 related to the loss on ignition. After all oxidation procedures and equilibration in 76 % RH, the step transitions decreased in intensity (Fig. 4.6). Only if the OM contents were reduced below 10 %, no glass transition-like step transitions were detected any more in the DSC thermograms (see A_{h1} sample of the

location Chorin in Fig. 4.6). For the samples which still reveal OM contents above 10 % after oxidation, there is a weak correlation between the OM contents and the *DC* values of the step transitions ($P < 0.004$).

The small transition intensity of samples with low C_{org} and their disappearance after removal of organic matter support the hypothesized interrelation with SOM. Even if it is assumed that each oxidation method also changes the mineral compounds, it is improbable that the mineral matrix alone is responsible for the transition. Otherwise, all oxidation methods would have to change the mineral soil phase in the same way. Either bulk SOM or organo-mineral interactions are most probably responsible for the transitions. The differences in DC_{OM} (Tab. 4.2), however, indicate effects of OM quality. The comparably low DC_{OM} of the anthropogenic locations Tiergarten and Buch point to a site-specific influence on transition intensity.

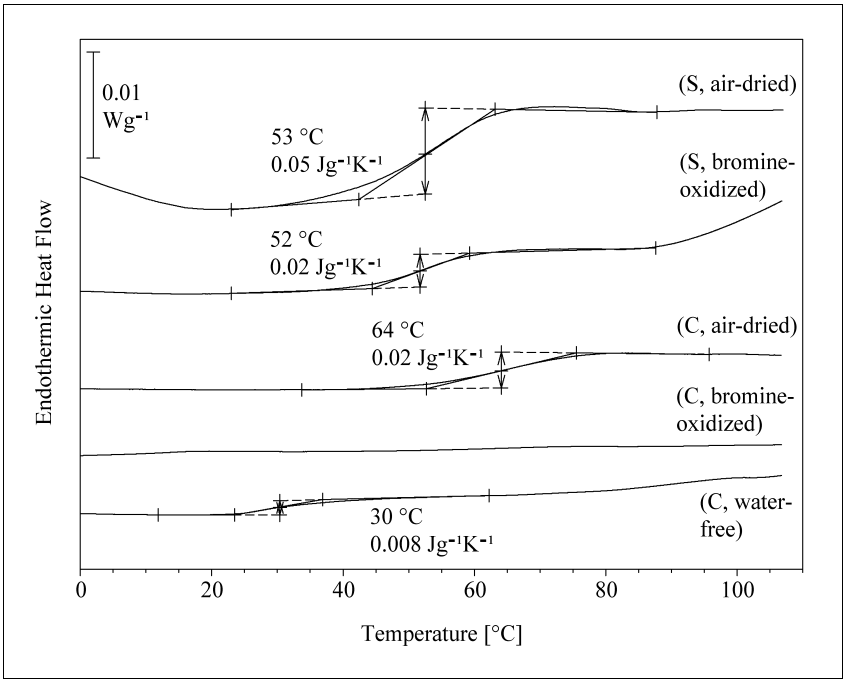

Fig. 4.6. DSC thermograms of air-dried and bromine-oxidized samples (C: A_{h1} horizon of the location Chorin (7.5 % OM after oxidation), S: A_h horizon of the southern taiga in Siberia (11.4 % OM after oxidation)). For the A_{h1} sample of the location Chorin (C), the glass transition of the water-free sample after a thermal pretreatment (open pan) is shown additionally. With the exception of the measurement in the open pan, the graph shows the DSC curves after baseline correction (subtraction of the second run from the first run).

In the tillage samples, changes of the structural composition of SOM by agricultural management, like a decrease of labile SOM fractions, containing peptides, lipids, carbohydrates, and an increase of recalcitrant N-heterocycles and polymethylen-type structures (Schulten and Leinweber 1996; Capriel 1997), may reduce the number of hydrogen bond sites and with that transition intensity. A similar effect can be assumed for Tiergarten and Buch. The inter-

relation between hydrogen bond sites and the glass transition-like behavior would further support the proposed HBCL model. In terms of this model, a large part of OM of anthropogenic locations is rubbery at ambient temperatures, causing linear sorption isotherms.

The TG thermograms of the different soil samples indicate three temperature ranges of distinct weight losses (Fig. 4.7), which is in consistence with classic thermogravimetric behavior of SOM (Shurygina et al. 1971; Schulten et al. 1993; Zuyi et al. 1997; Cuypers et al. 2002). The weight loss between 25 °C and 165 °C is caused by the water, which has remained in the sample despite of the previous tempering at 120 °C. The DTG peak between 130 °C and 320 °C is related to exothermic decarboxylation and dehydration reactions of thermo-labile compounds such as fatty acids, peptides, carbohydrates, cellulose, and hemicellulose. The exothermic process between 320 °C and 600 °C is due to the decomposition of thermostable SOM compounds with high C/H ratios (e.g. condensed aromatic nuclei) or the destruction of organo-mineral complexes. Tab. 4.3 summarizes the weight losses of the three temperature ranges for all the studied samples.

To obtain first indications whether black carbon may be responsible for the observed glass transition-like step transition, we divided the TG weight losses (Fig. 4.7) into a non-BC portion between 200 °C and 375 °C and a BC portion above 375 °C, in analogy to the thermal oxidation method applied by Cornelissen et al. (2004). No significant correlation between the weight losses above 375 °C and the DC_{OM} values was detected (Fig. 4.8). This may be due to either the absence of BC contribution to the transitions or to methodical restrictions, as (i) the combustion time in TG differs from that used by Cornelissen et al. (2004) or (ii) the combustion produces new thermostable substances above 375 °C which may reveal glassy character, but are not present in the samples before the combustion. For a definitive evidence of an interrelation between BC and the step transition characteristics, more detailed studies are required.

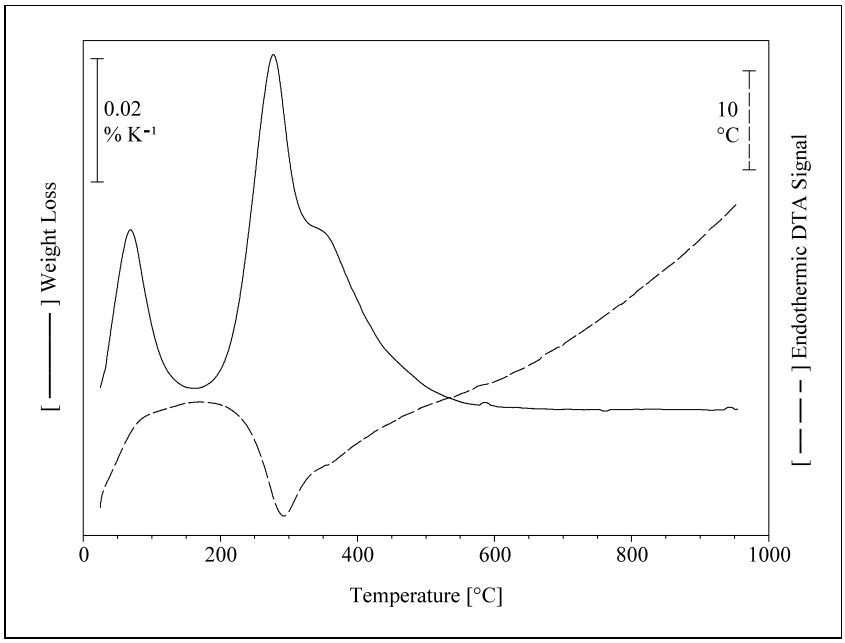

Fig. 4.7. Representative DTG and DTA signal of the air-dried A_{h1} sample of the location Chorin.

Tab. 4.3. Weight losses of the three characteristic temperature ranges (peaks 1-3) of the studied samples. For each sample, the limits of the temperature ranges were chosen corresponding to the minima between the peaks in the DTA signal.

Sample group	location, horizon	peak 1 start [° C]	peak 1 end [° C]	peak 1 weight loss [%]	peak 2 start [° C]	peak 2 end [° C]	peak 2 weight loss [%]	peak 3 start [° C]	peak 3 end [° C]	peak 3 weight loss [%]
C	Chorin, O_f	25	150	6.4 ± 0.1	150	340	20.7 ± 0.1	340	600	12.3 ± 0.1
	Chorin, A_{h1}	25	165	1.8 ± 0.1	165	320	4.2 ± 0.3	320	600	3.1 ± 0.3
	Chorin, A_{h2}	25	165	0.9 ± 0.1	165	320	1.6 ± 0.1	320	600	1.3 ± 0.1
	Chorin, $(B_v)A_h$	25	165	0.9 ± 0.1	165	320	1.3 ± 0.1	320	600	2 ± 1
	Chorin, $B_v(A_h)$	25	165	0.8 ± 0.1	165	330	1.0 ± 0.1	330	600	0.8 ± 0.1
	Chorin, B_v	25	165	0.5 ± 0.1	165	340	0.4 ± 0.1	340	600	0.4 ± 0.1
S	southern taiga, O	25	170	12 ± 2	170	320	29 ± 4	320	600	24 ± 2
	southern taiga, A_h	25	190	6 ± 2	190	330	7 ± 3	330	600	7 ± 2
	forest steppe, A_h	25	200	7 ± 2	200	340	6.7 ± 0.7	340	600	7 ± 2
	mountain forest steppe, A_h	25	180	4.4 ± 0.2	180	330	6.0 ± 0.2	330	188	5.3 ± 0.2
	steppe, A_h	25	200	5.5 ± 0.4	200	350	7 ± 1	350	600	6 ± 1
T	Tiergarten	25	175	1.9 ± 0.3	175	315	4 ± 1	315	600	3 ± 1
B	Buch	25	175	2.1 ± 0.2	175	340	4.3 ± 0.4	340	600	3.3 ± 0.3

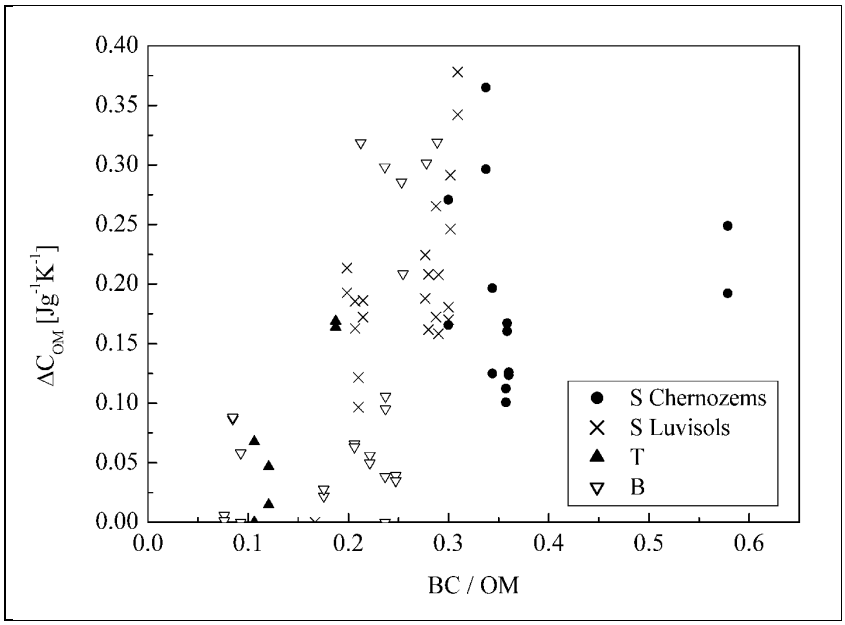

Fig. 4.8. Change of the specific heat capacity which is related to the mass of SOM (DC_{OM}) as a function of the ratio of the weight loss above 375 °C (assumed to be related to BC) and the OM content of the samples from Siberia, Tiergarten, and Buch. The Siberia samples are divided into Chernozems and Luvisols.

In order to test whether POM and MOM exhibit different transition behavior, they were analyzed separately (Fig. 4.9). As expected, in the O_h horizon of the F1 profile, the POM content is distinctly higher than the MOM content ((26 ± 1) % POM and (11 ± 1) % MOM). Between A_h and B_h horizon, POM and MOM contents do not differ significantly ((3 ± 1) % POM and (12 ± 1) % MOM in A_h and (2 ± 1) % POM and (11 ± 1) % MOM in B_h). POM and MOM fractions reveal comparable transitions in all investigated samples (Fig. 4.9). As in the originating samples, the transitions of the POM and the MOM fractions represent a combination of step and endothermic peak for the O and A horizons. In the B horizon, the step is however insignificant. The differences in DC_{OM} of the soil samples thus cannot be directly related to organo-mineral interactions. They may be overbalanced by the interactions of hydrophilic functional groups with water.

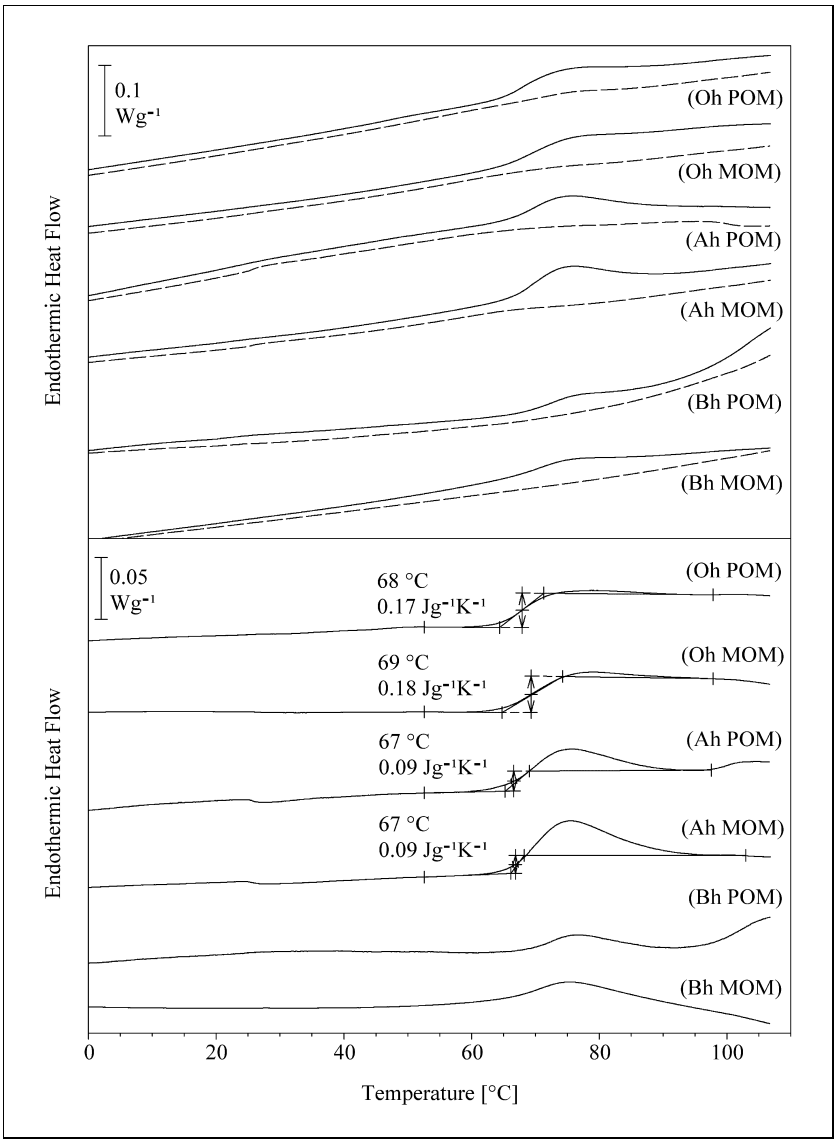

Fig. 4.9. DSC thermograms of POM and MOM fractions of samples of the forest location F1. The heat flow is related to the OM content of each fraction. The upper graph shows the original DSC curves (first run: solid line, second run: dashed line). The graph below shows the DSC curves after baseline correction (subtraction of the second run from the first run).

Fig. 4.10 exemplarily shows thermograms of the isolated humic fractions of the A_{h1} sample from Chorin, together with thermograms of the original whole sample and a mixture of the fractions according to their mass portions in the sample. Additionally, a calculated (fictive) sum curve of the four fractions is included in the graph. Since no second run could be calculated for the calculated sum curve, the thermograms in Fig. 4.10 are not baseline-corrected to better compare the respective thermograms. The curvature of the original thermograms, which is strongly pronounced for the fulvic acid, the humic acid, and the carbohydrate fractions as well as for the calculated sum curve, may result in high errors for T_g^* and *DC*, but the principal observation of a step accompanied by an endothermic peak is unaffected. The pronounced endothermic peaks of the humic and fulvic acids point to a closer

distribution of structural relaxation times linked with a more homogeneous structure of these fractions compared to the whole SOM (Cortés and Montserrat 1998; Hutchinson 1998).

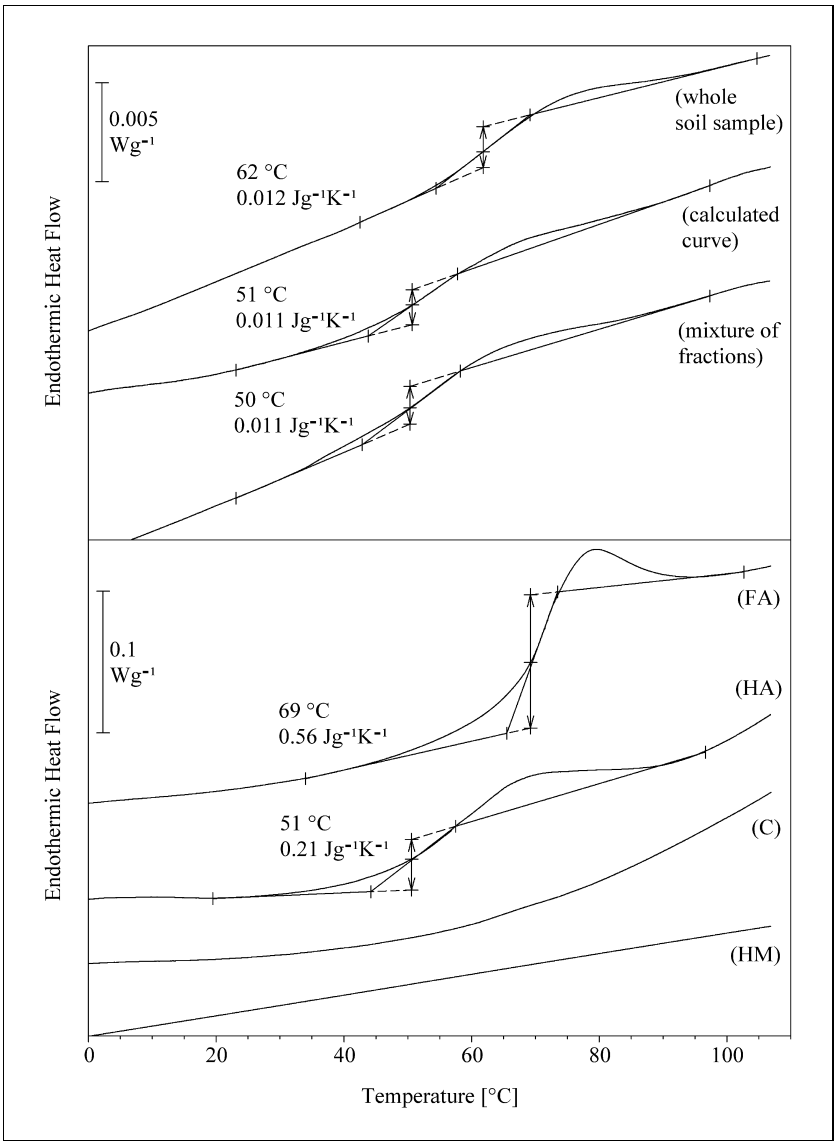

Fig. 4.10. DSC thermograms of the whole A_{h1} sample of the location Chorin and of a mixture of the humic fractions according to their mass portions in the whole sample together with a curve calculated from the thermograms of the isolated fractions (top). DSC thermograms of humic acid (HA), fulvic acid (FA), carbohydrate (C), and humin (HM) fraction of the same sample (bottom).

The humic and fulvic acids of the three samples show step transitions at (53 ± 5) °C and (69 ± 6) °C, respectively, while for the humin and carbohydrate fractions, no transitions were observed. The latter may be due to T_g^* beyond the investigated temperature range: T_g of dry cellulose, e.g., is 225 °C (Akim 1978), and the highly condensed structure of the humin fractions (Cuypers et al. 2002; Gunasekara and Xing 2003) most probably results in a T_g^* above 110 °C. Alternatively, the DSC sensitivity may be insufficient for the humin fractions, which contain only (14 ± 6) % OM, or the lower abundance of hydrophilic functional groups

does not allow for a significant vitrification by water bridges. Due to their high relevance for sorption behavior, humin fractions should be investigated with more sensitive methods such as TMA (Schaumann et al. 2005b).

The initially surprising difference between the MOM transition behavior and that of the humin fraction reflects their differences in composition: In contrast to the MOM fraction, the humin fraction does not contain fulvic or humic acid components. The MOM transitions thus are based on interactions between more hydrophilic compounds in the still heterogeneous mixture, while in the humin fraction, humin-humin interactions and organo-mineral interactions overbalance and contribute to classical transitions.

The mixture of the fractions (98.2 % humins, 1.0 % humic acids, 0.4 % fulvic acids, and 0.4 % carbohydrates) results in a thermogram qualitatively comparable to that of the original sample and to the curve calculated from the contributions of the individual fractions (Fig. 4.10). The transitions of the humic and the fulvic acids are not separated in the thermograms of the mixture, which underlines the limitation of standard DSC to separate overlapping transitions. Individual transitions thus may remain undetectable despite the high sensitivity of DSC.

The transition temperatures of the mixture, the calculated curve, and the whole soil differ within a range of 10 °C. It is improbable that different water states in the soil sample and the mixture of the fractions are responsible for these differences, because all samples were equilibrated in 76 % RH for three weeks prior to measurement and water contents in the soil sample and in the mixture then were not markedly different. Water contents differed according to the hydrophilic nature of the components ((0.1 ± 0.1) % in the humin, (2.2 ± 0.2) % in the humic acid, (10 ± 1) % in the fulvic acid, (3.9 ± 0.5) % in the carbohydrate fraction, (0.6 ± 0.1) % in the soil sample, and (0.2 ± 0.2) % in the mixture). The T_g^* differences may be explained with (i) chemical alterations during fractionation, (ii) errors in determination of the exact quantitative sample composition, and the high mass portion of the thermally inert humin fraction affecting solely the curvature, (iii) different cation contents between the fractions and the whole soil sample, or (iv) the hypothesis that the macromolecular structure has not yet formed directly after mixing the fractions. The last is supported by the observation that T_g^* of the mixture increased continually upon storage within at least 7 months. This increase points to aging effects due to structural relaxation in the young mixture, which are common for amorphous matrixes (Struik 1978).

This study suggests that glass transition-like step transitions accompanied by matrix softening occur in a number of natural soils, and transition intensity may be significantly reduced by anthropogenic impacts. The transition intensity is mainly affected by the OM content. From the differences between transition parameters for different locations, we conclude that SOM quality additionally affects the transitions. The study does not suggest involvement of the black carbon fraction; this unexpected finding, however, has to be verified in further studies. Our results point to a relation between transition intensity and the abundance of H bond

forming functional groups. This assumption will be verified with spectroscopic methods (NMR).

The results confirm the existence of two types of transitions, only one of which is related to classical glass transitions. Transitions reported by the group of LeBoeuf and Weber (e.g., LeBoeuf and Weber Jr. 1997; DeLapp and LeBoeuf 2004) are of this type. The classical glass transition characterizes structural properties of the water-free organic matrix and may be related with OM aromaticity (LeBoeuf and Weber Jr. 2000b; Xing 2001). The second transition type, here called glass transition-like step transition, shows changes in matrix rigidity with only slowly reversing character. The results suggest that glassiness is enhanced by water bridges, as hypothesized in the HBCL model (Schaumann 2005; Schaumann and LeBoeuf 2005), the formation and disruption of which are responsible for the slowly reversing behavior of this transition type. This is further supported by the rather narrow temperature range of T_g^* (51 to 67 °C), which also points to a superordinate transition mechanism. The transition depends on structural units providing hydrogen bond sites for water bridges, which may be found rather in labile and young SOM fractions. If verified by structural assessments with solid state NMR techniques, this hypothesis will provide explanations for the absence or low detectability of this transition in anthropogenically influenced sites.

The postulated water bridges (Schaumann and LeBoeuf 2005) may be easily disrupted by changes in external conditions, and glassy regions may suddenly become rubbery even at ambient temperatures below T_g^*, possibly leading to a sudden release of organic contaminants, which underlines the relevance of this type of glass transition under field conditions.

5. Influence of the sample history and the moisture status on the glass transition behavior of soil organic matter

5.1. Abstract

Recent studies indicate that glassiness represents a characteristic feature of soil organic matter (SOM). It is however unknown, to which extent the transitions detected in humic substances and whole soil samples correspond to common models of synthetic polymers providing the theoretical basis for explaining their glass transition characteristics. Physical aging associated with structural relaxation of amorphous substances below their glass temperature is one fundamental basis for the glass transition behavior of synthetic polymers. According to the results of this study, aging processes also occur in SOM. In whole soil samples, this process can be observed by the shift of glass transition-like step transitions to higher temperatures within the time scale of years. Not only the structural relaxation of the macromolecular organic substances, but also interactions with water molecules, which may exhibit both plasticizing and anti-plasticizing properties, influence the aging process of SOM. Especially under moistening or drying conditions, a differentiation between the effects of water and of alterations of the SOM structure in the course of time on the rigidity of the macromolecular network is difficult.

5.2. Introduction

In the last years, glass transitions have been discovered in humic and fulvic acids (LeBoeuf and Weber Jr. 1997) as well as in whole soil samples, sediments, and peat (Chapter 4; Schaumann and Antelmann 2000; DeLapp and LeBoeuf 2004; Schaumann and LeBoeuf 2005). To date, it is however not known whether the properties of glassy and rubbery regions in soil organic matter (SOM) are comparable to those of synthetic polymers. The interpretation of sorption isotherms of organic compounds to humous substances by a polymer model, which is based on the coexistence of properties known for the glassy and rubbery states of synthetic polymers (LeBoeuf and Weber Jr. 1997; Xing and Pignatello 1997), combined with the detection of glass transitions in SOM (Chapter 4; Schaumann and LeBoeuf 2005) supports the hypothesized comparability. However, due to the extremely heterogeneous structure of SOM in comparison with synthetic polymers, the macromolecular characteristics and processes possibly differ. The occurrence of two types of glass transitions in SOM also points to differences between the organic soil matrix and typical synthetic polymer systems, which only reveal one glass transition type.

In humous substances, in addition to a classical glass transition, which can be measured only in water-free samples, an atypical glass transition type is observable in water-containing samples. Because of the only slowly reversing character of this transition, it does not agree with the classical definition of glass transitions (Seyler 1994). To distinguish this transition type from the classical one, it is referred to as glass transition-like step transition with the

transition temperature T_g^* (see Chapter 4). The glass transition-like step transitions occur at higher temperatures and reveal higher intensities than the classical glass transitions of SOM. They can only be observed in closed systems, which prevent an evaporation of water out of the samples, and due to their only slowly reversing character, they disappear in a second run of the measurement (Chapter 4; Schaumann 2005; Schaumann and LeBoeuf 2005). The two types of glass transition behavior in SOM can be explained by the hydrogen bond-based crosslinking (HBCL) model proposed by Schaumann and LeBoeuf (Schaumann 2005; Schaumann and LeBoeuf 2005). This model supposes hydrogen bond-based crosslinks of water molecules between the molecular chains of SOM, resulting in an antiplasticization of the SOM structure for low water contents. If these crosslinks are disrupted by the removal of water out of the system, the chain mobility increases, and consequently the glass transition-like step transition shifts to significantly lower temperatures and becomes a reversible classical glass transition (Chapter 4; Schaumann 2005; Schaumann and LeBoeuf 2005). In closed pans, the glass transition-like step transition disappears in a second run of the measurement, because the water molecules have left their crosslinking positions during the heating of the first run. But, since they are still in the sample, they prevent interactions between the organic chains and with that the formation of a glassy SOM structure.

Formally, glass transitions appear to be second order transitions (McKenna 1989; Elias 1997). One deciding feature of glassiness is the occurrence of time-dependent characteristics due to the non-equilibrium nature of the glassy state (McKenna 1989; Höhne et al. 1996; Elias 1997). Consequently, glass transition events can only be insufficiently characterized by thermodynamical approaches (McKenna 1989; Höhne et al. 1996). Instead of applying classical thermodynamics, the time-dependent properties of the glassy state require kinetic models (Höhne et al. 1996). Below the glass transition temperature, amorphous polymers undergo a structural relaxation process, which also is called physical aging. In the course of this process, the physical properties of the amorphous phase change over time: These changes include reductions in segmental mobility, enthalpy, and free volume, causing an increase of density, yield stress, and elastic modulus (Struik 1978). The kinetics of enthalpy relaxation correspond to the relationship, proposed by Cowie and Ferguson (1986):

$$\Delta H(t_a, T_a) = \Delta H_\infty(T_a)\left[1 - \exp\left\{-\left(\frac{t_a}{\tau}\right)^{\beta}\right\}\right] \qquad (5.1)$$

where $DH_¥$ represents the maximum equilibrium enthalpy of the glassy matrix. t_a and T_a are annealing time and annealing temperature of the aging process, and t is the average relaxation time of the different compounds of the amorphous system undergoing the aging process at the temperature T_a. ß is the nonexponentiality parameter ($0 \le ß \le 1$), which is inversely correlated to the width of the distribution of relaxation times (Cortés and Montserrat 1998; Hutchinson 1998; Chung et al. 2004). The rate of the structural relaxation process increases with increasing annealing temperature, i.e. with decreasing difference T_g - T_a.

In well annealed glasses, endothermic annealing peaks (enthalpic overshoots) can be observed in Differential Scanning Calorimetry (DSC) thermograms. These annealing peaks reflect the aging process, which beforehand has occurred in the glassy matrix. With increasing annealing time or increasing annealing temperature during the aging process, the enthalpy loss and the peak temperature shift to higher values (Illekova 1994; Montserrat 1994; Hutchinson 1998; Chung et al. 2004), provided that T_a is distinctly below the glass temperature T_g. Additionally, the annealing peaks are influenced by the heterogeneity of the amorphous matrix. Chung et al (2004) showed that a high structural heterogeneity in starches (small *ß* values) yields a slow relaxation and with that small relaxation enthalpies, i.e. small annealing peak areas at a certain annealing time t_a. Generally, very wide distributions of relaxation times (small *ß* values) result in broad glass transition regions with weakly pronounced or no annealing peaks (Cortés and Montserrat 1998; Hutchinson 1998).

On the basis of the detected glass transition behavior of SOM (Chapter 4; DeLapp and LeBoeuf 2004; Schaumann and LeBoeuf 2005), it can be assumed that aging processes occur in soil samples, too. This study focused on the investigation of these hypothesized aging effects of SOM in unfractionated soil samples. By DSC measurements of the same samples after different periods of storage in defined relative humidities at temperatures below their glass transition-like step transitions, the influence of annealing on their thermal behavior was investigated. Due to the high heterogeneity of SOM, a wide distribution of relaxation times has to be expected for the structural relaxation process of SOM in the glassy state. This may explain that only weakly pronounced or no annealing peaks are observable in DSC thermograms of humous soil samples (Chapter 4), so that the aging process cannot be studied by means of these peaks. Consequently, the transition temperatures of the glass transition-like step transitions were applied for examining possible effects of sample storage on the glassiness of the organic soil phase.

An influence of water on aging processes is known for polymer systems in which it acts as plasticizer. Thus, Shogren (1992) performed DSC measurements for a cornstarch and observed that after sample annealing for constant periods of time t_a at a constant temperature T_a, the enthalpy of the annealing peak rose, if the moisture contents increased. The increasing enthalpy is due to the decrease of the difference $T_g - T_a$, resulting in a faster relaxation process. Only when the water content was so high that T_g was reduced below T_a, no annealing endotherm appeared any more (Shogren 1992). For aged epoxy resins, Ellis and Karasz (1986) likewise observed that the sorption of water, which also reveals plasticizing effects in this system, may result in the disappearance of annealing peaks and with that in the annihilation of all previously accumulated aging effects. For organic substances in soil, which always contain water under natural conditions, an influence of the water status on the aging process also has to be expected.

Generally, two processes which may alter the glass transition behavior of SOM in the course of time have to be taken into account: On the one hand, the pronounced influence of the water status (Chapter 4; Schaumann 2005; Schaumann and LeBoeuf 2005) is supposed to result in

slow changes of the glass transition-like step transitions. Thus, for constant low moisture contents, increasing transition temperatures in the course of time due to a gradual increase of the degree of SOM crosslinking by hydrogen bond water molecules are to be assumed. Contrary to these antiplasticizing effects of water for low water contents (Schaumann 2005; Schaumann and LeBoeuf 2005), water has been found to act as plasticizing agent in humic substances (LeBoeuf and Weber Jr. 1997) and in a soil sample for moderate to high water contents due to swelling (Schaumann and Antelmann 2000; Schaumann 2005; Schaumann and LeBoeuf 2005). Consequently, for high water contents, the transition temperatures of the glass transition-like step transitions are expected to decrease during the slow process of SOM swelling. On the other hand, a structural relaxation process of the organic substances may occur irrespective of the effects of water. Under field conditions, a differentiation of these two factors of influence is impossible, because the moisture content as well as the way of water bonding in the solid soil matrix usually change in the course of time.

As a result of possible plasticizing effects and possible antiplasticizing effects of water in SOM, the shifting of glass transition-like step transitions to higher temperatures due to possible structural relaxation processes of the organic substances in soil can be either increased or reduced by water uptake or water removal, depending on the moisture content in the system. By investigating the effect of time on the glass transition behavior of soil samples stored at different constant relative humidities, a differentiation between the effects of water and the aging effects which do not depend on the water status was attempted in this study. To the resulting water sorption data, different sorption models were applied in order to get an insight into the way of water bonding within the samples. The sorption isotherms thus were evaluated with the aim to obtain information, whether water acts as plasticizer or as antiplasticizer for the different relative humidities: Antiplasticizing effects of water require specific sorption sites within the SOM for the water molecules. By contrast, swelling and with that plasticization of the SOM matrix only is possible for high water contents, if there are more water molecules than crosslinking sites (Schaumann 2005; Schaumann and LeBoeuf 2005). SOM plasticization by water consequently is linked with a sorption process which is not based on specific sorption sites, but presumably on a partitioning mechanism of water molecules in the organic soil phase.

5.3. Sorption models

Depending on the assumed sorption mechanisms, the sorption of water to SOM can be described by different models. The Langmuir isotherm bases on specific sorption sites on a monomolecular adsorption layer (Wedler 1987):

$$N = \frac{N_m \cdot p}{b + p} \tag{5.2}$$

where N and N_m are the number of adsorbed molecules and the maximal number of molecules in a monolayer. p is the partial pressure of the adsorbate in the gas phase. The constant b is

inversely correlated to the affinity coefficient of the sorbate to the sorbent. Assuming a specific adsorption area A_S of water molecules on the SOM surface and a mass specific surface A_m of SOM, with the Avogadro constant N_A and the molar mass of water M, equation 5.2 can be transformed to a form applicable to the gravimetric sorption data of water from the gas phase to SOM:

$$\Theta = \frac{A_m}{A_S} \cdot N_A \cdot M \cdot \frac{N_m \cdot p_0 \cdot RH}{b + p_0 \cdot RH} = \Theta_m \cdot \frac{p_0 \cdot RH}{b + p_0 \cdot RH} \tag{5.3}$$

where Q_m is the maximal gravimetric monolayer water content, and RH is the relative humidity, which represents the quotient of the partial pressure p of water and the respective saturation vapor pressure p_0.

While the Langmuir model assumes a sorption enthalpy which is independent of the sorbed phase concentration, the Freundlich isotherm is based on a sorption enthalpy which logarithmically decreases with sorbed phase concentration (Wedler 1987):

$$N = a \cdot p^n \tag{5.4}$$

where a and n are adsorption coefficients. Since it has to be assumed that the sorption enthalpies of water to the different polar functional groups of humous substances are different, the Freundlich equation was transformed in the same way as described for the Langmuir isotherm (see equations 5.2 and 5.3) and applied fit the water sorption to SOM:

$$\Theta = \frac{A_m}{A_S} \cdot N_A \cdot M \cdot a \cdot (p_0 \cdot RH)^n = k_F \cdot (p_0 \cdot RH)^n \tag{5.5}$$

where the constant k_F unites the constants A_m, A_S, N_A, and a.

Due to their dipole moments, several layers of water molecules, which are bound by hydrogen bonds among each other, may adsorb to the porous SOM surfaces. With the BET isotherm, this multilayer adsorption can be modeled. (Wedler 1987):

$$\frac{p}{n \cdot (p_0 - p)} = \frac{1}{n_m \cdot b} + \frac{b-1}{n_m \cdot b} \cdot \frac{p}{p_0} \tag{5.6}$$

where n and n_m are the sorbed concentration and the maximal monolayer concentration (both in mol sorbate per g adsorbent). b represents a measure of the adsorption enthalpy. Transformation of equation 5.6 and the multiplication of the molar concentrations n and n_m by the molar mass of water M yields:

$$\Theta = \Theta_m \cdot \frac{b \cdot RH}{(1 - RH) \cdot [1 + (b-1) \cdot RH]} \tag{5.7}$$

with Q_m as the maximal monolayer water content.

Additionally, the polymer-based dual-mode model (DMM) for NOM (Xing and Pignatello 1997; Xia and Pignatello 2001), which commonly is used for the sorption of organic

molecules to SOM, was applied to the water sorption data. The DMM model assumes the coexistence of glassy and rubbery domains in SOM. For the glassy regions, a hole-filling mechanism linked with the sorption to fixed sorption sites is proposed. In addition to the resulting Langmuir term, a partitioning term is added for the rubbery regions, which are supposed to reveal comparable sorption behavior as a fluid, because of the high flexibility of their molecular chains:

$$\Theta = K_D \cdot p_0 \cdot RH + \frac{\Theta_m \cdot p_0 \cdot RH}{b + p_0 \cdot RH} \tag{5.8}$$

with K_D as the partition coefficient of the dissolution domain. Kamiya et al. (1986; 1998) extended the DMM and introduced a term that accounts for plasticization by the sorbate. For a high-organic soil, Xia and Pignatello (2001) have shown that the sorption of polar and apolar compounds agrees well with this extended DMM. However, an extensive data base over a wide concentration range is necessary for an evaluation of sorption isotherms with this model (Xia and Pignatello 2001). Up to now, the DMM as well as the extended DMM were only applied for modeling the sorption isotherms of organic compounds to NOM. It is unknown, if these models are appropriate for the sorption of water to humous substances. But, due to the supposed antiplasticizing effects of water in glassy SOM and the swelling of rubbery SOM at moderate to high water contents (Schaumann 2005; Schaumann and LeBoeuf 2005), the applicability of these models may be assumed.

The mechanisms involved in the process of water sorption to NOM are also indirectly described by the link solvation model (LSM) explaining the effects of organic matter hydration on the sorption of organic compounds (Borisover and Graber 2002; Borisover and Graber 2004). This model bases on the assumption that hydration-assisted sorption of organic sorbates results from the formation of new sorption sites upon solvation of noncovalently linked NOM moieties which are not available for the sorbate molecules in dry NOM due to strong intramolecular interactions, as e.g., H-bonding, proton-transfer phenomena, or bridging via metal cations (Borisover and Graber 2002; Borisover and Graber 2004). If only one compound is sorbed without a solvent-assisted sorption effect, corresponding to the water sorption to SOM examined in this study, the local sorption isotherm of the LSM model passes into the Freundlich isotherm (Borisover and Graber 2002).

5.4. Experimental Section

5.4.1. Soil samples

The main properties of the soil samples are specified in Tab. 5.1. Chapter 4.3.1 includes a more detailed description of the samples from the spruce forest locations and the southern taiga. The samples were used in air-dried, oven-dried, and vacuum-dried state. Before the measurements, the air-dried samples were equilibrated for at least three weeks in 31 % RH at 20 °C. The oven-dried subsamples were obtained by heating the air-dried samples for 24 h at

105 °C. The vacuum-dried subsamples were obtained by exposing the air-dried samples for 24 h in a 3 mm thick layer to a pressure of 80 Pa in a Christ Model Alpha 1-4 freeze drying system (Christ, Germany).

Tab. 5.1. Properties of the soil samples (OM: organic matter, Q: water content).

Location	soil type	soil texture	horizon	OM content [%]	Θ [%] of air-dried samples
Flossenbürg, Germany: spruce forest	Podzol	sandy loam	O_h A_h	37.1 14.3	3.3 ± 0.1 1.5 ± 0.1
Rothenkirchen, Germany: spruce forest	Cambisol	clay	O_h A_h	79.7 71.2	5.7 ± 0.1 6.2 ± 0.1
Siberia, southern taiga	Luvisol	loam	O_h A_h A_{h2}	60.4 20.0 12.7	4.1 ± 0.7 2.0 ± 0.2 2.3 ± 0.3
Warnowtal, Germany	peat		H_v	63.9	13.6 ± 0.4

To examine, if a long-term storage of soil samples influences their glass transition behavior, DSC measurements of the Siberia samples were performed just after sampling and after three years of sample storage. Before the first measurements after sampling, reproducible moisture contents were achieved by an equilibration of the samples for two weeks over saturated NaCl solution (76 % RH) at 20 °C. Then, the samples were stored for three years in PE containers at 20 °C and measured for a second time.

In order to study the effect of the water content on the glass transition-like step transitions, the air-dried samples from Flossenbürg and Rothenkirchen as well as the air-dried and oven-dried samples from the Warnowtal were equilibrated at different relative humidities (RH). RH of 20 %, 22 %, 23 %, 37 %, 47 %, 63 %, 78 %, 92 %, and 97 % were realized in 7 x 19 x 23 cm perspex desiccators at 20 °C with dried $CaCl_2$, saturated solutions of $ZnBr_2$, LiCl, $CaCl_2$, $Zn(NO_3)_2$, NaBr, NaCl and $ZnSO_4$, and distilled water, respectively. With electronic thermo-hygrometers, the relative humidities were measured in the desiccators. Due to the surface properties of the desiccators and because of the high ratio of the air volume in them to the surface area of the conditioning agents, these measured RH values deviate from literature values (Weast et al. 1986; Falbe and Regitz 1992). After distinct periods of time, subsamples were taken out of the desiccators for determining the gravimetrical water contents and for DSC analysis.

5.4.2. DSC experiments

The samples were analyzed with the TA Instruments Model Q1000 DSC (TA Instruments, Germany), as described in Chapter 4.3.3. For the standard measurements, the samples were heated in hermetically sealed aluminum pans from -50 °C to 110 °C with a heating rate of 10 K min^{-1}. In order to examine the reversibility of the transitions in air-dried samples, the pans with the Flossenbürg and Rothenkirchen samples were stored after the first DSC run and

measured again after several periods of time. To study the effect of water evaporation, further DSC measurements were carried out in pans in which three holes were punched. In these punched pans, the samples were pre-tempered for 30 min at 110 °C before the heating cycle. The cooling between the pre-tempering and the heating cycle was conducted in two ways: Method A involved an abrupt cooling from 110 °C to -50 °C within 6.5 min. In method B, the samples were cooled with a rate of -10 K min^{-1}.

Following a technique to determine the apparent activation energies of the structural relaxation process in the glassy state of organic and inorganic glass-forming substances (Moynihan et al. 1996; Cortés and Montserrat 1998), measurements with different heating rates were carried out for the air-dried samples from Flossenbürg, Rothenkirchen, and Siberia. Additionally to measurements with the heating rate of 10 K min^{-1}, measurements from -50 °C to 110 °C with heating rates of 1 K min^{-1}, 2.5 K min^{-1}, and 5 K min^{-1} were performed for these samples. But contrary to the method described by Moynihan et al. (1996), the samples were not cooled prior to the heating cycle from above their glass transition region with a cooling rate which is equal to or proportional to the heating rate. Due to the atypical glass transition behavior of the air-dried soil samples, it was not possible to measure glass transition-like step transitions after such a cooling cycle. For the different samples, the apparent activation energies DH^* of the aging process of SOM were determined by the slope m of the function (Moynihan et al. 1996):

$$m = \frac{d \ln q_h}{d\left(1/T_g\right)} = -\frac{\Delta H^*}{R} \tag{5.9}$$

where q_h is the heating rate, and R is the ideal gas constant.

The DSC data analysis was performed with the Thermal Advantage V4.0 software (TA Instruments). In order to obtain horizontal thermograms in the glass transition regions, linear baselines were subtracted. Since several thermal effects investigated in this study persist in subsequent DSC runs, a baseline correction as in Chapter 4 was not possible. For the evaluation of the classical glass transitions and the glass transition-like step transitions, tangent lines are applied to both limits of evaluation. The onset and the end point are defined as the intersections of these outer tangent lines with a central tangent line. The central tangent line is applied to the transition temperature T_g or T_g^*, which is determined as the temperature at the half height between onset and end point. The associated change of specific heat capacity DC, which is a measure for the transition intensity, is calculated from the difference between end and onset tangent lines at T_g or T_g^* and is related to the total mass of the soil sample.

For each sample, all measurements were executed with three replications, which served to estimate the errors of the data on the basis of the 95 % confidence interval.

5.5. Results and Discussion

5.5.1. Effects of the sample history on thermal events in the DSC thermograms

In hermetically sealed pans, step transitions of the studied air-dried soil samples only occur in the first DSC run (see curve 1 in Fig. 5.1 exemplarily for the O_h horizon from Rothenkirchen). Due to their irreversible character, which contradicts the classical definition of glass transitions (Seyler 1994), these transitions are assigned to glass transition-like step transitions with transition temperatures T_g^* (Chapter 4). For the measurements in open pans, Fig. 5.1 includes a comparison between the two cooling methods A and B after the pre-tempering of the samples at 110 °C (curves 2 and 3, respectively). While after the abrupt cooling by method A, no glass transition region was detected, the heating cycle after the cooling with the defined rate of -10 K min^{-1} by method B shows a glass transition at (37 ± 1) °C with *DC* of (0.02 ± 0.01) J g^{-1} K^{-1}. Because of the reversibility of this transition indicated by the reproducible transition temperature and intensity in subsequent heating cycles with cooling cycles of method B in between, it is assigned to classical glass transitions. The same behavior was observed for all the samples from Flossenbürg, Rothenkirchen, and Siberia. After the thermal pretreatment in open pans, all these samples showed reversible glass transitions at lower temperatures and with decreased intensities in comparison with the glass transition-like step transitions of the air-dried samples in closed pans.

After oven-drying, a step transition at (39 ± 1) °C comparable to that after the thermal pretreatment in the open pans was observed (see curves 3 and 5 in Fig. 5.1). Since the transition of the oven-dried sample also shows the same reversibility in subsequent runs as the transition after thermal pretreatment in open pans, we assume that these two transitions both represent classical transitions most probably based on the same mechanism responsible for glassy matrix rigidity. In contrast to the oven-dried status, the forest soil samples from Flossenbürg and Rothenkirchen revealed no transition directly after vacuum-drying (curve 4 in Fig. 5.1). This shows that for some samples the shifting of the step transition to lower temperatures requires both the removal of water and a thermal pretreatment of the samples before the DSC measurements. But, contrary to these samples, the thermograms of the oven-dried and the vacuum-dried peat sample from the Warnowtal (not shown) are comparable, as also described for another peat sample by Schaumann and LeBoeuf (2005). The oven- and the vacuum-dried peat samples from the Warnowtal both reveal a reversible step transition at (49 ± 2) °C with *DC* of (0.04 ± 0.01) J g^{-1} K^{-1}, whereas the air-dried peat sample shows a glass transition-like step transition at (62 ± 1) °C with *DC* of (0.13 ± 0.01) J g^{-1} K^{-1}.

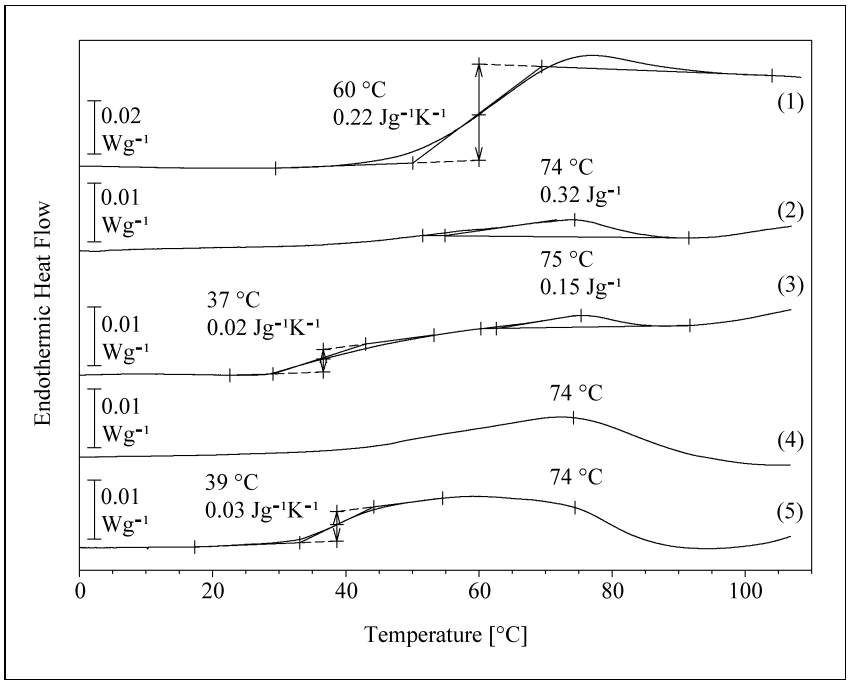

Fig. 5.1. DSC thermograms of air-dried (1), vacuum-dried (4), and oven-dried (5) samples of the O_h horizon from Rothenkirchen in hermetically sealed pans. The air-dried sample was additionally measured in punched pans after water removal by pre-tempering and subsequent cooling by method A (2) and method B (3). Due to unknown limits of the endothermic process at (74 ± 2) °C, a quantitative evaluation of the peak area is not possible. The evaluation of this peak in the thermograms 2 and 3 only yields a rough estimation of the energy required for the process.

The results of the different DSC measurement conditions (Fig. 5.1) are in accordance with the HBCL model and the findings of previous studies (Schaumann 2005; Schaumann and LeBoeuf 2005). Thus, for the water-containing air-dried soil samples in sealed pans, the disappearance of the glass transition-like step transition in a second DSC run conducted immediately after the first one can be explained by the disruption of water crosslinks during the first heating cycle (Chapter 4; Schaumann 2005; Schaumann and LeBoeuf 2005). Based on the HBCL model, the lower temperatures and decreased intensities of the transitions after a thermal pretreatment in open pans are due to a smaller degree of crosslinking of the organic substances because of the absence of water molecules (Schaumann and LeBoeuf 2005). But for some samples, the differences between the vacuum- and the oven-dried state indicate that besides the removal of water, a thermal pretreatment above 100 °C also is necessary for the occurrence of this classical glass transition type directly after the sample drying (Fig. 5.1). Supposing a kinetic control of the rearrangement of the SOM side chains and the formation of new crosslinks among themselves after the destruction of the water crosslinks, this process is accelerated by higher temperatures. Consequently, there may be more crosslinks in SOM after oven-drying than after vacuum-drying, leading to a detectable glass transition in the studied temperature range. For the occurrence of the classical glass transition type in the peat sample directly after vacuum-drying and the absence of this transition type in the forest samples directly after this drying procedure carried out without supplying the samples with heat,

differences in the SOM quality may be responsible. E.g., smaller distances between the molecular segments of SOM in peat than in the studied forest soils possibly cause smaller activation energies required to form crosslinks between the organic side chains of peat samples. To examine this hypothesis, detailed studies including a combination of DSC measurements and structural assessments of various soil samples covering a wide range of OM contents and humus forms are necessary.

The differences between the cooling methods A and B show that the way of cooling after the thermal pretreatment is also a deciding factor for the occurrence of a glass transition in the subsequent heating cycle. The glass transitions of the classical type only occur after a slow sample cooling by method B. This supports the hypothesis that the organic molecules need a certain time to rearrange and to form crosslinks between their side chains after the removal of water molecules out of the macromolecular network. These results show that the time is an important factor for the glass transition behavior in soil samples. In addition, the absence of transitions after the abrupt cooling by method A indicates that the transitions observed in the water-free samples also do not completely agree to the classical definition of glass transitions (Seyler 1994).

Besides the glass transitions of the classical type, the DSC thermograms in Fig. 5.1 which were recorded after a thermal pretreatment and after the evaporation of water reveal an endothermic process at (74 ± 2) °C. The process was observed for the O_h horizon from Flossenbürg, the O_h and A_h horizons from Rothenkirchen, and the O_h horizon from Siberia, whereas the thermograms of the A_h horizon from Flossenbürg and the A_h and A_{h2} horizons from Siberia do not show this endothermic event. It is noticeable that the peak maximum is located within a very small temperature range of (74 ± 2) °C for all the samples revealing this process. Because of the unknown peak limits and the overlapping with the step transitions in the thermograms, a quantitative evaluation of the enthalpy of the endothermic process is not possible.

The process at (74 ± 2) °C may be correlated to a the amount of organic matter (OM) in the samples: The significantly higher OM contents (Tab. 5.1) of the samples revealing the endothermic process (O_h horizon from Flossenbürg, O_h and A_h horizons from Rothenkirchen, and O_h horizon from Siberia) than of the samples without this process (A_h horizon from Flossenbürg and A_h and A_{h2} horizons from Siberia) indicate this interrelation. Until now, the origin of the endothermic process, which occurs in the thermograms immediately after the removal of water out of the samples as well as after a pre-tempering at 110 °C in closed pans (not shown) is unknown. It is improbable that it is an annealing peak, because annealing peaks only occur for well annealed amorphous polymers (Tsereteli and Smirnova 1992; Illekova 1994; Montserrat 1994; Cortés and Montserrat 1998; Hutchinson 1998). While a fast relaxation of the SOM molecules cannot be excluded after the evaporation of water, the occurrence of the peak directly after a thermal pretreatment in closed pans contradicts the theory for annealing peaks.

The endothermic peak at (74 ± 2) °C possibly is based on the melting of poly(methylene) crystallites, which were detected by solid-state NMR and X-ray diffraction in humic substances and peat samples (Hu et al. 2000; Chilom and Rice 2005). The melting temperature of these poly(methylene) crystallites, which make up less than 5 % of the total SOM material, depends on the crystallite size and varies among humous substances between 60 °C and 80 °C (Hu et al. 2000; Chilom and Rice 2005). The absence of a poly(methylene) melting peak in the thermograms of the air-dried samples in closed pans may be due to (i) the overlapping of the glass transition-like step transitions, which occur for the air-dried samples in the same temperature region or (ii) the absence of poly(methylene) crystallites in air-dried SOM, which partially would turn into crystallite units only after heating the samples to high temperatures. In contrast to the air-dried samples, the occurrence of the peak without a thermal pretreatment in water-free samples can be explained according to the HBCL model (Schaumann 2005; Schaumann and LeBoeuf 2005) by a higher flexibility of the polymeric chains, enabling the formation of poly(methylene) crystallites at lower temperatures. Assuming a melting enthalpy between 13 and 31 J g^{-1}, as determined by Chilom and Rice (2005) for the lipid fractions consisting of the crystalline poly(methylene) components, and 3 % poly(methylene) crystallites in SOM (Hu et al. 2000), the melting enthalpy should be between 0.3 and 0.8 J g^{-1} for the O_h horizon from Rothenkirchen. The enthalpies estimated on the basis of the areas of the endotherms at (74 ± 2) °C (Fig. 5.1) are of this magnitude supporting the hypothesis of a melting of poly(methylene) crystallites. For a verification of the hypothesis that the observed endothermic process is due to the melting of crystalline poly(methylene) units, solid-state NMR analyses or other measurements which allow the differentiation between amorphous and crystallite structures would be necessary.

For a better separation of the hypothesized melting process of the poly(methylene) crystallites and the two types of glass transitions (Fig. 5.1), further investigations including different methods to remove water and to supply the samples with heat before the DSC measurements are required. However, a comparison between the thermograms of the closed and the open pans (see curves 1-3 in Fig. 5.1) indicates that a distinct differentiation between the melting process and the glass transition-like step transition occurring in the same temperature range is possible. These results contradict the assumptions of Chilom and Rice (2005), who suggested that the reported glass transition behavior of SOM possibly may be the melting of crystallites. Investigations of Kögel-Knabner et al. (1992) and Hu et al. (2000) point to higher concentrations of poly(methylene) crystallites in SOM of deeper soil horizons, which is more rigid and more resistant to biodegradation than young humous material. Until now, it is not possible to correlate the enthalpy associated with the process at (74 ± 2) °C with the horizon depth of the samples investigated in this study. On the one hand, the overlapping with the step transitions and the difficulties to determine the limits in the thermograms (Fig. 5.1) prevent a quantitative evaluation of the peak areas. On the other hand, the examination of a possible interrelation between this peak and the soil depth is impeded by the absence of the process for samples from deep soil horizons with small OM contents.

5.5.2. Slow changes of the glass transition behavior of SOM in the course of time

The slowly reversing character of the glass transition-like step transition of the air-dried samples was studied by means of the pan storage experiment (Fig. 5.2): In hermetically sealed pans, this transition type disappears in a second DSC run performed directly after the first one (Fig. 5.2, curve 2). But, it reappears after storing the pans for one more week (curve 3; see also Schaumann and LeBoeuf 2005). After further storage, the transition shifts to higher temperatures (from (47 ± 1) °C to (52 ± 1) °C after 7 months for the A_h sample from Flossenbürg; Fig. 5.2) and reveals a significantly higher intensity. This behavior is comparable for all soil samples with glass transition-like step transitions. It is uncertain, if the original T_g^* and *DC* values of the first runs will be reached again at any time. Between one week and 7 months of sample storage, T_g^* increased by (4.5 ± 0.4) °C, and *DC* increased by (0.020 ± 0.008) J g^{-1} K^{-1} on average for the samples from Flossenbürg and Rothenkirchen. If a continuous increase of T_g^* and *DC* is assumed, it would take between one and two years to reach the original parameters of the glass transition-like step transition of the first runs. The reappearance of glass transition-like step transitions at decreased temperatures after one week of storing the pans and the increase of T_g^* and *DC* with proceeding time points to a slow rearrangement of the water molecules resulting in a new formation of water bridges within the SOM. These results consequently reflect the pronounced influence of time after a change of the water status on the glass transition behavior of SOM.

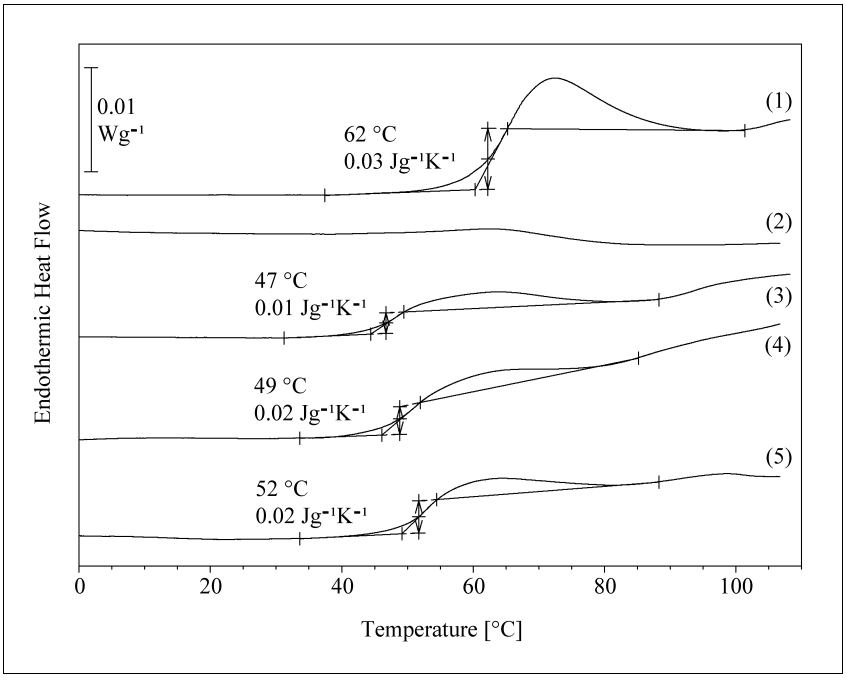

Fig. 5.2. DSC thermograms of the air-dried A_h sample from Flossenbürg in hermetically sealed pans. Directly after the first run (1), a second run (2) was performed with the same pan. Then, the pan was stored and measured again after one week (3), after further 8 weeks (4), and further 7 months (5).

Changes of the glass transition behavior of SOM in the course of time also occur without preceded alterations of the water status by thermal pretreatment or drying of the samples. Thus, the three-year storage of the NaCl equilibrated Siberia samples in closed containers resulted in a significant increase of the transition temperatures T_g^* (Tab. 5.2). The intensity of the transitions showed no significant change.

Tab. 5.2. T_g^* and *DC* of the NaCl equilibrated Siberia samples soon after sampling and after three years of storing them.

Horizon	T_g^* after 2 weeks	*DC* after 2 weeks	T_g^* after 3 years	*DC* after 3 years
O_h	52 ± 2	0.05 ± 0.04	61 ± 2	0.13 ± 0.07
A_h	56 ± 2	0.03 ± 0.01	61 ± 1	0.03 ± 0.01
A_{h2}	56 ± 2	0.04 ± 0.01	60 ± 1	0.02 ± 0.01

For the three-year storage of the NaCl equilibrated samples, it can be assumed that the effects of water on the changes of the glass transition-like step transitions are smaller than after alterations of the water status (Fig. 5.2). Consequently, structural relaxation of the humous substances including reductions in segmental mobility and free volume (Tsereteli and Smirnova 1992; Illekova 1994; Cortés and Montserrat 1998; Hutchinson 1998) also may contribute to the increase of T_g^* during this period of time. The aging studies described in the above mentioned publications were performed with synthetic organic polymers and gelatin as well as with metallic and chalcogenide glasses, which were annealed for up to 70 days at temperatures below their T_g. In contrast to the soil samples, already after annealing times of few hours, these glasses reveal endothermic annealing peaks which are distinctly higher than their glass transition steps. As depicted in the introduction, the enormous heterogeneity of SOM and with that a presumably wide range of different relaxation times (small *ß* values) may explain the minor annealing peaks in the soil samples (Cortés and Montserrat 1998; Hutchinson 1998; Chung et al. 2004). In addition, it cannot be excluded that the water remaining in the air-dried or NaCl conditioned samples causes a reduction of the annealing peaks. In contrast to the studies by Ellis and Karasz (1986) and Shorgen (1992) dealing with the influence of moisture on the aging process (see introduction), the water molecules most probably exhibit antiplasticizing effects in the air-dried or NaCl conditioned soil samples. Consequently, the difference between transition temperature and annealing temperature T_g - T_a may be increased by the water in the soil samples, causing a slower relaxation rate and a lowering of the annealing peaks.

In Fig. 5.3, the transition temperature T_g^* of the air-dried O_h sample from Rothenkirchen, which was measured as a function of the heating rate q_h, is shown in a special plot, which serves to determine the apparent activation energy of the structural relaxation process. According to Moynihan et al. (1996), the fitted linear function yields an apparent activation energy of (200 ± 20) kJ mol^{-1} for the O_h sample from Rothenkirchen. For all the other samples from Flossenbürg, Rothenkirchen, and Siberia, the activation energies range between 120 and 370 kJ mol^{-1} and show no correlation to the OM content, to the locations, or to the different

soil horizons. The deviation of the data points for the lowest heating rate of 1 K min^{-1} from the linear trend (Fig. 5.3) was observed for three out of the 19 samples for which the measurements with different heating rates were performed. Possibly, only the small heating rates ensure for all samples that the temperatures prescribed by the temperature protocol are really reached within the porous soil samples in the DSC pans.

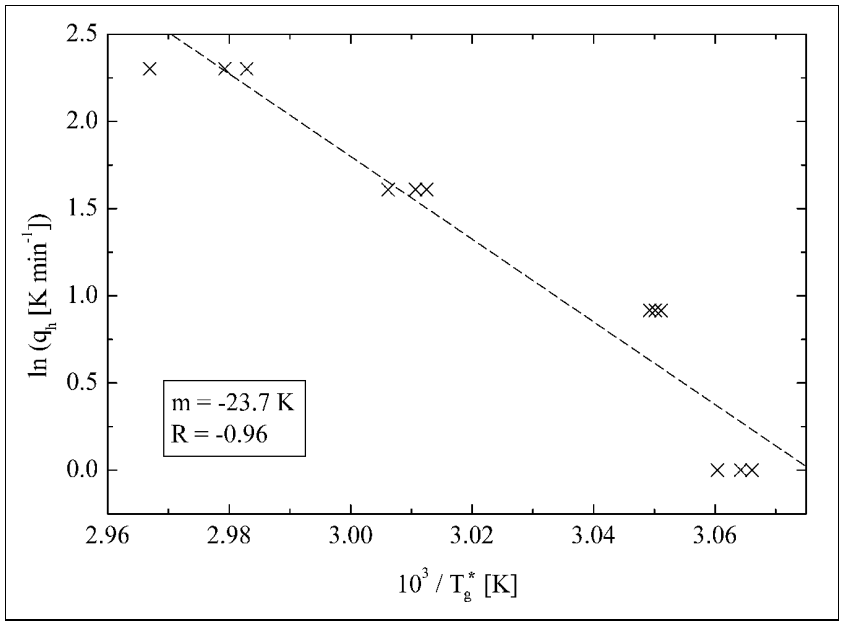

Fig. 5.3. Logarithm of the heating rate q_h versus reciprocal of transition temperature T_g^* for the air-dried O_h sample from Rothenkirchen. The slope and the correlation coefficient of the linear regression are specified in the box.

The determined apparent activation energies of the structural relaxation process of the air-dried soil samples are smaller than the activation energies quoted for synthetic organic polymers (Montserrat 1994; Cortés and Montserrat 1998; Hutchinson 1998) and inorganic glasses (Moynihan et al. 1996; Hutchinson 1998). According to structural relaxation models for synthetic polymers (Cortés and Montserrat 1998), the low activation energies would indicate small barriers to internal rotations of the backbone bonds of the SOM molecules and high relaxation rates. However, it is questionable, if these models for pure polymer systems can be transferred to soil samples, in which interrelations with the mineral matrix, ions, and water molecules may control the mobility of the organic substances.

5.5.3. Influence of the moisture status

After four weeks of equilibration over the different conditioning agents, the water contents of the soil samples had reached equilibrium values. Later on, no significant changes of the water contents were observed. The water sorption isotherms show a sigmoidal shape (see Fig. 5.4 for the oven-dried and Fig. 5.5 for the air-dried peat sample from the Warnowtal), as also observed by Miyamoto et al. (1972).

For RH ≤ 0.8, the water sorption data of the oven-dried and the air-dried samples can be modeled by both the Langmuir and the Freundlich isotherm ($Chi^2 < 0.0001$ for both isotherms). Due to the almost congruent curve progressions of these two isotherms, only the Langmuir isotherms are shown exemplarily in Fig. 5.4 and Fig. 5.5. The fitting results of the Langmuir model for RH ≤ 0.8 yield maximal water contents Q_m of (0.6 ± 0.1) and (0.3 ± 0.1) for the oven-dried and the air-dried peat sample, respectively. The Langmuir constant *b* which is inversely correlated to the sorption affinity of the water molecules amounts to $(5 \cdot 10^3 \pm 1 \cdot 10^3)$ Pa for the oven-dried sample and to $(1.8 \cdot 10^3 \pm 0.5 \cdot 10^3)$ Pa for the air-dried sample. The higher maximal water content Q_m of the oven-dried sample in combination with the comparable Langmuir constants *b* of both samples indicates that oven-drying causes sample alterations linked to higher amounts of water uptake. The fitting of the Freundlich isotherm for RH ≤ 0.8 results in Freundlich exponents *n* of (0.83 ± 0.04) for the oven-dried sample and (0.65 ± 0.07) for the air-dried sample, pointing to nonlinear sorption. The yielded k_F values are $(3.0 \cdot 10^{-4} \pm 0.1 \cdot 10^{-4})$ $Pa^{-0.83}$ for the oven-dried and $(1.3 \cdot 10^{-3} \pm 0.1 \cdot 10^{-3})$ $Pa^{-0.65}$ for the air-dried peat sample.

The fitting was not improved by application of the DMM instead of the simple Langmuir isotherm. Both models yield almost identical curve progressions with $R^2 > 0.95$ and $Chi^2 < 0.0001$ for the air-dried and the oven-dried samples. Neither the data for RH ≤ 0.8 nor the whole data set of the water sorption of the peat sample do agree with the BET model. By a vertical shifting of the BET function, the fitting results slightly improved, but nevertheless are insufficient to describe the data (Fig. 5.4 and Fig. 5.5).

The water sorption isotherms indicate that for RH ≤ 0.8, sorption of water molecules to specific sites represents the dominating mechanism, whereas for RH > 0.8, partitioning of the water molecules linked to swelling of SOM may become relevant. Specific sorption sites for low RH can be assumed due to the nonlinearity of the isotherms. The fact that the fitting results cannot be improved by applying the DMM instead of the Langmuir model also is in accordance with fixed adsorption sites without partitioning-like behavior. However, the differentiation between these sorption models is difficult because of the small number of data points. The unsuitability of the BET isotherm, which is based on a fixed surface for adsorption, most probably is caused by swelling of SOM for RH > 0.8. The BET model characterizes multilayer sorption, but it does not include the severe increase of the water contents for RH > 0.8 presumably caused by the development of additional surface areas and the increasing relevance of partitioning due to swelling. For a humic and a fulvic acid, Chen and Schnitzer (1976) also obtained poor fitting results by the BET model for RH > 0.5 - 0.6. They assumed that the condensation of water vapor into clusters around COOH groups of the humic substances caused this divergence from the BET model at high RH. Orchiston (1953) gives a range of only 0.05 to 0.35 RH for the applicability of the BET isotherm to soils.

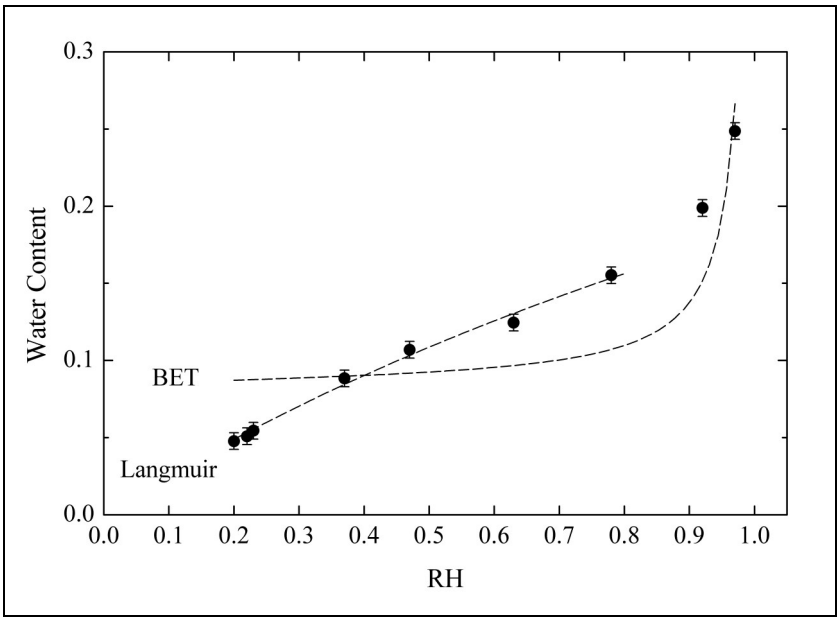

Fig. 5.4. Water content as a function of relative humidity for the oven-dried peat sample from the Warnowtal after 9 months conditioning time and BET sorption model fit as well as Langmuir fit for RH £ 0.8.

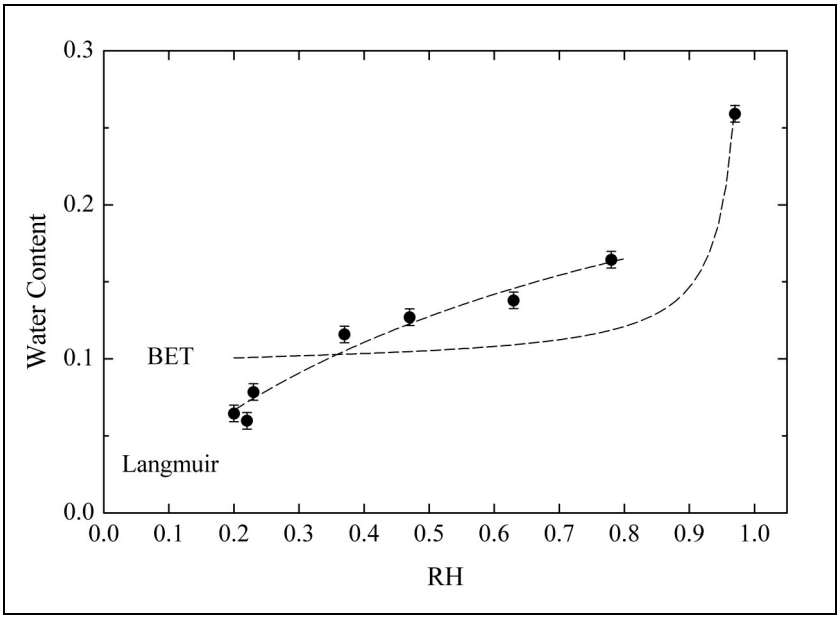

Fig. 5.5. Water content as a function of relative humidity for the air-dried peat sample from the Warnowtal after 9 months conditioning time and BET sorption model fit as well as Langmuir fit for RH £ 0.8.

In contrast to the predictions of the extended DMM by Kamiya et al. (1986), a linear or exponential function, fitted to the data points for RH > 0.8, does not intersect the origin, but intersects the abscissa at RH = (0.7 ± 0.2) for the air-dried and the oven-dried sample. This points to a plasticizing effect of water only for RH > (0.7 ± 0.2), i.e. for water contents of above (15 ± 4) %. For lower water contents, the interactions between SOM and water are

most probably dominated by crosslinks within the organic molecules by water molecules resulting in an antiplasticizing effect.

The transition temperatures T_g^* of the samples which were stored in the different RH slowly increased despite the constant water contents reached after four weeks. Fig. 5.6 and Fig. 5.7 show T_g^* as a function of time for the oven-dried and for the air-dried peat sample from the Warnowtal. Only in 20 % and 22 % RH, no gradual increase of T_g^* was observed for the air-dried samples (Fig. 5.7). Interestingly, these two relative humidities are the only ones which caused a significant drying of this sample (to water contents of (6 ± 1) % and (7 ± 1) %), while the other RH resulted in comparable or higher water contents with reference to the air-dried sample ((13.6 ± 0.4) %). Because of the low water contents of the air-dried samples from Flossenbürg and Rothenkirchen (see Tab. 5.1) and the absence of water in the oven-dried peat sample from the Warnowtal, none of the relative humidities caused further drying of these samples. As for the oven-dried peat sample, but in contrast to the air-dried peat sample, the transition temperatures T_g^* of the air-dried samples from Flossenbürg and Rothenkirchen also increased during the sample equilibration in 20 % and 22 % RH (not shown).

In summary, the equilibration of the soil samples in different RH has shown that sample drying does not necessarily show a significant trend of T_g^*, while constant or increasing water amounts in the samples cause a rise of T_g^*. Contrary to the results for the peat sample from the Warnowtal, Schaumann (2005) observed for another peat sample from the Rhinluch (Germany) an increase of the transition temperatures in the course of time under hydration as well as under dehydration conditions. Additionally, the investigations of the Rhinluch sample (Schaumann 2005) have shown that the transition temperatures distinctly decreased in the first days after water attachment or water removal, and only after this fast decrease, slowly increased within a time scale of weeks. The initial decrease was attributed to a fast disruption of water crosslinks occurring as a result of alterations of the water status irrespective of the direction of the moisture content changes (Schaumann 2005). Only in comparison to the fast initial decrease of the transition temperature, the subsequent slow increase was identifiable. Since for the peat sample from the Warnowtal investigated in this study, the development of the transition temperatures was not observed in the time scale of days, but in the time scale of months, a possible fast decrease of T_g^* in the first days could not be detected. Consequently, T_g^* increases which can only be identified in comparison to such a fast T_g^* decrease also could not be identified.

According to the HBCL model (Schaumann 2005; Schaumann and LeBoeuf 2005), the slow T_g^* increase of the peat sample from the Warnowtal for constant or increasing amounts of water within the SOM matrix can be explained by a strengthening of the degree of SOM crosslinking due to hydrogen bond bridges in the course of time. Following this model, an evaporation of water molecules out of the samples results in a decrease of the amount of hydrogen bond-based crosslinks yielding a higher flexibility of the organic side chains and with that a lower transition temperature.

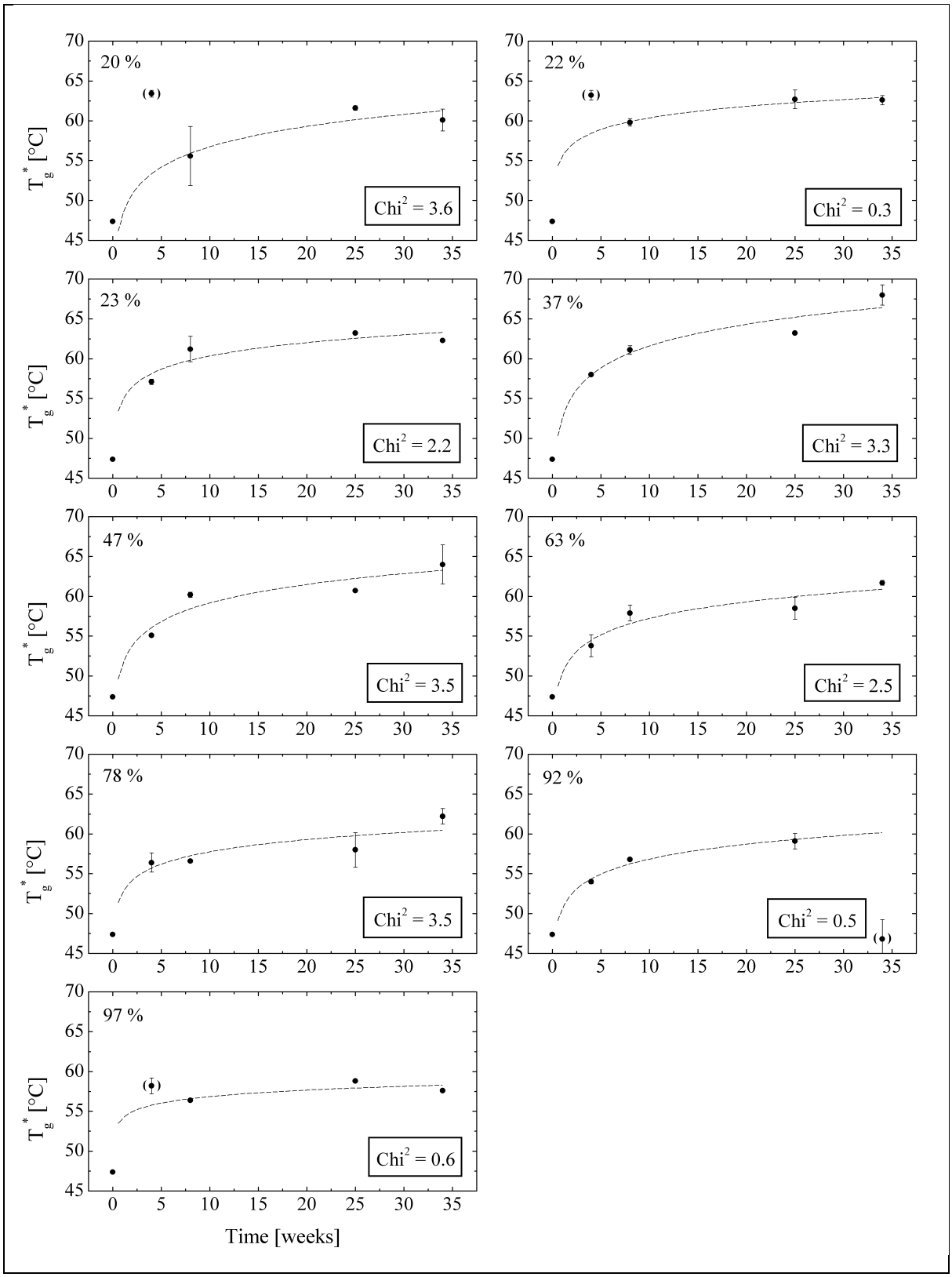

Fig. 5.6. Transition temperatures T_g^* of the oven-dried peat sample from the Warnowtal as a function of time for sample equilibration in RH of 20 %, 22 %, 23 %, 37 %, 47 %, 63 %, 78 %, 92 %, and 97 %. For each fitted logarithmic function, Chi² is given in the plots. Data points in brackets were not included in the fitting procedure.

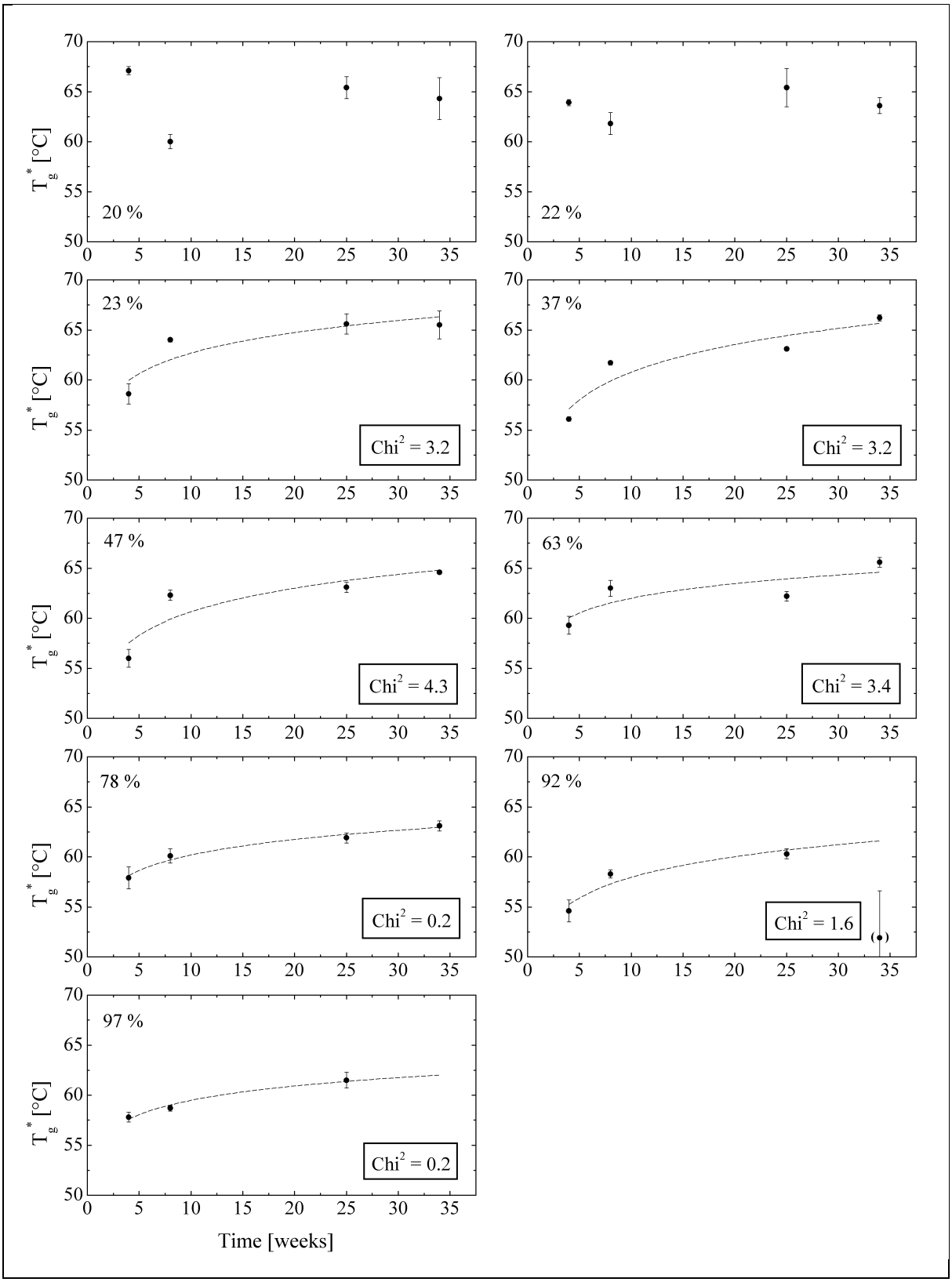

Fig. 5.7. Transition temperatures T_g^* of the air-dried peat sample from the Warnowtal as a function of time for sample equilibration in RH of 20 %, 22 %, 23 %, 37 %, 47 %, 63 %, 78 %, 92 %, and 97 %. For each fitted logarithmic function, Chi² is given in the plots. Data points in brackets were not included in the fitting procedure.

The transition temperatures T_g^* reached at the end of the sample equilibration experiment (Fig. 5.8) also reflect the influence of the different water contents caused by the different RH. If the moisture contents were reduced, T_g^* decreased probably due to the reduction of the number of hydrogen bond-based crosslinks. Especially, distinctly reduced water contents (below 6 %), are linked to low transition temperatures T_g^*, which are more than 5 °C lower than the highest T_g^* values reached for water contents about 10 % (Fig. 5.8). For further increasing moisture contents above 10 %, the transition temperatures again show a decreasing trend, which may be a consequence of beginning swelling and with that plasticizing effects of the additional water molecules.

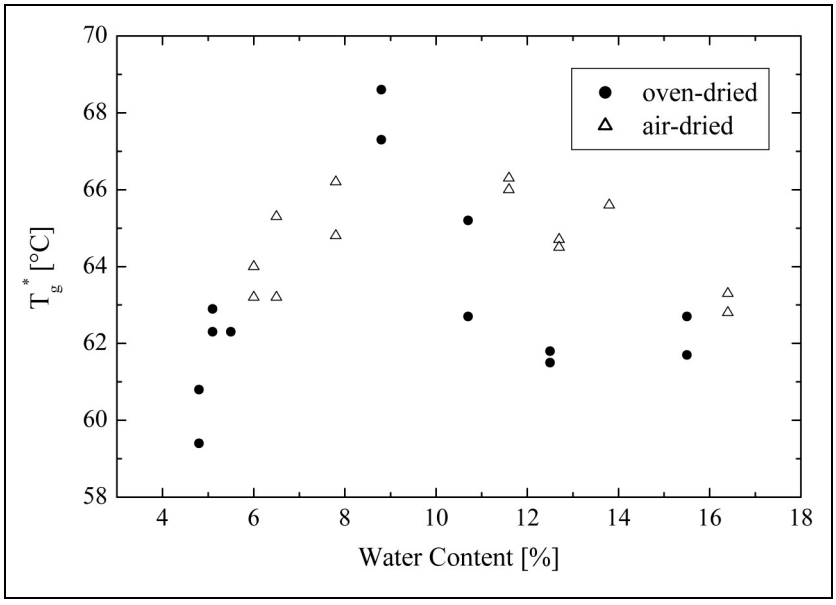

Fig. 5.8. Transition temperatures T_g^* of the oven-dried and the air-dried peat sample from the Warnowtal as a function of the water contents reached 9 months after starting the sample equilibration in different RH.

Besides the effects of water, structural relaxation of SOM may occur in the course of time. The increase of T_g^* for constant or increasing water contents (Fig. 5.6 and Fig. 5.7) presumably reflects the whole aging process of SOM, which includes both mechanisms. The absence of a T_g^* trend of the peat sample under drying conditions (20 % and 22 % RH in Fig. 5.7) may be due to the antagonistic effects of crosslink disruption and structural relaxation of the organic phase.

The slow increase of T_g^* under constant moisture status or hydration conditions is in accordance with physical aging studies, where the annealing peak temperatures of amorphous polymer materials increase linearly with $\log t_a$ (Shogren 1992; Montserrat 1994; Chung et al. 2004). For different starches, Chung et al. (2004) found that the annealing peak temperatures are positively correlated with the glass transition temperatures T_g, so that a logarithmic dependence of T_g or T_g^* on the aging time can be expected, too. The results of the sample conditioning in different RH indicate that the transition temperatures of SOM increase with a

very slow rate: For the air-dried samples, T_g^* rose by (7 ± 2) °C within 30 weeks, and for the oven-dried samples, T_g^* rose by (13 ± 1) °C within 34 weeks. The slow increase of the transition temperatures T_g^* of the soil samples may reflect the heterogeneous structure and high crosslinking density of SOM. However, for the underlying process occurring during the sample conditioning in different RH (Fig. 5.6 and Fig. 5.7), the rate of the T_g^* increase is faster than for the process which is observable in closed DSC pans after heating the samples above 100 °C (Fig. 5.2). Due to the absence of a wetting process, the water molecules from the vapor phase probably penetrate more rapidly into the SOM network and thus need a shorter period of time to build new crosslinks than the liquid water molecules in the closed DSC pans.

The increase of T_g^* during the sample conditioning in different RH (Fig. 5.6 and Fig. 5.7) can be described by logarithmic or exponential functions. But, because of the low number of data points, it is not possible to assign specific functions to the development of the transition temperatures in the course of time. Since the physical aging of glassy polymers is reflected by a logarithmic increase of the annealing peak temperatures (Shogren 1992; Montserrat 1994; Chung et al. 2004), Fig. 5.6 and Fig. 5.7 exemplarily show the fitting results for the function:

$$T_g^* = T_{g0}^* + k \cdot \log(t) \tag{5.10}$$

where T_{g0}^* represents the transition temperature T_g^* at the beginning of the sample conditioning. The constant k indicates the extent of the T_g^* increase in the course of the sample equilibration time (in weeks). Due to the higher T_g^* of the air-dried sample compared with T_g of the oven-dried sample, the original air-dried sample (t = 0) could not be included into these functions (Fig. 5.7). For both the oven-dried and the air-dried peat sample, k amounts to values between 3 °C and 9 °C and shows no interrelation to the RH used for sample equilibration. The T_{g0}^* fitting results, which also show no correlation to RH, are (52 ± 3) °C for the oven-dried and (54 ± 2) °C for the air-dried sample. The fitting of the T_g^* development in the course of time by exponential functions (not shown), likewise yields no significant differences between the oven-dried and the air-dried sample and no interrelations between the fitting parameters and RH. The time constants of the exponential functions are between 2 and 8 days for all sample conditioning variants. Due to the low number of data, no further quantitative information on the aging process and its dependence on the water status can be obtained the by the fitting results. The possibility to describe the T_g^* development as a function of $\log t_a$ implies that the changes of the glassy SOM matrix may depend in a comparable way on time as physical aging processes in synthetic polymer systems.

The results of the conditioning experiments point to an aging process of SOM, which occurs irrespective of the water content of the soil samples. This process can only be observed, if the water content remains constant or increases in the course of time. The divergent T_g^* development of the peat sample under drying conditions (20 % and 22 % RH) may be attributed to an antagonistic effect caused by the disruption of hydrogen bond-based crosslinks in SOM due to the evaporation of water. For a more detailed differentiation

between the effects of aging associated with structural changes of the organic molecules and the effects due to a change of the water content, further studies of samples with different water contents are required.

5.6. Conclusions

The water sorption to humous soil samples does not easily follow from polymer theory. Instead, the sigmoidal form of the sorption isotherms indicates that the sorption of water molecules to SOM is governed by different mechanisms depending of the moisture contents of the samples. For low water contents, the applicability of the Langmuir and the Freundlich model indicates some type of specific sorption. Either restricted sorption sites or sorption enthalpies decreasing as a function of the amount of sorbed water may explain these nonlinear sorption isotherms and are in accordance with the hypothesized antiplasticizing effects of water in the low water content region according to the HBCL model (Schaumann 2005; Schaumann and LeBoeuf 2005). For moderate to high moisture contents, the pronounced increase of water sorption presumably is a result of disruption of water crosslinks between hydrophilic sorption sites linked with SOM swelling and plasticizing effects of water.

The study has shown that the glass transition behavior of soil samples is strongly influenced by time and thermal history. The shift of glass transition-like step transitions to higher temperatures during sample storage below T_g^* points to an aging process comparable to synthetic polymers. Changes of the moisture status in the soil samples distinctly affect this aging process. If a drying of the samples occurs in the course of annealing, possibly no increase of T_g^* can be observed, because the effect of lowering T_g^* by the removal of hydrogen bond bridges of water molecules may superimpose the effect of aging. The new formation of hydrogen bond bridges in SOM by water molecules probably is as slow or even slower than the structural relaxation of SOM, resulting in difficulties to separate these two parallel running processes.

In some samples, an endothermic process was observed at (74 ± 2) °C, which may be related with the melting of poly(methylene)crystallites. To verify the hypothesis of crystalline poly(methylene) units in SOM, these samples will be investigated by NMR before and after thermal treatment.

6. Synthesis and general Conclusions

6.1. Wetting of soil samples

The investigation of the hydration kinetics of soil samples by direct gravimetric measurements of the water contents in the course of time has shown that differences in the wetting process only occur, if the water is supplied via the liquid phase. The results of these gravimetric measurements indicate that water repellent properties of the organic matrix may be linked with first-order wetting processes which last up to three weeks. This period of time agrees with ^{1}H NMR Relaxometry results of Todoruk et al. (2003b) and Schaumann et al. (2005a) and is distinctly higher than the water drop penetration time (WDPT) of the samples, suggesting that the WDPT only is a measure for the first wetting step, i.e. for the first interactions between the water molecules and the SOM surfaces. The hypothesis that water molecules are bound in a different way to the solid phase of wettable and water repellent samples was corroborated by differences in the phase transition temperatures and in the mean freezing enthalpies of water molecules in the samples. For the studied sample pairs, the water molecules in the water repellent samples on average revealed lower freezing enthalpies than in the wettable samples. According to studies dealing with unfreezable water in natural and synthetic polymer systems and in peat (Quinn et al. 1988; McBrierty et al. 1996; Nishinari et al. 1997), a higher degree of bonding can be assumed for the water molecules in the water repellent samples. However, these differences are most probably a consequence of the different moisture contents of the water repellent and the wettable samples. Thus, the differences disappeared three weeks after the moisture contents of the samples had been adjusted. After adding water to the samples, the portion of unfreezable water abruptly decreased, but then, it slowly increased, pointing to rising bond strengths of the water molecules. The ^{1}H NMR results indicate that in water repellent samples, these rising bond strengths presumably occurring in the course of sample wetting are linked to a redistribution process of the water molecules from coarse to fine pores (Schaumann et al. 2005a). An inclusion of water in fine pores at the end of this process may be the reason for their unfreezability (Berezin et al. 1973; Pfeifer et al. 1985). Contrary to the samples from the location Chorin (Schaumann et al. 2004), no swelling process, which would cause changes of the peak positions in the NMR relaxation time distribution, was observed for the sample pairs from the location Tiergarten (Schaumann et al. 2005a).

Like the temperatures and enthalpies of the phase transitions, the wetting characteristics of the initially water repellent and the initially wettable samples of the different sample pairs from the locations Tiergarten and Buch have approached each other, if the samples were subjected to the same moisture conditions. Thus, the WDPT measurements after different sample pretreatments and in the course of drying-remoistening cycles have shown that the wetting behavior is distinctly influenced by the moisture content. The dependence of the soil wettability on the moisture content is in accordance with concepts presented in literature for water repellency (e.g., King 1981; Ritsema and Dekker 1998; Quyum et al. 2002). However,

our experiments also have shown that after the different sample pretreatments and during the drying-remoistening cycles, the WDPT of the initially water repellent samples always remain higher than the WDPT of the initially wettable samples. Consequently, between the water repellent and the wettable samples, a general difference linked to another mechanism, which is responsible for the wettability behavior irrespective of the water status, has to be assumed. Contrary to our expectations, neither the superior structure observed by ESEM nor the molecular structure of SOM studied by infrared spectroscopy revealed differences between the water repellent and the wettable samples. The results of the analyses of the soil extracts indicate that the mechanisms which control soil wettability differ between different locations. Only for the location Tiergarten, an interrelation between the wetting behavior and pH and ionic strength was observed. High electrolyte contents and especially the protonation of negatively charged functional groups probably result in an aggregation of molecular chains at solid SOM surfaces, as it is known for humic substances in solution (Avena et al. 1999; Rice et al. 2000; Sanyal 2001). This aggregation may cause low wettability for soil regions with low pH and high electrolyte content. The water repellency for soil samples from these regions thus may be based on a SOM conformation, where hydrophilic groups may approach each other, while the hydrophobic groups are orientated outwards. For a final ascertainment, whether pH and electrolyte content are really reasons for water repellency or consequences of it, as proposed by Ritsema and Dekker (1998), further studies are necessary. By examining the effects of artificially induced pH changes on the wettability of soil samples, the underlying mechanisms can be analyzed (Bayer and Schaumann 2006).

The observed smaller surface tensions of the extracts of the water repellent samples in comparison with the wettable samples represented a surprising result for both studied locations. The amount of soluble amphiphilic substances at the SOM surfaces of water repellent soil regions consequently is higher than for the wettable regions. In the field, where water repellent and wettable regions are directly neighbored, the dissolution of surface active substances from the water repellent regions possibly enables a gradual adjustment of the wetting properties. Additionally, the drying-remoistening cycles have indicated that the time has to be taken into account as factor of influence for soil wettability. After changes of the water status, slow changes of the wetting behavior may occur, which also can cause that the wetting characteristics of different soil regions approach each other.

6.2. Glass transition behavior

The detection of glass transition behavior in 52 out of the 102 analyzed soil samples by DSC measurements strongly supports the polymer model for SOM (LeBoeuf and Weber Jr. 1997; Xing and Pignatello 1997). Two types of glass transitions can be distinguished in the samples: One of them agrees with the classical definition of glass transitions (Seyler 1994) and can be observed only in water-free samples. The other one occurs only in the first heating cycle of water-containing soil samples in closed systems and is strongly affected by the water status in the samples. According to Schaumann and LeBoeuf (2005), in this thesis, this atypical glass

transition is designated as glass transition-like step transition due to its only slowly reversing character. For all the studied air-dried samples, the transition temperatures of the glass transition-like step transition ranged between 51 °C and 67 °C, pointing to a superordinate mechanism controlling matrix rigidity. According to the hydrogen bond-based crosslinking (HBCL) model (Schaumann 2005; Schaumann and LeBoeuf 2005), crosslinks by water molecules may be responsible for the comparable glassiness of the amorphous SOM matrix in air-dried samples. In addition to the small range of transition temperatures of the air-dried samples, the observed distinctly lower temperatures of the transitions of water-free samples together with their decreased intensity and broadness suggest the general validity of the HBCL model for humous soil samples.

The assumption of antiplasticizing effects of water for low water contents according to the HBCL model and of plasticizing effects linked with SOM swelling for moderate to high water contents is further supported by the water adsorption isotherms. Their sigmoidal form indicates that below a certain moisture content, the sorption process of the soil samples is governed by specific sorption sites and consequently can be described by the Langmuir isotherm. Above this moisture content, the sorption of water distinctly increases pointing to a pronounced swelling of the organic matrix (Xia and Pignatello 2001). The increasing amount of water molecules in the swollen SOM presumably results in an increasing disruption of the water crosslinks between hydrophilic sorption sites.

The hypothesized interrelation of the glass transition behavior with the organic soil phase was demonstrated by the correlation between transition intensity and C_{org} content of the samples as well as by decreasing transition intensities with increasing SOM removal out of the samples. Contrary to our expectations based on studies of the sorption characteristics of charcoal-like substances or soot (Chiou et al. 2000; Cornelissen et al. 2004), an influence of the thermoresistant black carbon-like fraction was not observed. The particulate (POM) and the mineral-associated organic matter (MOM) fractions also showed no influence on the glass transition characteristics. Possibly, effects of different SOM fractions are superimposed by the effects of the hydrogen bond-based crosslinks. Thus, the non-uniform development of the transition temperatures with soil depth also points to the existence of different factors of influence. On the one hand, the more condensed structure of organic substances with a higher degree of decomposition (Schulten and Leinweber 1996; Xing and Chen 1999; Cuypers et al. 2002) is expected to result in higher transition temperatures. On the other hand, the lower abundance of young SOM fractions with high contents of hydrophilic groups may cause decreased transition temperatures in deep soil horizons because of a smaller amount of hydrogen bond sites. This possible correlation between hydrophilic functional groups and the glass transition behavior probably also yields the explanation for the smaller intensities or the complete absence of glass transition-like step transitions in the DSC thermograms of samples from anthropogenically affected locations. Thus, e.g., the reduction of labile SOM fractions as a result of agricultural management (Schulten and Leinweber 1996; Capriel 1997) may be

linked with a decreased number of hydrogen bond sites and consequently with a reduced transition intensity.

Due to the assumed pronounced influence of the hydrogen bond-based crosslinks, the glass transition-like step transition of the air-dried samples is supposed to reflect rather the field-moist sample state (Schaumann and LeBoeuf 2005), while the classical glass transition of the water-free samples probably is solely dependent on structural properties of SOM, as e.g., the aromaticity of the humic substances (LeBoeuf and Weber Jr. 2000b; Xing 2001). The analysis of the glass transition behavior of humic fractions, however, has shown that the glass transition-like step transitions of soil samples represent a combination of the sum of the transitions of the different humic fractions and of effects of the proceeding time probably due to a matrix relaxation process of the humic substances. Contrary to the whole soil samples, the isolated humic and fulvic acid fractions revealed pronounced annealing peaks following the step transitions. The occurrence of these peaks may reflect the less heterogeneous composition of the humic fractions in comparison with the complete SOM matrix of the soil samples, which yields broad transitions without or with only weakly pronounced annealing peaks (Cortés and Montserrat 1998; Hutchinson 1998). In the humin fraction, surprisingly no thermal events were observed in the studied temperature range below 110 °C. In the rigid humin structure (Cuypers et al. 2002; Gunasekara and Xing 2003), the amount of hydrophilic groups providing hydrogen bond sites possibly is too small for an influential crosslinking of the organic matrix by water molecules. Classical glass transitions at high temperatures basing on interactions between the organic substances or between the mineral and the organic phase consequently may play a part for the glass transition behavior of the humin fraction.

The observation of aging processes in soil samples further supports the polymeric view of SOM. For air-dried samples, the glass transition-like step transitions have shifted to 5 - 10 °C higher temperature within three years. Because of the small intensity or complete absence of annealing peaks, which may be a consequence of the extreme heterogeneity of SOM (Cortés and Montserrat 1998; Hutchinson 1998; Chung et al. 2004), the transition temperatures of the glass transition-like step transitions were used instead of the annealing peaks to trace the aging process. By the evaluation of the transition temperatures as a function of the DSC heating rate (Moynihan et al. 1996; Cortés and Montserrat 1998), apparent activation energies between 120 and 370 kJ mol^{-1} were determined for the relaxation process of the air-dried soil samples. These values are smaller than the activation energies of synthetic organic polymers (Montserrat 1994; Cortés and Montserrat 1998; Hutchinson 1998) or inorganic glasses (Moynihan et al. 1996; Hutchinson 1998). It is, however, questionable, if the processes which occur in SOM in the glassy state are comparable to the structural relaxation process of synthetic glassy materials. In contrast to synthetic polymer systems, the aging of SOM may be affected by the interactions of a high number of different organic compounds as well as by the mineral phase partially directly attached to the organic substances. The measurement of the transition temperatures in the course of time for samples stored in different relative humidities (RH) has indicated that aging of water-containing soil samples may consist of two processes:

Structural relaxation of the polymeric network as well as the formation of hydrogen bond crosslinks by water molecules may cause a slowly increasing rigidity of the amorphous SOM matrix. For the studied samples with low moisture contents, a rise of the transition temperatures due to aging only occurred, if the moisture content remained constant or increased. Under drying conditions, however, no increase of the transition temperatures was observed. This can be explained by the disruption of crosslinks of water molecules in the organic phase due to evaporation, which may counteract the structural relaxation process. As also assumed for the structural relaxation process, the formation of new water crosslinks after their disruption or after an increase of the moisture content is a very slow process (Schaumann and LeBoeuf 2005). After the disruption of hydrogen bond-based crosslinks by heating the air-dried samples in closed pans to 110 °C, the slow changes of the observed glass transition parameters indicate that the reorganization of the water-crosslinked SOM structure lasts one to two years. In contrast, the reorganization of the polymeric chains to the amorphous glassy structure after transferring water-free soil samples to the rubbery state occurs within a time scale of minutes.

Another interesting result of the DSC measurements was an endothermic peak at (74 ± 2) °C, which occurred for soil samples with high OM content, if they were measured in the water-free state or after a thermal pretreatment at 110 °C. According to solid-state NMR and wide-angle X-ray scattering (WAXS) studies of humic substances by Hu et al. (2000), this peak may be attributed to the melting of poly(methylene) crystallites.

6.3. Conclusions for the macromolecular SOM structure and its interactions with water

The results of this thesis show that in addition to the molecular structure, the macromolecular structure of humous soil substances has to be taken into account in order to understand many aspects of SOM behavior. Thus, swelling of SOM as well as the slow wetting process of water repellent soil samples can only be interpreted in terms of conformational changes within the macromolecular organic network. Hysteresis effects of the soil wettability in the course of drying-remoistening cycles also point to the relevance of slow changes of the conformation of the complex SOM matrix, which is composed of an immense number of different structural units. Especially, slow changes of the orientation of hydrophilic and hydrophobic groups at the surfaces of the organic soil matrix (Ma'shum and Farmer 1985; Valat et al. 1991; Roy et al. 2000) are expected to be responsible for the slow rates of alterations of the wettability characteristics after changes of the moisture status. Possibly, the observed interrelation between water repellency and pH and ionic strength for the location Tiergarten also bases on changes of the macromolecular arrangement in dependence on the electrolyte content. Thus, a more aggregated SOM conformation because of shielding of its charges by ions in the soil solution may result in a lower wettability (see Chapter 6.1). Above all, the glass transition behavior of SOM is supposed to react very sensitively on conformational changes associated with the matrix rigidity, i.e. the degree of crosslinking and

aggregation of the molecular chains. The structural relaxation as the main factor of influence for the glass transition parameters bases on changes of the amorphous glassy structure towards a more rigid structure. These slow changes towards equilibrium usually do not include alterations of the molecular composition, but only of the conformational arrangement of the macromolecular structure (Struik 1978; Donth 1992; Cortés and Montserrat 1998).

All the above mentioned processes reveal close interrelations between water molecules and the organic soil matrix. Polar functional groups of SOM, as represented mainly by carboxylic, amino, and phenolic hydroxyl groups, provide bond sites for water molecules. Within the macromolecular SOM network, the sorption of water may result in two opposite effects, depending on the amount of available water molecules. For low water contents, a hydrogen bond-based crosslinking of SOM segments by water molecules, as suggested by the HBCL model (Schaumann 2005; Schaumann and LeBoeuf 2005), probably results in a more rigid structure. For moderate to high water contents, water on the other hand may act as plasticizer and may cause SOM swelling associated with the arising of gel properties (Benedetti et al. 1996; Schaumann et al. 2000; Schaumann and LeBoeuf 2005). These different effects of water are distinctly reflected by the sorption isotherms of water in humous soil samples and by their glass transition behavior: Most probably, for each soil sample, one moisture status is linked with a maximal transition temperature, as observed by Schaumann and LeBoeuf (2005) for a peat sample. Drying of the sample may cause a lowering of the transition temperature because of the reduction of the antiplasticizing effect of water. The addition of water also is supposed to result in the disruption of crosslinks of bridging water molecules (Schaumann 2005). For further increasing water contents, classical plasticization of the SOM matrix linked with swelling additionally may contribute to a decrease of the transition temperature (Schaumann and LeBoeuf 2005). At the surface of the organic substances in soil, the interfacial properties may be altered by the sorption of water. The slow conversion of water repellent surfaces to wettable ones after the contact with water molecules most probably is based on the orientation of hydrophilic molecule groups to the outside and of hydrophobic molecule groups to the inside of the organic macromolecules or molecule associates (Ma'shum and Farmer 1985; Valat et al. 1991; Roy et al. 2000). Conversely, the removal of water is supposed to cause a slow reorientation of the polar and apolar groups turning the surface characteristics again to a more water repellent behavior (Bayer and Schaumann 2006). Consequently, the water status has to be considered a decisive factor of influence for the conformation and with that for ecologically relevant properties of SOM.

Because of the low reaction rates of wetting and swelling processes of SOM, the time represents an additional important factor besides the water status for the conformational structure of humous substances. In accordance with the results of sorption studies by Altfelder et al. (1999), our results also point to a period of time up to three weeks which is necessary to reach equilibrium conditions after a change of the moisture content. The underlying slow processes can be traced by direct approaches to observe the wetting and swelling kinetics, as measurements of the water content and assessments of the bond strengths of water molecules

and their distribution in different pore types in the course of hydration time. Additionally, the gradual changes of SOM wetting characteristics with time after a change of the water content reflect the slow alterations of the SOM conformation induced by moistening or drying. Especially, the increasing transition temperatures of the glass transition-like step transition due to aging of the amorphous matrix indicate the distinct influence of the time on the macromolecular SOM structure.

6.4. Outlook

6.4.1. Wetting and swelling

For investigating wetting and swelling processes in soil, ^{1}H NMR Relaxometry has been established as an excellent tool (Todoruk et al. 2003b; Schaumann et al. 2004; Schaumann et al. 2005a). This technique allows a differentiation between wetting and swelling, the first of these processes causing a shift of the peak positions in the relaxation time distributions and the latter being reflected by a change of the water distribution within different relaxation time ranges. Due to the lack of information on the surface relaxivities of the different soil components, the pore geometries, and the effects of paramagnetic soil compounds (mainly iron and manganese) on the relaxation times, up to now, only a qualitative description of the redistribution of water in different pore types or changes of the sizes or properties of soil pores is possible. For a quantitative characterization of the pores which are involved in these processes, careful investigations of well-characterized reference systems are required. The porous solid phases of such systems have to be provided with known pore size distributions, uniform pore geometries, and known surface relaxivities, which do not change in the course of time due to the contact with the wetting agent. For the liquid phase, the content of paramagnetic substances and the bulk relaxation time have to be known. Meantime, Fabian Jäger deals with these mentioned issues within the scope of the DFG project SCH849/5.

In a second step, synthetic swellable substances can be used to study the effects of swelling on the relaxation time distributions. However, the interpretation of the NMR results is difficult, if swelling processes occur, because both the solid and the liquid phase are affected by swelling (Elias 1997). On the one hand, the distance affected by surface relaxation of the solid phase is supposed to increase, and the bulk relaxation time in the liquid phase probably becomes smaller, resulting in decreasing relaxation times in the course of swelling. On the other hand, the sizes of macropores may increase, causing higher relaxation times due to swelling. In order to evaluate the individual contributions of these mechanisms, additional analyses to observe the gel formation during the swelling process are necessary. Changes of the pore sizes and the formation of visible gel phases at the surfaces of the macromolecular network may be observed by microscopic techniques (Mackie et al. 1998; Yamul and Lupano 2002; Tian et al. 2003). Especially by atomic force microscopy (AFM), a technique which allows the observation of aqueous samples, the gelation process can be followed in detail (Mackie et al. 1998). Alterations of the composition of the liquid phase due to the dissolution

of substances initially associated with the solid phase should be analyzed, and particularly the study of rheological properties in the course of swelling would yield additional important information on the gel characteristics (Ross-Murphy 1994; Kavanagh and Ross-Murphy 1998).

6.4.2. Water repellency

The measured surface tensions of the soil extracts of water repellent and wettable samples point to an important role of amphiphilic substances for the actual wetting properties in soil. Morley et al. (2005) found more polar compounds of high relative molecular mass, which also may exhibit amphiphilic character, in water repellent than in wettable soil samples. Our results, however, indicate that at the SOM surfaces, amphiphilic groups may be enriched in water repellent soils. To confirm this assumption, detailed investigations of the structural composition at the surfaces of humous soil compounds are required. For this purpose, surface sensitive methods, as e.g., diffuse reflectance Fourier transform infrared (DRIFT) spectroscopy or attenuated total reflectance-Fourier transform infrared (ATR-FTIR) spectroscopy, are necessary.

In order to understand the effects of time on the wetting behavior, further studies including the observation of soil wettability in the course of time after different moistening and drying methods have to be performed. First results of Bayer et al. (2005) have shown that the development of soil wettability during sample drying is affected by the drying temperature and that significant changes of the wettability also occur after a constant water content has been reached. The mechanisms which cause the alterations of the wetting behavior in the course of moistening or drying could be determined by analyzing the structural changes at the SOM surfaces at different points of time during slow moistening and drying procedures.

Our results show that the wetting behavior of the studied soil samples is influenced by intrinsic SOM properties. However, the degree of water repellency of each sample varies with the water content. This indicates that the interfacial tension of the organic substances in soil does not depend only on the molecular composition and their conformation at the SOM surfaces, but the water film which is formed at the surfaces also has a pronounced effect on the interfacial properties. By means of the thickness of this water film, the often observed maximum of repellency at a specific water content (King 1981; de Jonge et al. 1999; Bachmann and van der Ploeg 2002) can be explained (Goebel et al. 2004): For completely dry soils, the portion of high-energy surfaces (especially mineral surfaces and hydrophilic groups of the organic matrix) results in small contact angles for the first adsorbed water molecules. With increasing moisture content, the adsorbed water molecules cause a decrease of the surface free energy, resulting in a lower wettability. At a certain water content, the influence of the solid surface on the adsorbed water molecules gets smaller, and additional water molecules undergo bonding types more and more similar to free water. At this specific water content, the wettability again begins to increase. A comprehensive study of this water film and of its effect on soil wettability would yield important information on the mechanisms

which are responsible for alterations of the wetting behavior with the water status. ^{1}H solid state NMR and DSC investigations of the water freezability would enable a characterization of the mobility of the water molecules and with that of the film thickness. Model substances with different contents of hydrophilic and apolar groups at their surfaces presumably reveal different interrelations between water status (i.e. moisture content and hydration or drying time) and the degree of water bonding in the superficial water film. By understanding the dependence of the water film on the surface characteristics of the solid phase, soil wettability may be interpreted as a function of structural surface composition and water status of the samples.

All these approaches will help to understand the wetting processes occurring in soil and elucidate possible factors of influence for water repellency. Nevertheless, an exact prediction of the wetting characteristics on the basis of specific soil properties most probably will remain impossible, because the underlying mechanisms differ from location to location. In this work, these site-specific mechanisms became noticeable for the anthropogenic locations Tiergarten and Buch. However, the site-specific influences on the wetting mechanisms in soil are commonly accepted (e.g., Doerr et al. 2000).

6.4.3. Glass transition behavior

In humous soil substances, two types of glass transitions can be distinguished: The atypical glass transition, here called glass transition-like step transition, which only can be observed in closed systems in the first heating cycle, reacts very sensitively to changes of the external conditions, as e.g., the water status (Schaumann 2005; Schaumann and LeBoeuf 2005). The second transition type of the water-free samples rather reflects the structural properties of SOM. But, because of the low intensity of this classical glass transition in soil samples, the DSC sensitivity is insufficient to correlate the transition parameters (especially ΔC) with other soil properties. More sensitive methods, as e.g., WISE (wideline separation) solid-state NMR (Mao et al. 2002), are required for a better quantitative analysis of this transition. Especially for the quantification of weak step transitions, TMA additionally may represent a more sensitive method than DSC (Schaumann et al. 2005b) despite the restrictions of TMA investigations of thermal transitions in soil samples (Schaumann et al. 2005b).

The observed site-specific influences on the glass transition-like step transition point to a correlation between its intensity and the amount of hydrophilic functional groups providing hydrogen bond sites for water bridges in SOM. The content of hydrophilic groups is expected to be higher in young labile SOM fractions than in decomposed material (Kögel-Knabner 1993; Baldock et al. 1997). Anthropogenic impacts, as agricultural management, also may reduce hydrophilic structural units due to the SOM transformation to more condensed recalcitrant substances (Leinweber and Schulten 1992; Schulten and Leinweber 1996; Capriel 1997). A verification of the interrelation between transition intensity and the number of hydrogen bond sites by solid state NMR would yield an explanation for the occurrence or absence of the glass transition-like step transition in samples of different locations.

In most cases, the crosslinking of the SOM matrix by water molecules probably superimposes the effects of the molecular and conformational structure of the organic soil substances and their interactions with the mineral matrix. However, if the amount of hydrogen bond sites is low, the intermolecular and intramolecular interactions of the humous substances also may influence the glass transition behavior of water-containing soil samples. Consequently, samples without or with only small amounts of hydrophilic groups have to be analyzed in order to separate the effect of condensed organic matter structures on the glass transition behavior from the effect of hydrogen bond-based crosslinking of SOM. Possibly, the humin fractions of different soil samples are suitable for such studies. For these fractions, which reveal distinctly smaller contents of polar groups than the humic acid, fulvic acid, and carbohydrate fractions (Stevenson 1994), an interrelation between the transition temperature and the content of highly condensed rigid organic structures can be assumed for water-containing samples. In addition to the DSC measurements, structural assessments, as pyrolysis-GC/MS or CPMAS ^{13}C NMR studies have to be applied to identify these structures.

For both glass transition types, it is important to know to which extent they correspond to general polymer models. In this context, especially the aging process and its kinetics are of importance. According to the general aging theory for amorphous polymers and other glassy materials (Struik 1978; Donth 1992; Cortés and Montserrat 1998), this process, which is directly connected with the glass transition characteristics, is expected to lead to structural changes of the glassy SOM matrix and with that to changes of related properties, as e.g., the sorption behavior. For water-containing samples, the processes of structural relaxation of the organic molecules and of increasing crosslinking by water molecules most probably overlap during sample annealing, as indicated by the different developments of the transition temperatures in different relative humidities. In order to differentiate the effects of these two processes on the glass transition behavior, an extensive study of various samples with different water retention properties of their humous substances is necessary. Alternatively, the study of the development of the glass temperature of water-free samples in the course of time would be a possibility to observe the structural relaxation of SOM without additional effects of water. However, from our experience, it is very difficult or even impossible to store samples for a long time in a completely water-free state.

Usually, the kinetics of physical aging are studied by means of the area and the position of the annealing peaks (Illekova 1994; Montserrat 1994; Hutchinson 1998; Chung et al. 2004). But, in complete soil samples, these annealing peaks do not occur or if at all, they reveal a very small intensity, most probably due to the heterogeneous structure of SOM. For this reason, we used the transition temperature of the glass transition-like step transition instead of the annealing peak temperature to observe the annealing effects. The correlation of glass temperature and annealing peak temperature for amorphous polymer materials (Chung et al. 2004) justifies this procedure. However, the analysis of physical aging processes of humous substances by means of distinctly pronounced annealing peaks would enforce the importance

of the occurrence of aging processes in SOM. More homogenous SOM constituents, as fulvic or humic acids, or precursor substances, as e.g., cellulose, may be used for such studies.

A comprehensive understanding of the aging mechanisms in SOM would yield a new method to describe transformation processes of the organic soil matrix from the macromolecular point of view. Due to the extremely complex and irregular molecular structure of organic substances in soil, this approach possibly results in the only method of general applicability to detect slow alterations of SOM induced by changes of the external conditions. Additionally, the question of an interrelation between SOM aging and the aging of contaminants in soil will be of fundamental importance.

7. References

Akim, E. L. 1978. Cellulose - bellwether or old hat. *Chemtech* 8, 676-682.

Almendros, G.; Gonzalez-Vila, F. J.; Martin, F.; Fruend, R.; Luedemann, H. D. 1992. Solid state NMR studies of fire-induced changes in the structure of humic substances. *Sci. Total Environ.* 117-118, 63-74.

Altfelder, S.; Streck, T.; Richter, J. 1999. Effect of air-drying on sorption kinetics of the herbicide chlortoluron in soil. *J. Environ. Qual.* 28, 1154-1161.

Avena, M. J.; Vermeer, A. W. P.; Koopal, L. K. 1999. Volume and structure of humic acids studied by viscometry pH and electrolyte concentration effects. *Colloids Surfaces A* 151, 213-224.

Bachmann, J.; van der Ploeg, R. R. 2002. A review on recent developments in soil water retention theory: Interfacial tension and temperature effects. *J. Plant Nutr. Soil Sci.* 165, 468-478.

Baes, A. U.; Bloom, P. R. 1988. Effect of ionic strength on swelling and the exchange of alkaline earth cations in soil organic matter. *Soil Sci.* 146, 67-72.

Baldock, J. A.; Oades, J. M.; Nelson, P. N.; Skene, T. M.; Golchin, A.; Clarke, P. 1997. Assessing the extent of decomposition of natural organic materials using solid-state 13C NMR spectroscopy. *Aust. J. Soil Res.* 35, 1061-1084.

Bartoli, F.; Philippy, R. 1990. Al-organic matter associations as cementing substances of ochreous brown soil aggregates: Preliminary examination. *Soil Sci.* 150, 745-751.

Bayer, J.; Hurraß, J.; Schaumann, G. E. 2005. Influence of pH and drying conditions on the wettability of soil samples. *Geophysical Research Abstracts* 7, EGU05-A-00416; SSS8-1FR5P-0147.

Bayer, J.; Schaumann, G. E. 2006. Development of soil water repellency in the course of isothermal drying and upon ph changes in two urban soils. *Hydrol. Process.*, submitted.

Benedetti, M. F.; van Riemsdijk, W. H.; Koopal, L. K. 1996. Humic substances considered as a heterogeneous Donnan gel phase. *Environ. Sci. Technol.* 30, 1805-1813.

Berezin, G. I.; Kiselev, A. V.; Kozlov, A. A. 1973. Equilibrium of adsorbate and capillary condensate with bulk crystal phase at temperatures below the normal melting point. *J. Colloid Interf. Sci.* 45, 190-197.

Berglöf, T.; Koskinen, W. C.; Kylin, H.; Moorman, T. B. 2000. Characterization of triadimefon sorption in soils using supercritical fluid (SFE) and accelerated solvent (ASE) extraction techniques. *Pest Manag. Sci.* 56, 927-931.

Birkett, J. W.; Jones, M. N.; Bryan, N. D.; Livens, F. R. 1997. Computer modeling of partial specific volumes of humic substances. *Eur. J. Soil Sci.* 48, 131-137.

Birkett, J. W.; Jones, M. N.; Bryan, N. D.; Livens, F. R. 1998. The effects of solution conditions on partial specific volumes of humic substances. *Anal. Chim. Acta* 362, 299-308.

Blackwell, P., 1997. Water repellent soils: Managing water repellent soils. Farmnote 109/96, Western Australian Department of Agriculture.

Borisover, M.; Graber, E. R. 2002. Simplified link solvation model (LSM) for sorption in natural organic matter. *Langmuir* 18, 4775-4782.

Borisover, M.; Graber, E. R. 2004. Hydration of natural organic matter: Effect on sorption of organic compounds by natural organic matter fractions vs natural organic matter source material. *Environ. Sci. Technol.* 38, 4120-4129.

Cambardella, C. A.; Elliott, E. T. 1992. Particulate soil organic-matter changes across a grassland cultivation sequence. *Soil Sci. Soc. Am. J.* 56, 777-783.

Cameron, R. S.; Thornton, B. K.; Swift, R. S.; Posner, A. M. 1972. Molecular weight and shape of humic acid from sedimentation and diffusion measurements on fractionated extracts. *J. Soil Sci.* 23, 394-408.

Capriel, P. 1997. Hydrophobicity of organic matter in arable soils: Influence of management. *Eur. J. Soil Sci.* 48, 457-462.

Capriel, P.; Beck, T.; Borchert, H.; Gronholz, J.; Zachmann, G. 1995. Hydrophobicity of the organic matter in arable soils. *Soil Biol. Biochem.* 27, 1453-1458.

Carale, T. R.; Pham, Q. T.; Blankschtein, D. 1994. Salt effects on intramicellar interactions and micellization of nonionic surfactants in aqueous solutions. *Langmuir* 10, 109-121.

Chen, Y.; Schnitzer, M. 1976. Water adsorption on soil humic substances. *Can. J. Soil Sci.* 56, 521-524.

Chen, Y.; Schnitzer, M. 1978. The surface tension of aqueous solutions of soil humic substances. *Soil Sci.* 125, 7-15.

Chenu, C.; Le Bissonnais, Y.; Arrouays, D. 2000. Organic matter influence on clay wettability and soil aggregate stability. *Soil Sci. Soc. Am. J.* 64, 1479-1486.

Chilom, G.; Rice, J. A. 2005. Glass transition and crystallite melting in natural organic matter. *Org. Geochem.*, in press.

Chiou, C. T.; Kile, D. E.; Malcolm, R. L. 1988. Sorption of vapors of some organic liquids on soil humic acid and its relation to partitioning of organic compounds in soil organic matter. *Environ. Sci. Technol.* 22, 298-303.

Chiou, C. T.; Kile, D. E.; Rutherford, D. W. 2000. Sorption of selected organic compounds from water to a peat soil and its humic-acid and humin fractions: Potential sources of the sorption nonlinearity. *Environ. Sci. Technol.* 34, 1254-1258.

Chiou, C. T.; Shoup, T. D. 1985. Soil sorption of organic vapors and effects of humidity on sorptive mechanism and capacity. *Environ. Sci. Technol.* 19, 1196-1200.

Chung, H.-J.; Chang, H.-I.; Lim, S.-T. 2004. Physical aging of glassy normal and waxy rice starches: Effect of crystallinity on glass transition and enthalpy relaxation. *Carbohydr. Polym.* 58, 101-107.

Conte, P.; Piccolo, A. 1999. Conformational arrangement of dissolved humic substances. Influence of solution composition on association of humic molecules. *Environ. Sci. Technol.* 33, 1682-1690.

Cornelissen, G.; Kukulska, Z.; Kalaitzidis, S.; Christanis, K.; Gustafsson, O. 2004. Relations between environmental black carbon sorption and geochemical sorbent characteristics. *Environ. Sci. Technol.* 38, 3632-3640.

Cortés, P.; Montserrat, S. 1998. Physical aging studies of amorphous linear polyesters. Part II. Dependence of structural relaxation parameters on the chemical structure. *J. Polymer Sci. Part B* 36, 113-126.

Cowie, J. M. G.; Ferguson, R. 1986. The aging of poly(vinyl methyl ether) as determined from enthalpy relaxation measurements. *Polymer* 27, 258-260.

Cuypers, C.; Grotenhuis, T.; Nierop, K. G. J.; Franco, E. M.; de Jager, A.; Rulkens, W. 2002. Amorphous and condensed organic matter domains: The effect of persulfate oxidation on the composition of soil/sediment organic matter. *Chemosphere* 48, 919-931.

de Jonge, L. W.; Jacobsen, O. H.; Moldrup, P. 1999. Soil water repellency: Effects of water content, temperature, and particle size. *Soil Sci. Soc. Am. J.* 63, 437-442.

de Wit, J. C. M.; van Riemsdijk, W. H.; Koopal, L. K. 1993. Proton binding to humic substances. 1. Electrostatic effects. *Environ. Sci. Technol.* 27, 2005-14.

DeBano, L.F., 1981. Water repellent soils: A state-of-the-art. USDA Forest Service General Technical Report PSW-46, Berkeley, California.

Dekker, L. W.; Ritsema, C. J. 2000. Wetting patterns and moisture variability in water repellent Dutch soils. *J. Hydrol.* 231-232, 148-164.

DeLapp, R. C.; LeBoeuf, E. J. 2004. Thermal analysis of whole soils and sediment. *J. Environ. Qual.* 33, 330-337.

Dittmar, T.; Kattner, G. 2003. Recalcitrant dissolved organic matter in the ocean: Major contribution of small amphiphilics. *Mar. Chem.* 82, 115-123.

Doerr, S. H.; Dekker, L. W.; Ritsema, C. J.; Shakesby, R. A.; Bryant, R. 2002. Water repellency of soils: The influence of ambient relative humidity. *Soil Sci. Soc. Am. J.* 66, 401-405.

Doerr, S. H.; Shakesby, S. H.; Walsh, R. P. D. 2000. Soil water repellency: Its causes, characteristics and hydro-geomorphological significance. *Earth Sci. Rev.* 51, 33-65.

Doerr, S. H.; Thomas, A. D. 2000. The role of soil moisture in controlling water repellency: New evidence from forest soils in Portugal. *J. Hydrol.* 231-232, 134-147.

Donth, E.-J. 1992. Relaxation and thermodynamics in polymers: Glass transition. Berlin: Akademie Verlag.

Elias, H.-G. 1997. An introduction to polymer science. Weinheim: VCH.

Ellerbrock, R. H.; Gerke, H. H. 2004. Characterisation of organic matter from aggregate coatings and biopores by Fourier transform infrared spectroscopy. *Eur. J. Soil Sci.* 55, 219-228.

Ellerbrock, R. H.; Gerke, H. H.; Bachmann, J.; Goebel, M. O. 2005. Composition of organic matter fractions for explaining wettability of three forest soils. *Soil Sci. Soc. Am. J.* 69, 57-66.

Ellis, T. S.; Karasz, F. E. 1986. Enthalpy recovery and physical aging of polymer-diluent binary systems: A network epoxy and water. *Polym. Eng. Sci.* 26, 290-296.

Falbe, P. D. J.; Regitz, P. D. M., Eds. 1992. Römpp Chemie Lexikon. Stuttgart: Georg Thieme Verlag.

Franco, C. M. M.; Clarke, P. J.; Tate, M. E.; Oades, J. M. 2000. Hydrophobic properties and chemical characterisation of natural water repellent materials in Australian sands. *J. Hydrol.* 231-232, 47-58.

Goebel, M.-O.; Bachmann, J.; Woche, S. K.; Fischer, W. R.; Horton, R. 2004. Water potential and aggregate size effects on contact angle and surface energy. *Soil Sci. Soc. Am. J.* 68, 383-393.

Graber, E. R.; Borisover, M. D. 1998a. Evaluation of the glassy/rubbery model for soil organic matter. *Environ. Sci. Technol.* 32, 3286-3292.

Graber, E. R.; Borisover, M. D. 1998b. Hydration-facilitated sorption of specifically interacting organic compounds by model soil organic matter. *Environ. Sci. Technol.* 32, 258-263.

Gregorich, E. G.; Carter, M. R.; Angers, D. A.; Monreal, C. M.; Ellert, B. H. 1994. Towards a minimum data set to assess soil organic matter quality in agricultural soils. *Can. J. Soil Sci.* 74, 367-385.

Gruenberg, B.; Emmler, T.; Gedat, E.; Shenderovich, I.; Findenegg, G. H.; Limbach, H.-H.; Buntkowsky, G. 2004. Hydrogen bonding of water confined in mesoporous silica MCM-41 and SBA-15 studied by 1H solid-state NMR. *Chem. Eur. J.* 10, 5689-5696.

Gunasekara, A. S.; Xing, B. 2003. Sorption and desorption of naphthalene by soil organic matter: Importance of aromatic and aliphatic components. *J. Environ. Qual.* 32, 240-246.

Guo, J. H. 1993. Effects of plasticizers on water permeation and mechanical properties of cellulose acetate: Antiplasticization in slightly plasticized polymer film. *Drug. Dev. Ind. Pharm.* 19, 1541-1545.

Haynes, R. J. 2005. Labile organic matter fractions as central components of the quality of agricultural soils: An overview. *Adv. Agron.* 85, 221-268.

Hinedi, Z. R.; Chang, A. C.; Anderson, M. A. 1997. Quantification of microporosity by nuclear resonance relaxation of water imbibed in porous media. *Water Resour. Res.* 31, 2687-2704.

Höhne, G. W. H.; Hemminger, W.; Flammersheim, H.-J. 1996. Differential scanning calorimetry. An introduction for practitioners. Berlin: Springer.

Hu, W.-G.; Mao, J.; Xing, B.; Schmidt-Rohr, K. 2000. Poly(methylene) crystallites in humic substances detected by nuclear magnetic resonance. *Environ. Sci. Technol.* 34, 530-534.

Huang, W.; Weber Jr., W. J. 1997. A distributed reactivity model for sorption by soils and sediments. 10. Relationships between desorption, hysteresis, and the chemical characteristics of organic domains. *Environ. Sci. Technol.* 31, 2562-2569.

Hudson, R. A.; Traina, S. J.; Shane, W. W. 1994. Organic matter comparison of wettable and nonwettable soils from bentgrass sand greens. *Soil Sci. Soc. Am. J.* 58, 361-367.

Hutchinson, J. M. 1998. Characterizing the glass transition and relaxation kinetics by conventional and temperature-modulated differential scanning calorimetry. *Thermochim. Acta* 324, 165-174.

Illekova, E. 1994. Review of structural relaxation models with the mutual correlation of their activation enthalpies. *Int. J. Rap. S.* 8, 195-224.

Illinger, J. L. 1977. Interaction of water with hydrophilic polyether polyurethanes: DSC studies of the effects of polyether variations. *Polym. Sci. Technol.* 10, 313-325.

Jackson, B. L. J.; Gillingham, A. G. 1985. Lime soil moisture relationships. In: Jackson, B. L. J.; Edmeades, D. C., Eds. *Proceedings of the Workshop on Lime in New Zealand Agriculture*.

Kaiser, K.; Guggenberger, G. 2003. Mineral surfaces and soil organic matter. *Eur. J. Soil Sci.* 54, 219-236.

Kamiya, Y.; Hirose, T.; Mizoguchi, K.; Naito, Y. 1986. Gravimetric study of high-pressure sorption of gases in polymers. *J. Polymer Sci. Part B* 24, 1525-1539.

Kamiya, Y.; Mizoguchi, K.; Terada, K.; Fujiwara, Y.; Wang, J.-S. 1998. CO2 sorption and dilation of poly(methyl methacrylate). *Macromolecules* 31, 472-478.

King, P. M. 1981. Comparison of methods for measuring severity of water repellence of sandy soils and assessment of some factors that affect its measurement. *Aust. J. Soil Res.* 19, 275-285.

Kögel-Knabner, I. 1993. Biodegradation and humification processes in forest soils. In: Bollag, J.-M.; Stotzky, G., Eds. Soil biochemistry. New York: Marcel Dekker, 101-137.

Kögel-Knabner, I. 1997. 13C and 15N NMR spectroscopy as a tool in soil organic matter research. *Geoderma* 80, 243-270.

Kögel-Knabner, I.; Hatcher, P. G.; Tegelaar, E. W.; de Leeuw, J. W. 1992. Aliphatic components of forest soil organic matter as determined by solid-state carbon-13 NMR and analytical pyrolysis. *Sci. Total Environ.* 113, 89-106.

Kölling, C. 2000. Luftverunreinigungen und Auswirkungen in den Wälder Bayerns. Bayerische Landesanstalt für Wald und Forstwirtschaft (LWF).

Krahmer, U.; Hennings, V.; Mueller, U.; Schrey, H.-P. 1995. Evaluation of soil physical parameters as a function of soil texture, effective density, and humus content. *Z. Pflanzenernähr. Bodenkd.* 158, 323-331.

Kuntz, I. D.; Kauzmann, W. 1974. Hydration of proteins and polypeptides. *Adv. Protein Chem.* 28, 239-345.

Landoldt-Börnstein 1982. Numerical data and functional relationships in science and technology. Heidelberg: Springer.

LeBoeuf, E. J.; Weber Jr., W. J. 1997. A distributed reactivity model for sorption by soils and sediments. 8. Sorbent organic domains: Discovery of a humic acid glass transition and an argument for a polymer-based model. *Environ. Sci. Technol.* 31, 1697-1702.

LeBoeuf, E. J.; Weber Jr., W. J. 2000a. Macromolecular characteristics of natural organic matter. 1. Insights from glass transition and enthalpic relaxation behavior. *Environ. Sci. Technol.* 34, 3623-3631.

LeBoeuf, E. J.; Weber Jr., W. J. 2000b. Macromolecular characteristics of natural organic matter. 2. Sorption and desorption behavior. *Environ. Sci. Technol.* 34, 3632-3640.

Leinweber, P.; Schulten, H. R. 1992. Differential thermal analysis, thermogravimetry and in-source pyrolysis-mass spectrometry studies on the formation of soil organic matter. *Thermochim. Acta* 200, 151-67.

Leinweber, P.; Schulten, H. R.; Horte, C. 1992. Differential thermal analysis, thermogravimetry and pyrolysis-field ionization mass spectrometry of soil organic matter in particle-size fractions and bulk soil samples. *Thermochim. Acta* 194, 175-187.

Lu, Y.; Pignatello, J. J. 2002. Demonstration of the "conditioning effect" in soil organic matter in support of a pore deformation mechanism for sorption hysteresis. *Environ. Sci. Technol.* 36, 4553-4561.

Lu, Y.; Pignatello, J. J. 2004. History-dependent sorption in humic acids and a lignite in the context of a polymer model for natural organic matter. *Environ. Sci. Technol.* 38, 5853-5862.

Lucht, L. M.; Larson, J. M.; Peppas, N. A. 1987. Macromolecular structure of coals. 9. Molecular structure and glass transition temperature. *Energy Fuels* 1, 56-58.

Lyon, W. G.; Rhodes, D. E. 1993. Molecular size exclusion by soil organic materials estimated from their swelling in organic solvents. *Environ. Toxicol. Chem.* 12, 1405-1412.

Kavanagh, G. M.; Ross-Murphy, S. B. 1998. Rheological characterization of polymer gels. *Progr. Polym. Sci* 23, 533-562.

Mackie, A. R.; Gunning, A. P.; Ridout, M. J.; Morris, V. J. 1998. Gelation of gelatin. Observation in the bulk and at the air-water interface. *Biopolymers* 46, 245-252.

Mao, J.; Ding, G.; Xing, B. 2002. Domain mobility of humic acids investigated with one- and two-dimensional nuclear magnetic resonance: Support for dual-mode sorption model. *Commun. Soil Sci. Plant Anal.* 33, 1679-1688.

Ma'shum, M.; Farmer, V. C. 1985. Origin and assessment of water repellency of a sandy South Australian soil. *Aust. J. Soil Res.* 23, 623-626.

McBrierty, V. J.; Martin, S. J.; Karasz, F. E. 1999. Understanding hydrated polymers: The perspective of NMR. *J. Mol. Liq.* 80, 179-205.

McBrierty, V. J.; Wardell, G. E.; Keely, C. M.; O'Neill, E. P.; Prasad, M. 1996. The characterization of water in peat. *Soil Sci. Soc. Am. J.* 60, 991-1000.

McKenna, G. B. 1989. Glass formation and glassy behavior. In: Allen, G., Ed. Comprehensive polymer science. Oxford: Pergamon Press, 311-362.

McKenna, G. B.; Simon, S. L. 2002. The glass transition: Its measurement and underlying physics. *Handbook of thermal analysis and calorimetry* 3, 48-109.

Meiboom, S.; Gill, D. 1958. Modified spin-echo method for measuring nuclear relaxation times. *Rev. Sci. Instrum.* 29, 688-691.

Merbach, W.; Garz, J.; Schliephake, W.; Stumpe, H.; Schmidt, L. 2000. The long-term fertilization experiments in Halle (Saale), Germany - introduction and survey. *J. Plant Nutr. Soil Sci.* 163, 629-638.

Mitra, S.; Dungan, S. R. 1997. Micellar properties of quillaja saponin. 1. Effects of temperature, salt and pH on solution properties. *J. Agr. Food Chem.* 45, 1587-1595.

Miyamoto, S.; Letey, J.; Osborn, J. 1972. Water vapor adsorption by water-repellent soils at equilibrium. *Soil Sci.* 114, 180-184.

Monreal, C. M.; Schnitzer, M.; Schulten, H. R.; Campbell, C. A.; Anderson, D. W. 1995. Soil organic structures in macro and microaggregates of a cultivated brown chernozem. *Soil Biol. Biochem.* 27, 845-853.

Montserrat, S. 1994. Physical aging studies in epoxy resins. I. Kinetics of the enthalpy relaxation process in a fully cured epoxy resin. *J. Polymer Sci. Part B* 32, 509-522.

Morley, C. P.; Mainwaring, K. A.; Doerr, S. H.; Douglas, P.; Llewellyn, C. T.; Dekker, L. W. 2005. Organic compounds at different depths in a sandy soil and their role in water repellency. *Aust. J. Soil Res.* 43, 239-249.

Moynihan, C. T.; Easteal, J.; Wilder, J.; Tucker, J. 1974. Dependence of the glass transition temperature on heating and cooling rate. *J. Phys. Chem.* 78, 2673-2677.

Moynihan, C. T.; Lee, S. K.; Tatsumisago, M.; Minami, T. 1996. Estimation of activation energies for structural relaxation and viscous flow from DTA and DSC experiments. *Thermochim. Acta* 280/281, 153-162.

Myneni, S. C. B.; Brown, J. T.; Martinez, G. A.; Meyer-Ilse, W. 1999. Imaging of humic substance macromolecular structures in water and soils. *Science* 286, 1335-1337.

Nishinari, K.; Watase, M.; Hatakeyama, T. 1997. Effects of polyols and sugars on the structure of water in concentrated gelatin gels as studied by low temperature differential scanning calorimetry. *Colloid. Polym. Sci.* 275, 1078-1082.

Orchiston, H. D. 1953. Adsorption of water vapor: I. Soils at 25°C. *Soil Sci.* 76, 453-465.

Orchiston, H. D. 1954. Adsorption of water vapor: II. Clays at 25°C. *Soil Sci.* 77, 463-479.

Perminova, I. V.; Frimmel, F. H.; Kovalevskii, D. V.; Abbt-Braun, G.; Kudryavtsev, A. V.; Hesse, S. 1998. Development of a predictive model for calculation of molecular weight of humic substances. *Wat. Res.* 32, 872-881.

Pfeifer, H.; Oehme, W.; Siegel, H. 1985. Freezing of water in porous solids; glass transition or phase transition? *Ann. Physik* 42, 496-506.

Piccolo, A. 2002. The supramolecular structure of humic substances: A novel understanding of humus chemistry and implications in soil science. *Adv. Agron.* 75, 57-134.

Piccolo, A.; Conte, P. 2000. Molecular size of humic substances. Supramolecular associations versus macromolecular polymers. *Adv. Environ. Res.* 3, 508-521.

Piccolo, A.; Mbagwu, J. S. C. 1999. Role of hydrophobic components of soil organic matter in soil aggregate stability. *Soil Sci. Soc. Am. J.* 63, 1801-1810.

Pignatello, J.; Xia, G. 2000. Extended dual-mode sorption of organic chemicals on soil organic matter. *Abstr. Pap. Am. Chem. Soc.* 220, ENVR-109.

Pignatello, J. J. 2003. Polymer sorption theory applied to macromolecular forms of natural organic matter. In: *Preprints of Extended Abstracts presented at the ACS National Meeting, American Chemical Society, Division of Environmental Chemistry* 43, 883-888.

Ping, Z. H.; Nguyen, Q. T.; Chen, S. M.; Zhou, J. Q.; Ding, Y. D. 2001. States of water in different hydrophilic polymers - DSC and FTIR studies. *Polymer* 42, 8461-8467.

Quinn, F. X.; Kampff, E.; Smyth, G.; McBrierty, V. J. 1988. Water in hydrogels. 1. A study of water in poly(N-vinyl-2-pyrrolidone/methyl methacrylate) copolymer. *Macromolecules* 21, 3191-3198.

Quyum, A.; Achari, G.; Goodman , R. H. 2002. Effect of wetting and drying and dilution on moisture migration through oil contaminated hydrophobic soils. *Sci. Total Environ.* 296, 77-87.

Randall, E. W.; Mahieu, N.; Ivanova, G. I. 1997. NMR studies of soil, soil organic matter and nutrients: Spectroscopy and imaging. *Geoderma* 80, 307-325.

Regnery, J., 2003. Einfluß einer Wiedervernässungsmaßnahme auf den Schwefelstatus eines degradierten Niedermoores. Diploma thesis, Institut für Pflanzenbauwissenschaften, Humboldt Universität, Berlin.

Rhue, R. D.; Rao, P. S. C.; Smith, R. E. 1988. Vapor-phase adsorption of alkylbenzenes and water on soils and clays. *Chemosphere* 17, 727-741.

Rice, J. A.; Guetzloff, T. F.; Tombacz, E. 2000. Investigations of humic materials aggregation with scattering methods. *Special Publication - Royal Society of Chemistry* 259, 135-141.

Ritsema, C. J.; Dekker, L. W. 1998. Three-dimensional patterns of moisture, water repellency, bromide and pH in a sandy soil. *J. Contam. Hydrol.* 31, 295-313.

Ritsema, C. J.; Dekker, L. W. 2000. Preferential flow in water repellent sandy soils: Principles and modeling implications. *J. Hydrol.* 231-232, 308-319.

Robens, E.; Wenzig, J. 1996. Water storing and releasing properties of peat. *Int. Peat J.* 6, 88-100.

Ronaldo de Macedo, J.; Meneguelli, N. d. A.; Ottoni Filho, T. B.; Lima, J. A. d. S. 2002. Estimation of field capacity and moisture retention based on regression analysis involving chemical and physical properties in Alfisols and Ultisols of the state of Rio de Janeiro. *Commun. Soil Sci. Plant Anal.* 33, 2037-2055.

Ross-Murphy, S. B. 1994. Rheological Characteristics of Gels. *J. Texture Stud.* 26, 391-400.

Roy, C.; Gaillardon, P.; Montfort, F. 2000. The effect of soil moisture content on the sorption of five sterol biosynthesis inhibiting fungicides as a function of their physicochemical properties. *Pest Manag. Sci.* 56, 795-803.

Roy, J. L.; McGill, B.; Rawluk, P. 1999. Petroleum residues as water-repellent substances in weathered nonwettable oil-contaminated soils. *Can. J. Soil Sci.* 79, 367-380.

Rutherford, D. W.; Chiou, C. T. 1992. Effect of water saturation in soil organic matter on the partition of organic compounds. *Environ. Sci. Technol.* 26, 965-970.

Sanyal, S. K. 2001. Colloid chemical properties of soil humic substances: A relook. *J. Indian Soc. Soil Sci.* 49, 537-569.

Seyler, R. J., Ed. 1994. Assignment of the glass transition. Philadelphia: American Society for Testing and Materials.

Schaumann, G. E. 2005. Matrix relaxation and change of water state during hydration of peat. *Colloids Surfaces A* 265, 163-170.

Schaumann, G. E.; Antelmann, O. 2000. Thermal characteristics of soil organic matter measured by DSC: A hint on a glass transition. *J. Plant Nutr. Soil Sci.* 163, 179-181.

Schaumann, G. E.; Hurraß, J.; Müller, M.; Rotard, W. 2004. Swelling of organic matter in soil and peat samples: Insights from proton relaxation, water absorption and PAH extraction. In: Ghabbour, E. A.; Davies, G., Eds. Humic substances: Nature's most versatile materials. New York: Taylor and Francis, Inc., 101-117.

Schaumann, G. E.; Hobley, E.; Hurraß, J.; Rotard, W. 2005a. H-NMR relaxometry to monitor wetting and swelling kinetics in high organic matter soils. *Plant Soil* 275, 1-20.

Schaumann, G. E.; LeBoeuf, E. J. 2005. Glass transitions in peat - their relevance and the impact of water. *Environ. Sci. Technol.* 39, 800-806.

Schaumann, G. E.; LeBoeuf, E. J.; DeLapp, R. C.; Hurraß, J. 2005b. Thermomechanical analysis of air-dried whole soil samples. *Thermochim. Acta* 436, 83-89.

Schaumann, G. E.; Siewert, C.; Marschner, B. 2000. Kinetics of the release of dissolved organic matter (DOM) from air-dried and pre-moistened soil material. *J. Plant Nutr. Soil Sci.* 163, 1-5.

Scheffer, F.; Schachtschabel, P. 1992. Lehrbuch der Bodenkunde. Stuttgart: Ferdinand Enke Verlag.

Schulten, H. R.; Leinweber, P. 1996. Characterization of humic and soil particles by analytical pyrolysis and computer modeling. *J. Anal. Appl. Pyrolysis* 38, 1-53.

Schulten, H. R.; Leinweber, P. 2000. New insights into organic-mineral particles: Composition, properties and models of molecular structure. *Biol. Fertil. Soils* 30, 399-432.

Schulten, H.-R.; Leinweber, P.; Sorge, C. 1993. Composition of organic matter in particle-size fractions of an agricultural soil. *J. Soil Sci.* 44, 677-691.

Seyler, R. J., Ed. 1994. Assignment of the glass transition. Philadelphia: American Society for Testing and Materials.

Sharma, M. L.; Uehara, G.; Mann Jr., J. A. 1969. Thermodynamic properties of water adsorbed on dry soil surfaces. *Soil Sci.* 107, 86-93.

Shatemirov, K. S.; Usupbaeva, C. A.; Sagymbaev, K. S. 1972. Physicochemical properties of some humates. *Tr. Kirg. Univ., Ser. Khim. Nauk*, 123-127.

Shogren, R. L. 1992. Effect of moisture content on the melting and subsequent physical aging of cornstarch. *Carbohydr. Polym.* 19, 83-90.

Shurygina, E. A.; Larina, N. K.; Chubarova, M. A.; Kononova, M. M. 1971. Differential thermal analysis and thermogravimetry of soil humus substances. *Sov. Soil Science*, 35-44.

Siewert, C. 2001. Investigation of the thermal and biological stability of soil organic matter. Aachen: Shaker.

Stawinski, J. 1983. The influence of exchangeable cations on the adsorption of water vapor on soils. *Zesz. Probl. Postepow Nauk Roln.* 220, 453-458.

Steenhuis, T. S.; Rivera, J. C.; Hernández, C. J. M.; Walter, M. T.; Bryant, R. B.; Nektarios, P. 2001. Water repellency in New York State soils. *Int. Turfgrass Soc. Res. J.* 9, 624-628.

Stevenson, F. J. 1994. Humus chemistry : Genesis, composition, reactions. New York: Wiley.

Struik, L. C. E. 1978. Physical aging in amorphous polymers and other materials. Amsterdam: Elsevier.

Summers, R. S.; Roberts, P. V. 1988. Activated carbon adsorption of humic substances. II. Size exclusion and electrostatic interactions. *J. Colloid Interf. Sci.* 122, 382-97.

Swift, R. S. 1996. Organic matter characterization. In: Sparks, D. L.; Page, A. L.; Helmke, P. A. et al., Eds. Methods of soil analysis: Part 3-chemical methods. Madison, WI: SSSA and ASA, 1018-1020.

Swift, R. S. 1999. Macromolecular properties of soil humic substances: Fact, fiction, and opinion. *Soil Sci.* 164, 790-802.

Tajima, K. 1971. Radiotracer studies on adsorption of surface-active substance at aqueous surface. III. Effects of salt on the adsorption of sodium dodecyl sulfate. *Bull. Chem. Soc. Japan* 44, 1767-1771.

Tarchitzky, J.; Hatcher, P. G.; Chen, Y. 2000. Properties and distribution of humic substances and inorganic structure-stabilizing components in particle-size fractions of cultivated mediterranean soils. *Soil Sci.* 165, 328-342.

Täumer, K.; Stoffregen, H.; Wessolek, G. 2005. Determination of repellency distribution using soil organic matter and water content. *Geoderma* 125, 107-115.

Thiele-Bruhn, S.; Seibicke, T.; Schulten, H. R.; Leinweber, P. 2004. Sorption of sulfonamide pharmaceutical antibiotics on whole soils and particle-size fractions. *J. Environ. Qual.* 33, 1331-1342.

Tian, Q.; Zhao, X.-A.; Tang, X.-Z.; Zhang, Y.-X. 2003. Fluorocarbon-containing hydrophobically modified poly(acrylic acid) gels: Gel structure and water state. *J. Appl. Polym. Sci.* 89, 1258-1265.

Todoruk, T. R.; Langford, C. H.; Kantzas, A. 2003a. Pore-scale redistribution of water during wetting of air-dried soils as studied by low-field NMR relaxometry. *Environ. Sci. Technol.* 37, 2707-2713.

Todoruk, T. R.; Litvina, M.; Kantzas, A.; Langford, C. H. 2003b. Low-field NMR relaxometry: A study of interactions of water with water-repellant soils. *Environ. Sci. Technol.* 37, 2878-2882.

Tschapek, M. 1984. Criteria for determining the hydrophilicity - hydrophobicity of soils. *Z. Pflanzenernähr. Bodenkd.* 147, 137-149.

Tsereteli, G. I.; Smirnova, O. I. 1992. DSC study of melting and glass transition in gelatins. *J. Thermal Anal.* 38, 1189-1201.

Unger, D. R.; Lam, T. T.; Schaefer, C. E.; Kosson, D. S. 1996. Predicting the effect of moisture on vapor-phase sorption of volatile organic compounds to soils. *Environ. Sci. Technol.* 30, 1081-1091.

Valat, B.; Jouany, C.; Rivière, L. M. 1991. Characterization of the wetting properties of air-dried peats and composts. *Soil Sci.* 152, 100-107.

Wagoner, D. B.; Christman, R. F. 1998. Molar masses and radii of humic substances measured by light scattering. *Acta hydrochim. hydrobiol.* 26, 191-195.

Waksmundzki, A.; Staszczuk, P. 1983. Apparatus for measuring adsorption and desorption of water vapor on soils. *Zesz. Probl. Postepow Nauk Roln.* 220, 459-466.

Wallis, M. G.; Horne, D. J. 1992. Soil water repellency. *Adv. Soil Sc.* 20, 91-146.

Weast, R. C.; Astle, M. J.; Beyer, W. H., Eds. 1986. CRC Handbook of Chemistry and Physics. Boca Raton, Florida: CRC Press, Inc.

Wedler, G. 1987. Lehrbuch der physikalischen Chemie. Weinheim: VCH.

Wershaw, R. L. 1999. Molecular aggregation of humic substances. *Soil Sci.* 164, 803-813.

Xia, G.; Pignatello, J. J. 2001. Detailed sorption isotherms of polar and apolar compounds in a high-organic soil. *Environ. Sci. Technol.* 35, 84-94.

Xing, B. 2001. Sorption of naphthalene and phenanthrene by soil humic acids. *Environ. Poll.* 111, 303-309.

Xing, B.; Chen, Z. 1999. Spectroscopic evidence for condensed domains in soil organic matter. *Soil Sci.* 164, 40-47.

Xing, B.; Pignatello, J. J. 1997. Dual-mode sorption of low-polarity compounds in glassy poly(vinyl chloride) and soil organic matter. *Environ. Sci. Technol.* 31, 792-799.

Yamul, D. K.; Lupano, C. E. 2002. Properties of gels from whey protein concentrate and honey at different pHs. *Food. Res. Int.* 36, 25-33.

Young, K. D.; LeBoeuf, E. J. 2000. Glass transition behavior in a peat humic acid and an aquatic fulvic acid. *Environ. Sci. Technol.* 34, 4549-4553.

Zhang, H.; Hartge, K. H. 1992. Effects of differently humified organic matter on soil aggregate stability by reducing aggregate wettability. *Z. Pflanzenernähr. Bodenkd.* 155, 143-149.

Zuyi, T.; Shifang, L.; Fan, Z. Z.; Yuhui, Y. 1997. Thermal transformation of humic and fulvic acids in soils. Part 2. Thermogravimetry. *Chem. Ecol.* 14, 21-30.

8. Annex

8.1. List of Figures

8.2. List of Tables

8.3. Contact

The number of data which were measured and evaluated in the context of this thesis would exceed the limited size of a printed annex. Therefore, the reader is kindly asked to contact me or the Department of Environmental Chemistry of the Institute of Environmental Technology of the TU Berlin and to request an electronic version of individual data.

Contact: Julia Hurraß
TU Berlin
Fachgebiet Umweltchemie
Institut für Technischen Umweltschutz
Fakultät für Prozesswissenschaften
Sekr: KF 3
Straße des 17. Juni 135
10623 Berlin
Tel: (030) 314-73638
(030) 314-25220 (office of the Department of Environmental Chemistry)
Fax: (030) 314-29319
e-mail: Julia.Hurrass@TU-Berlin.de